

# Generalized Psuedospectral Shattering and Inverse-Free Matrix Pencil Diagonalization

James Demmel<sup>\*</sup>Ioana Dumitriu<sup>†</sup>Ryan Schneider<sup>†</sup>

## Abstract

We present a randomized, inverse-free algorithm for producing an approximate diagonalization of any  $n \times n$  matrix pencil  $(A, B)$ . The bulk of the algorithm rests on a randomized divide-and-conquer eigensolver for the generalized eigenvalue problem originally proposed by Ballard, Demmel, and Dumitriu [Technical Report 2010]. We demonstrate that this divide-and-conquer approach can be formulated to succeed with high probability as long as the input pencil is sufficiently well-behaved, which is accomplished by generalizing the recent pseudospectral shattering work of Banks, Garza-Vargas, Kulkarni, and Srivastava [Foundations of Computational Mathematics 2022]. In particular, we show that perturbing and scaling  $(A, B)$  regularizes its pseudospectra, allowing divide-and-conquer to run over a simple random grid and in turn producing an accurate diagonalization of  $(A, B)$  in the backward error sense. The main result of the paper states the existence of a randomized algorithm that with high probability (and in exact arithmetic) produces invertible  $S, T$  and diagonal  $D$  such that  $\|A - SDT^{-1}\|_2 \leq \varepsilon$  and  $\|B - SIT^{-1}\|_2 \leq \varepsilon$  in at most  $O(\log(n) \log^2(\frac{n}{\varepsilon}) T_{\text{MM}}(n))$  operations, where  $T_{\text{MM}}(n)$  is the asymptotic complexity of matrix multiplication. This not only provides a new set of guarantees for highly parallel generalized eigenvalue solvers but also establishes nearly matrix multiplication time as an upper bound on the complexity of exact arithmetic matrix pencil diagonalization.

---

<sup>\*</sup>Department of Mathematics, University of California Berkeley

<sup>†</sup>Department of Mathematics, University of California San Diego

# Contents

<b>1</b>	<b>Introduction</b>	<b>3</b>
1.1	The Generalized Eigenvalue Problem . . . . .	3
1.2	Divide-and-Conquer Eigensolvers . . . . .	3
1.3	Pseudospectra and Random Matrix Theory . . . . .	4
1.4	Matrix Pencil Diagonalization . . . . .	5
1.5	Complexity and Numerical Stability . . . . .	6
1.6	Outline . . . . .	6
<b>2</b>	<b>Background</b>	<b>7</b>
2.1	Matrix Pencils, Eigenvalues, and Eigenvectors . . . . .	7
2.2	Pseudospectra . . . . .	9
<b>3</b>	<b>Pseudospectral Shattering for Matrix Pencils</b>	<b>12</b>
3.1	Preliminaries . . . . .	13
3.2	Multi-Parameter Tail Bound . . . . .	14
3.3	Shattering . . . . .	16
<b>4</b>	<b>Inverse-Free Divide-and-Conquer</b>	<b>20</b>
4.1	Motivation . . . . .	20
4.2	Numerical Building Blocks . . . . .	21
4.2.1	Implicit Repeated Squaring (IRS) . . . . .	21
4.2.2	RURV and GRURV . . . . .	23
4.2.3	DEFLATE . . . . .	24
4.3	Divide-and-Conquer Routine . . . . .	26
<b>5</b>	<b>Randomized Pencil Diagonalization</b>	<b>34</b>
5.1	Diagonalization Routine . . . . .	34
5.2	Forward Error Guarantee and Computational Complexity . . . . .	38
<b>6</b>	<b>Numerical Examples</b>	<b>41</b>
<b>7</b>	<b>Conclusion</b>	<b>47</b>
<b>8</b>	<b>Acknowledgements</b>	<b>48</b>
<b>A</b>	<b>Alternative Versions of Bauer-Fike for Matrix Pencils</b>	<b>49</b>
<b>B</b>	<b>Finite Arithmetic Analysis</b>	<b>50</b>
B.1	Black-Box Assumptions . . . . .	50
B.2	Two Matrix GRURV . . . . .	51
B.3	Finite Arithmetic IRS . . . . .	53

# 1 Introduction

## 1.1 The Generalized Eigenvalue Problem

Given matrices  $A, B \in \mathbb{C}^{n \times n}$ , the generalized eigenvalue problem seeks pairs  $(\lambda, v) \in \mathbb{C} \times \mathbb{C}^n$  with  $v \neq 0$  such that

$$Av = \lambda Bv. \quad (1.1.1)$$

As the name implies, this is a generalization of the standard, single-matrix eigenvalue problem, which we recover by setting  $B = I$ . When  $(A, B)$  is *regular*, meaning the characteristic polynomial  $\det(A - \lambda B)$  is not identically zero, solutions to (1.1.1) yield a generalized eigenvalue  $\lambda$  and a generalized eigenvector  $v$  of the matrix pencil  $(A, B)$ .

Solutions to generalized eigenvalue problems are important in a variety of research disciplines and applications. The ESPRIT algorithm and other matrix pencil methods in signal processing [35, 43], for example, recover signal parameters from noisy data as generalized eigenvalues. Generalized eigenvectors, meanwhile, have found application in binary classification problems [29, 40]. Finally, as in the single-matrix eigenvalue problem, we can draw motivation from linear differential equations, where the generalized eigenvalues and eigenvectors of  $(A, B)$  can be used to construct solutions to the first-order differential equation  $Bu'(t) = Au(t)$  [30, §7.1].

Unlike the single-matrix case, however, the generalized eigenvalue problem may have infinitely many solutions or admit infinite eigenvalues. In particular, any complex number satisfies (1.1.1) if  $A$  and  $B$  are both singular with overlapping null spaces, as the characteristic polynomial  $\det(A - \lambda B)$  is identically zero. In this case the pencil is *singular* (i.e., non-regular) and we need to be more careful about how we define generalized eigenvalues and eigenvectors (to be made precise later). In short, we cannot rely on (1.1.1) alone; some generalized eigenpairs may only formally satisfy (1.1.1) – e.g., in the infinite eigenvalue case – and more importantly there may be solutions that we consider trivial and wish to discard.

When  $B$  is nonsingular,  $(A, B)$  and  $B^{-1}A$  have the same set of eigenvalues and eigenvectors. This prompts a first approach to the problem: explicitly form  $B^{-1}A$  and apply any method for finding the eigenvalues and eigenvectors of an individual matrix. This is unsatisfactory for two reasons. First, many important applications (for example the signal processing methods mentioned above) feature pencils where one or both of the matrices involved is singular. Even when this approach would be viable, numerical stability concerns prompt us to avoid taking inverses if possible. We comment more on this in Section 1.5. Going forward, we will only consider approaches that work with both  $A$  and  $B$  rather than  $B^{-1}A$ .

The most ubiquitous method for solving the generalized eigenvalue problem is the QZ algorithm of Moler and Stewart [41], which obtains generalized eigenvalues and eigenvectors of  $(A, B)$  by first producing its generalized Schur form via implicit application of shifted QR to  $AB^{-1}$ . A significant amount of research has focused on exploring the performance of this approach as well as developing a variety of extensions [36, 56, 57]. The main drawback to QZ is its relative difficulty to parallelize. Efforts to do so [1] require a non-trivial reworking of the numerical details and to our knowledge are not widely used. Methods for extracting only a certain subset of generalized eigenvalues/eigenvectors for sparse problems include the trace minimization algorithm [46], projection methods [45], and extensions of the Lanczos procedure [22].

In this paper, we present a new, naturally parallelizable method that, given any matrix pencil  $(A, B)$ , constructs a full set of approximate generalized eigenvalues and eigenvectors. For simplicity, we will drop the label “generalized” in the subsequent sections and simply refer to eigenvalues and eigenvectors of  $(A, B)$ .

## 1.2 Divide-and-Conquer Eigensolvers

To construct an easily parallelizable method, we employ a divide-and-conquer strategy that recursively splits the original problem  $(A, B)$  into smaller ones with disjoint spectra. By ensuring that these subproblems share no eigenvalues (and therefore have no overlapping eigenspaces), we can handle them in parallel. Moreover, as long as the spectrum of each subproblem is contained in its predecessor’s, we can reconstruct a set of eigenvalues/eigenvectors for  $(A, B)$  from those of the smallest subproblems, which are either  $1 \times 1$  and therefore trivial or small enough to handle with existing techniques. One step of divide-and-conquer consists of the following:

1. Divide the eigenvalues into two disjoint sets (opposite sides of a line, inside/outside a circle, etc.).

2. Compute unitary projectors onto the corresponding eigenspaces.
3. Apply the projectors to the original problem, splitting it in two.

Note that if we are able to consistently split the eigenvalues into sets of roughly equal size, only  $O(\log(n))$  steps of divide-and-conquer are required to find a full set of eigenvalues/eigenvectors.

Parallel divide-and-conquer methods for eigenvalue problems have a rich history in the literature. Early approaches for dense matrices emerged following work of Beavers and Denman [12], which demonstrated that the matrix sign function of Roberts [42] could be used to compute projectors onto certain eigenspaces. While it is possible to adapt the sign function for the generalized eigenvalue problem [26], it requires taking inverses which, as mentioned above, we'd prefer to avoid. An alternative, inverse-free method was outlined by Malyshev [39] and subsequently explored, for both pencils and individual matrices, in work of Bai, Demmel, and Gu [5]. In this approach, spectral projectors are approximated by repeatedly and implicitly squaring  $A^{-1}B$ , where eigenvalues are split by the unit circle.

The requirement to have unitary projectors in each step of divide-and-conquer is non-trivial. In fact, neither the sign function nor the inverse-free, repeated squaring approach of Malyshev produce explicitly unitary projectors; instead, rank-revealing factorizations are applied to guarantee a unitary result. The rank-revealing aspect is important here, as the rank of each projector tells us how many eigenvalues lie in a corresponding region of the complex plane. While there are many ways to compute a rank-revealing factorization [14, 28, 50], we are particularly interested in a randomized, rank-revealing URV factorization introduced by Demmel, Dumitriu, and Holtz [17] and later generalized by Ballard, Demmel, and Dumitriu [6].

The method we present combines this randomized, rank-revealing factorization with the inverse-free approach of Malyshev. A technical report of Ballard, Demmel, and Dumitriu [6] already explored this combination, though it left one fundamental question unanswered: how do we reliably split the spectrum at each step? The importance of this cannot be understated, as divide-and-conquer can only hope to be efficient if the split is significant (i.e., close to 50/50) at each step. And while we might hope that randomly selecting a dividing line/circle may work with high probability, the method will fail if whatever we choose intersects the spectrum or even pseudospectrum. Our most important contribution, we resolve this problem by adapting recent work of Banks et al. [9], demonstrating that by adding a bit of randomness to the problem we can state the inverse-free procedure in a way that succeeds with high probability.

### 1.3 Pseudospectra and Random Matrix Theory

The pseudospectrum of a matrix or matrix pencil consists of all eigenvalues of nearby matrices/pencils. We will define them precisely in Section 2.2, but for now we can think of the  $\epsilon$ -pseudospectrum as containing the eigenvalues of matrices or pencils that are, in a matrix-norm sense,  $\epsilon$ -away. In general, each pseudospectrum consists of connected components in  $\mathbb{C}$  containing at least one true eigenvalue, to which they collapse as  $\epsilon \rightarrow 0$ . For more background, see the standard reference [54].

Looking toward finite arithmetic implementations where error may accumulate at each step, we expect that divide-and-conquer eigensolvers are most likely to fail when the  $\epsilon$ -pseudospectra for small  $\epsilon$  (say close to machine precision) cover large areas of the complex plane, in which case it becomes difficult to select a dividing line/circle that will significantly split the spectrum without causing the process to break down. This is particularly important for matrix pencils, since infinite eigenvalues are a possibility.

To work around this, our algorithm begins by adding small perturbations to the input matrices, swapping the pencil  $(A, B)$  for  $(\tilde{A}, \tilde{B}) = (A + \gamma G_1, B + \gamma G_2)$ , where  $\gamma$  is a tuning parameter and  $G_1$  and  $G_2$  are independent, complex Ginibre random matrices – i.e., matrices whose entries are independent and identically distributed (i.i.d.) standard complex Gaussian with mean zero and variance  $1/n$ . It is well-known that random matrices with i.i.d. entries have a number of useful properties [4, 18, 19]; not only are they almost surely invertible, but in many cases distributions for their smallest singular values are known [44, 53]. The perturbation applied to  $(A, B)$  leverages these properties to regularize the problem, replacing what could be a poorly-conditioned or singular input pencil with one whose eigenvalue problem is well-behaved (in a way to be defined precisely later).

The concept of using a random perturbation to regularize a matrix – considered a linear algebra extension of smoothed analysis – has been well-studied [2, 23, 47]. Of particular relevance here, Banks et al. [10] showed that adding a Ginibre perturbation to a matrix provides a probabilistic bound on its smallest singular value

while also controlling its eigenvector condition number. In a subsequent work [9] they demonstrated that these perturbations also regularize  $\epsilon$ -pseudospectra, breaking them into small connected components around distinct eigenvalues. Banks et al. used this phenomena, referred to as *pseudospectral shattering*, as the basis for a divide-and-conquer eigensolver, which proceeds as follows:

1. Perturb the input matrix, shattering its pseudospectra into distinct components.
2. Construct a random grid that contains the spectrum of the matrix. Shattering implies that a fine enough grid does not intersect them, and each eigenvalue of the perturbed matrix is contained in a unique grid box with high probability.
3. Run divide-and-conquer (using the sign function), each time splitting the eigenvalues by a grid line.

This rough outline obscures the numerical details but captures the core idea: by perturbing, we obtain a matrix whose pseudospectra are sufficiently well-behaved for divide-and-conquer to succeed using a simple random grid.

We generalize these results here, proving our own version of pseudospectral shattering for matrix pencils and using it to complete the divide-and-conquer algorithm originally posed by Ballard, Demmel, and Dumitriu [6]. This is not the first approach that solves the generalized eigenvalue problem by perturbing the input matrices. A method of Hochstenbach, Mehl, and Plestenjak [33], for example, finds the eigenvalues of a singular pencil via QZ by first applying rank-completing perturbations. Note that because our perturbations are random, and because we use a random rank-revealing factorization, convergence is only available with high probability.

## 1.4 Matrix Pencil Diagonalization

Another consequence of the perturbation is that only backward error accuracy guarantees are available. Given an input  $(A, B)$ , the eigensolver we present produces approximations of the eigenvalues/eigenvectors of the nearby pencil  $(\tilde{A}, \tilde{B})$ . While perturbation results for the generalized eigenvalue problem are well-developed in the literature, see for example [51, §VI], little can be said about the accuracy of an individual eigenvalue or eigenvector found this way in the absence of additional, expensive information like a condition number. That is, the eigenvalues of  $(\tilde{A}, \tilde{B})$  may vary significantly from those of  $(A, B)$  even when  $\|A - \tilde{A}\|_2$  and  $\|B - \tilde{B}\|_2$  are small. Take the following  $2 \times 2$  matrices as an example:

$$A = B = \begin{pmatrix} 1 & 0 \\ 0 & 10^{-10} \end{pmatrix}, \quad \tilde{A} = \begin{pmatrix} 1 & 0 \\ 0 & 1.5 \times 10^{-10} \end{pmatrix}, \quad \tilde{B} = \begin{pmatrix} 1 & 0 \\ 0 & 5 \times 10^{-11} \end{pmatrix}. \quad (1.4.1)$$

By construction,  $\|A - \tilde{A}\|_2 = \|B - \tilde{B}\|_2 = 5 \times 10^{-11}$  while  $\Lambda(A, B) = \{1\}$  and  $\Lambda(\tilde{A}, \tilde{B}) = \{1, 3\}$ ; a tiny perturbation in  $A$  and  $B$  results in macroscopic changes to the eigenvalues. This is a consequence of the instability of the second eigenvalue of  $(A, B)$ , which itself is due to the near singularity of  $B$ . Guarantees are even worse when the matrix  $B$  is actually singular. In particular, our algorithm always produces a set of finite eigenvalues, even though the input pencil may have one or many eigenvalues at infinity.

With this in mind, we consider the related problem of joint diagonalization. A pair of nonsingular matrices  $S$  and  $T$  jointly diagonalize  $A$  and  $B$ , or equivalently diagonalize the pencil  $(A, B)$ , if  $S^{-1}AT$  and  $S^{-1}BT$  are both diagonal. The connection to the generalized eigenvalue problem is fairly straightforward, as the pencils  $(A, B)$  and  $(S^{-1}AT, S^{-1}BT)$  have the same set of eigenvalues. Moreover any regular matrix pencil with distinct eigenvalues can be diagonalized by matrices  $S$  and  $T$  containing its left and right eigenvectors respectively [51, §VI Corollary 1.12].

It is in this context that our method produces provably accurate results, in a backward error sense, regardless of the input pencil  $(A, B)$ . The main result of the paper (presented technically as [Theorem 5.1](#) and [Proposition 5.3](#) below) may be summarized as follows:

**Theorem 1.1.** *There exists an exact arithmetic, inverse-free, and randomized algorithm that for any matrix pencil  $(A, B)$  with  $A, B \in \mathbb{C}^{n \times n}$  and any accuracy  $\epsilon < 1$  produces in nearly matrix multiplication time nonsingular matrices  $S, T$  and a diagonal matrix  $D$  such that*

$$\|A - S D T^{-1}\|_2 \leq \epsilon \quad \text{and} \quad \|B - S I T^{-1}\|_2 \leq \epsilon$$

*with probability at least  $1 - O(\frac{1}{n})$ .*

As we will see, this result provides forward error guarantees on approximate eigenvalues and eigenvectors in certain cases ([Theorem 5.2](#)).

## 1.5 Complexity and Numerical Stability

In [Theorem 1.1](#) above, “in nearly matrix multiplication time” means the asymptotic complexity of the algorithm is the same as the complexity of matrix multiplication,  $T_{\text{MM}}(n)$ , up to  $\log(n)$  factors. This is accomplished by showing that (1) one step of divide-and-conquer runs in nearly matrix multiplication time, and (2) that only  $O(\log(n))$  steps are needed to obtain the approximate diagonalization. As alluded to earlier, (2) is guaranteed as long as the eigenvalue split at each step is significant. Claim (1), meanwhile, stems from using only QR and matrix multiplication, both of which can be implemented stably in  $O(T_{\text{MM}}(n))$  operations (see work of Demmel, Dumitriu, and Holtz [[17](#)]). In fact, matrix multiplication and QR have  $O(T_{\text{MM}}(n))$  implementations that are respectively forward and backwards stable – i.e., the relative forward/backward error is bounded by machine precision  $\mathbf{u}$  times an appropriate condition number.

This combination of efficiency and stability is our motivation for stating an inverse-free approach. While it is possible to invert a matrix in  $O(T_{\text{MM}}(n))$  operations, such implementations are only logarithmically stable [[17](#), §3], meaning a polylogarithmic increase in precision is required to obtain the same error as a truly backward stable version. Accordingly, the pseudospectral method of Banks et al., which requires inversion to compute the sign function, is built on a logarithmically stable black-box inversion algorithm [[9](#), Definition 2.7]. This lack of stability carries over into their finite arithmetic analysis, which yields a slightly weaker-than-logarithmic stability guarantee for the divide-and-conquer routine as a whole.

We do not state any results in finite arithmetic in this paper (though we do outline some progress in that direction in [Appendix B](#)). Nevertheless, we anticipate that the inverse-free approach presented here can produce a logarithmically stable method for computing an approximate diagonalization of any pencil or matrix. In this way, we position our work as not only a generalization of the algorithm of Banks et al. but also as a more stable alternative for the single-matrix case. Echoing Bai, Demmel, and Gu [[5](#)], we may even consider the two methods as a multi-step approach to the problem; since the sign function version is likely to be faster, we could first attempt to form  $B^{-1}A$  or  $A^{-1}B$  and apply the algorithm of Banks et al. before defaulting to ours.

Up to this point, efficiency has been characterized by the number of arithmetic operations being performed. Alternatively, we could focus on communication costs, both between multiple processors and/or between levels of memory hierarchy. This is especially relevant for the algorithm presented here, which is highly parallel and primed for memory-constrained applications; in particular, divide-and-conquer can be used to reduce a problem to fit in available fast memory if necessary. With this in mind, we may consider a communication optimal implementation in the vein of Ballard et al. [[8](#)]. In fact, the variant of our approach presented by Ballard, Demmel, and Dumitriu [[6](#)] was shown to achieve asymptotic communication lower bounds for  $O(n^3)$  eigensolvers. While we won’t analyze in detail the communication costs of our algorithm, we mention this here to emphasize the flexibility of the high level strategy: the method may be easily reformulated to minimize communication costs if desired.

## 1.6 Outline

To improve readability, we summarize the main contributions of each of the remaining sections here.

1. In [Section 2](#), we define the pseudospectrum of a matrix pencil and explore some of its properties, culminating in our version of Bauer-Fike [[11](#)] for pencil pseudospectra ([Theorem 2.20](#)).
2. In [Section 3](#), we prove pseudospectral shattering for matrix pencils ([Theorem 3.11](#)). The proof presented is a fairly straightforward generalization of the single-matrix case done by Banks et al. [[9](#)].
3. In [Section 4](#), we state our divide-and-conquer eigensolver and prove that it succeeds with high probability in exact arithmetic ([Theorem 4.8](#)).
4. In [Section 5](#), we use the eigensolver to construct an algorithm that produces an accurate diagonalization of any matrix pencil with high probability, thereby proving [Theorem 1.1](#).

5. In [Section 6](#) we present a handful of numerical experiments to demonstrate that the algorithm works in finite arithmetic.
6. Finally in the appendices, we consider alternative versions of Bauer-Fike for matrix pencils ([Appendix A](#)) and discuss progress towards a finite arithmetic analysis of the algorithm ([Appendix B](#)).

## 2 Background

### 2.1 Matrix Pencils, Eigenvalues, and Eigenvectors

In this section, we review necessary background information from linear algebra as presented in the standard references [\[34, 51\]](#). Here and in the subsequent sections,  $\|\cdot\|_2$  is the  $L_2$  or operator norm,  $A^H$  and  $A^{-H}$  denote the Hermitian transpose and inverse Hermitian transpose of  $A$  respectively, and  $\kappa(A)$  is the  $L_2$  condition number of  $A$ . Throughout,  $(A, B)$  is a matrix pencil with  $A, B \in \mathbb{C}^{n \times n}$ ,  $\Lambda(A)$  and  $\Lambda(A, B)$  denote the spectra of  $A$  and  $(A, B)$  respectively, and  $\rho(A)$  is the spectral radius. We assume familiarity with the basic definitions of the single-matrix eigenvalue problem.

**Definition 2.1.** The matrix pencil  $(A, B)$  is regular if its characteristic polynomial  $\det(A - \lambda B)$  is not identically zero. If  $(A, B)$  is not regular, it is singular.

The distinction between regular and singular pencils is fundamental: only in the regular case does any solution to [\(1.1.1\)](#) correspond to an eigenvalue and eigenvector of the pencil.

**Definition 2.2.** A nonzero vector  $v \in \mathbb{C}^n$  is a right eigenvector of a regular pencil  $(A, B)$  if  $Av = \lambda Bv$  for some  $\lambda \in \mathbb{C}$ . In this case, the eigenvalue  $\lambda$  is a root of the characteristic polynomial  $\det(A - \lambda B)$  and  $(\lambda, v)$  is an eigenpair of  $(A, B)$ . Similarly, a nonzero vector  $w$  is a left eigenvector of  $(A, B)$  if  $w^H A = \lambda w^H B$ .

Technically, [Definition 2.2](#) only defines finite eigenpairs of a regular pencil; missing are the infinite eigenvalues that correspond to nontrivial vectors in the null space of  $B$ , which in some sense formally satisfy  $\frac{1}{\lambda}Av = Bv$  (though of course infinity cannot be a root of the characteristic polynomial). Ultimately, eigenvectors with infinite eigenvalues are included for completeness: since the characteristic polynomial of  $(A, B)$  has degree less than  $n$  if  $B$  is singular, we only obtain a full set of  $n$  eigenvalues for regular pencils if we include those at infinity. As is standard, we will use “eigenvector” to refer to right eigenvectors unless stated otherwise.

For singular  $(A, B)$ , [Definition 2.2](#) would imply that every complex number is an eigenvalue. While it would be convenient to stick with this definition or simply not define eigenvalues in this case, doing so would miss interesting and (depending on the application) important information. In particular, a pencil  $(A, B)$  with overlapping null spaces may have a nonzero pair  $(\lambda, v)$  such that  $Av = \lambda Bv$  while  $Av \neq 0$  and  $Bv \neq 0$ . In other words, a singular pencil can have eigenvalues as in the regular case, though [Definition 2.2](#) cannot differentiate them from the trivial “eigenvalues” created by the singularity of the pencil. With this in mind, we have a separate definition<sup>1</sup> for the eigenvalues and eigenvectors of singular pencils.

**Definition 2.3.** Let  $(A, B)$  be a singular pencil and let  $r$  be the rank of  $(A - xB)$  over the field of fractions of  $\mathbb{C}[x]$ . Then  $\lambda$  is a finite eigenvalue of  $(A, B)$  if  $\text{rank}(A - \lambda B) < r$ . Meanwhile, the vector  $v$  is a corresponding right eigenvector if  $Av = \lambda Bv$  with  $Bv \neq 0$  and the row vector  $w$  is a left eigenvector if  $wA = \lambda wB$  with  $wB \neq 0$ .

As in the regular case, a singular pencil can have eigenvalues at infinity, which occur when  $\text{rank}(B) < r$ . While we are primarily focused on finding the eigenvalues of regular pencils, we would still like to recover those of a singular pencil if possible, and we comment on the challenges of doing so in the subsequent sections.

Throughout, we are interested in factorizations of  $A$  and  $B$  that reveal the eigenvalues of  $(A, B)$ . First, we consider a generalization of Schur form [\[51, §I\]](#) to matrix pencils.

---

<sup>1</sup>[Definition 2.3](#) can also be used to define the finite eigenvalues of regular pencils, and in that case is equivalent to [Definition 2.2](#) since  $r = n$ . We choose to state [Definition 2.2](#) for regular pencils since it follows more intuitively from the single-matrix eigenvalue problem. We note also that the more general definition is required to define the Kronecker canonical form [\[37\]](#), which is a generalization of Jordan form to pencils.



**Definition 2.4.**  $(A, B) = (UT_A V^H, UT_B V^H)$  is a generalized Schur form of  $(A, B)$  if  $U, V \in \mathbb{C}^{n \times n}$  are unitary and  $T_A$  and  $T_B$  are upper triangular.

$(A, B)$  and its Schur form are equivalent, meaning they have the same set of eigenvalues. Moreover, the eigenvalues of  $(A, B)$  are given by  $\frac{T_A(i, i)}{T_B(i, i)}$ , where zeros on the diagonal of  $T_B$  correspond to eigenvalues at infinity. It is not hard to show that every regular matrix pencil has a Schur form (see for example [51, §VI Theorem 1.9]).

Just as in the single-matrix case, we can build a Schur decomposition by constructing  $V$  so that any leading set of columns is an orthonormal basis for a space spanned by a collection of right eigenvectors of  $(A, B)$ . In fact, the columns of  $V$  span right deflating subspaces for the pencil.

**Definition 2.5.** Subspaces  $\mathcal{X}, \mathcal{Y} \subseteq \mathbb{C}^n$  are right and left deflating subspaces of  $(A, B)$  respectively if  $\dim(\mathcal{X}) = \dim(\mathcal{Y})$  and  $\text{span}\{Ax, Bx : x \in \mathcal{X}\} = \mathcal{Y}$ .

The right and left deflating subspaces of a pencil generalize the invariant eigenspaces of an individual matrix. That is, a collection of eigenvectors of  $(A, B)$  span a right deflating subspace, which, as long as the pencil is regular, are “mapped” to a corresponding left deflating subspace. Despite the similarity in naming, the left deflating subspace of  $(A, B)$  corresponding to a set of right eigenvectors is not usually spanned by left eigenvectors.

Note that if  $(A, B) = (UT_A V^H, UT_B V^H)$  is the Schur form of a regular pencil then the first  $k$  columns of  $U$  span the left deflating subspace corresponding to the first  $k$  columns of  $V$  (this follows from  $AV = UT_A$  and  $BV = UT_B$  since  $T_A$  and  $T_B$  cannot both have a zero in the same diagonal entry). Moreover, if we take the first  $k$  columns of  $U$  as a right deflating subspace of  $(A^H, B^H)$  then the first  $k$  columns of  $V$  span the corresponding left deflating subspace since  $A^H U = VT_A^H$  and  $B^H U = VT_B^H$ . In this way, taking a Hermitian transpose swaps left and right deflating subspaces.

Moving beyond Schur form, we next generalize diagonalization to pencils.

**Definition 2.6.** Nonsingular matrices  $S$  and  $T$  diagonalize  $(A, B)$  if  $S^{-1}AT = D_1$  and  $S^{-1}BT = D_2$  are both diagonal.

Once again,  $(A, B)$  and its diagonalization  $(D_1, D_2)$  have the same set of eigenvalues with infinite eigenvalues corresponding to zeros on the diagonal of  $D_2$ . When  $(A, B)$  is regular, the columns of  $T$  and rows of  $S^{-1}$  contain right and left eigenvectors of  $(A, B)$ .

As in the single-matrix problem, not every pencil is diagonalizable. Instead, the diagonalization given in Definition 2.6 is a special case of the Kronecker canonical form [37], which generalizes Jordan form to matrix pencils. Of particular use here, note that if  $B$  is invertible and  $T$  contains right eigenvectors of  $(A, B)$  then  $S = BT$  produces a diagonalization with  $D_2 = I$ .

To prove pseudospectral shattering in Section 3, we will need the following definitions related to the eigenvalues/eigenvectors of an individual matrix. While each of these generalizes to pencils in a fairly straightforward way, we state them first for the single-matrix case to match how they are used in the analysis to come.

**Definition 2.7.** The eigenvector condition number of a diagonalizable matrix  $M$  is  $\kappa_V(M) = \inf_V \kappa(V)$ , where the infimum is taken over nonsingular matrices  $V$  that diagonalize  $M$ .

**Definition 2.8.** Let  $\lambda_1(M), \dots, \lambda_n(M)$  be the eigenvalues of  $M$  repeated according to multiplicity. The eigenvalue gap of  $M$  is  $\text{gap}(M) = \min_{i \neq j} |\lambda_i(M) - \lambda_j(M)|$ .

Under the right conditions, we can also define a condition number for each eigenvalue of a diagonalizable matrix.

**Definition 2.9.** If  $\lambda_i$  is an eigenvalue of a matrix  $M$  with distinct eigenvalues and  $v_i$  and  $w_i$  are right and left eigenvectors corresponding to  $\lambda_i$  normalized so that  $w_i^H v_i = 1$ , then the condition number of  $\lambda_i$  is

$$\kappa(\lambda_i) = \|v_i w_i^H\|_2 = \|v_i\|_2 \|w_i\|_2$$

Together, the eigenvector/eigenvalue condition numbers and the eigenvalue gap give an indication of how well-behaved a matrix’s eigenvalue problem is. To generalize this to the eigenvalues/eigenvectors of a matrix pencil, we can adapt  $\kappa_V(M)$  and  $\text{gap}(M)$  to  $(A, B)$  as follows.



**Definition 2.10.** The right eigenvector condition number of diagonalizable  $(A, B)$  is  $\kappa_V(A, B) = \inf_T \kappa(T)$ , where the infimum is taken over all invertible  $T$  containing a full set of right eigenvectors of  $(A, B)$ .

Though  $\kappa_V(A, B)$  depends only on the right eigenvectors, we will refer to it as simply the eigenvector condition number going forward.

**Definition 2.11.** Let  $\lambda_1(A, B), \dots, \lambda_n(A, B)$  be the eigenvalues of  $(A, B)$  repeated according to multiplicity. The eigenvalue gap of  $(A, B)$  is  $\text{gap}(A, B) = \min_{i \neq j} |\lambda_i(A, B) - \lambda_j(A, B)|$ .

Of course, these definitions are not the only possible condition numbers for generalized eigenvalues/eigenvectors [3, 31]. We justify our choice in Section 5.1, where we show that a backward error diagonalization of a suitably well-behaved pencil provides forward error approximations of its eigenvalues and eigenvectors in terms of  $\kappa_V(A, B)$  and  $\text{gap}(A, B)$  (Theorem 5.2). Note that when  $B$  is invertible,  $\kappa_V(A, B) = \kappa_V(B^{-1}A)$  and  $\text{gap}(A, B) = \text{gap}(B^{-1}A)$ .

Finally, we consider an important building block of divide-and-conquer eigensolvers: spectral projectors.

**Definition 2.12.**  $P$  is a spectral projector of  $M$  if  $P^2 = P$  and  $MP = PM$ .

The simplest spectral projector is  $vw^H$  for  $v$  and  $w$  right and left eigenvectors of  $M$  corresponding to the same eigenvalue  $\lambda$  and scaled so that  $w^H v = 1$ . In this case, we have by Cauchy's integral formula

$$vw^H = \frac{1}{2\pi i} \oint_{\Gamma} (z - M)^{-1} dz \quad (2.1.1)$$

for  $\Gamma$  any closed, rectifiable curve that separates  $\lambda$  from the rest of the spectrum of  $M$ . More generally, any spectral projector can be expressed as

$$P = V \begin{pmatrix} I_k & 0 \\ 0 & 0 \end{pmatrix} V^{-1} \quad (2.1.2)$$

for  $V$  a matrix containing the right eigenvectors of  $M$ , again appropriately scaled.

As mentioned above, an important component of any divide-and-conquer eigensolver is approximating spectral projectors onto certain sets of eigenvectors. For our purposes, since  $(A, B)$  and  $B^{-1}A$  have the same eigenvectors if  $B$  is nonsingular, it will be sufficient to approximate the spectral projectors for  $B^{-1}A$  without explicitly forming it.

To wrap up this section, we state a few general linear algebra results/facts that will be useful later on. First is the stability of singular values, which follows from Weyl's inequality [51, §IV Corollary 4.9]

**Lemma 2.13** (Stability of Singular Values). *For  $M_1, M_2 \in \mathbb{C}^{n \times n}$ ,*

$$|\sigma_i(M_1) - \sigma_i(M_2)| \leq \|M_1 - M_2\|_2$$

*for all  $1 \leq i \leq n$ .*

Second, we note that the matrix  $L_2$ -norm is often generalized to pencils by setting  $\|(A, B)\|_2$  equal to the  $L_2$ -norm of the  $n \times 2n$  matrix obtained by concatenating  $A$  and  $B$ . Throughout we use the loose upper bound  $\|(A, B)\|_2 \leq \|A\|_2 + \|B\|_2$ .

## 2.2 Pseudospectra

In this section, we define pseudospectra for both individual matrices and matrix pencils. We start with the single matrix case, where the definition is standard.

**Definition 2.14.** For any  $\epsilon > 0$ , the  $\epsilon$ -pseudospectrum of  $M$  is

$$\Lambda_\epsilon(M) = \{z : \text{there exists } u \neq 0 \text{ with } (M + E)u = zu \text{ for some } \|E\|_2 \leq \epsilon\}.$$

Each pseudospectrum  $\Lambda_\epsilon(M)$  consists of connected components in  $\mathbb{C}$  containing at least one eigenvalue of  $M$ . As  $\epsilon \rightarrow 0$  these connected components collapse to the true eigenvalues of the matrix. If  $M$  is diagonalizable, we can quantify this explicitly via the Bauer-Fike Theorem [11].

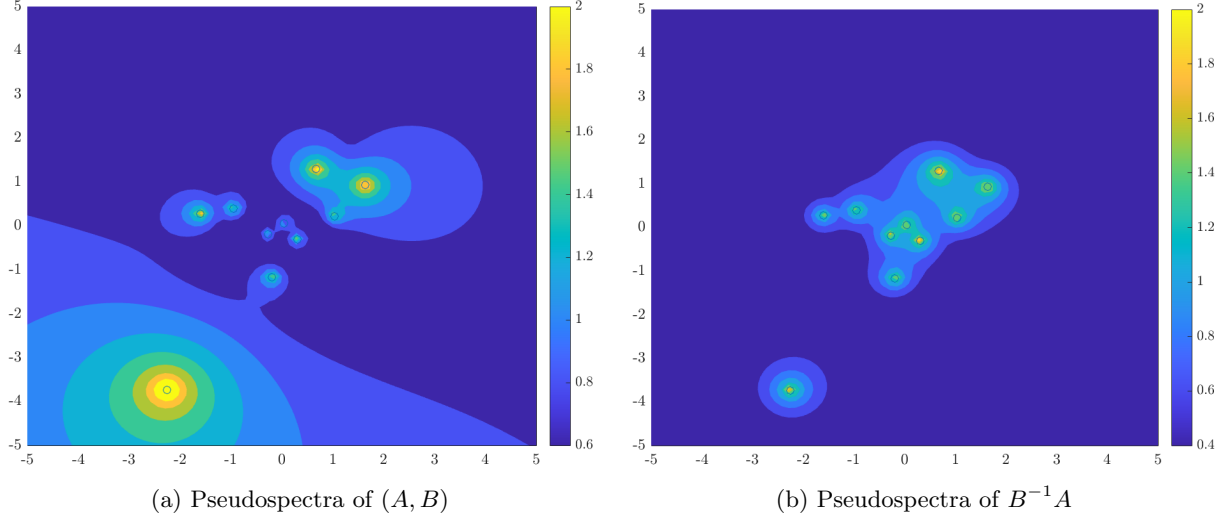


Figure 1: Pseudospectra of  $(A, B)$  and  $B^{-1}A$  for Gaussian  $A, B \in \mathbb{C}^{10 \times 10}$  following Definition 2.16 and Definition 2.14 respectively. Eigenvalues are plotted with open circles. Pseudospectra were obtained by graphing the level curves of  $\log_{10} [(1 + |z|) \|(A - zB)^{-1}\|_2]$  and  $\log_{10} [\|(B^{-1}A - zI)^{-1}\|_2]$  in Matlab R2023a.

**Theorem 2.15** (Bauer-Fike). *If  $\lambda_1, \dots, \lambda_n$  are the eigenvalues of  $M \in \mathbb{C}^{n \times n}$  and  $V$  is any invertible matrix that diagonalizes  $M$ , then*

$$\bigcup_{i=1}^m B_\epsilon(\lambda_i) \subseteq \Lambda_\epsilon(M) \subseteq \bigcup_{i=1}^m B_{\epsilon \kappa(V)}(\lambda_i)$$

where  $B_r(z)$  is the ball of radius  $r$  centered at  $z$ .

To extend this to matrix pencils, we must first decide how to define  $\Lambda_\epsilon(A, B)$  – the  $\epsilon$ -pseudospectrum of a pencil  $(A, B)$ . Unlike the single matrix case there is no standard choice here (see Trefethen and Embree [54, §45] for a discussion of various options). In this paper, we follow a definition originally due to Frayssé et al. [25].

**Definition 2.16.** For any  $\epsilon > 0$ , the  $\epsilon$ -pseudospectrum of  $(A, B)$  is

$$\Lambda_\epsilon(A, B) = \{z : \text{there exists } u \neq 0 \text{ with } (A + \Delta A)u = z(B + \Delta B)u \text{ for some } \|\Delta A\|_2, \|\Delta B\|_2 \leq \epsilon\}.$$

Figure 1 plots the pseudospectra of  $(A, B)$  and  $B^{-1}A$  for one (randomly chosen) pair  $A, B \in \mathbb{C}^{10 \times 10}$ . Clearly, the pseudospectra of  $(A, B)$  and  $B^{-1}A$  as defined above differ significantly. Informally, we might say that the pseudospectra of  $(A, B)$  are less well-behaved than those of  $B^{-1}A$ , despite the fact that both coalesce around the same set of eigenvalues.

In their paper Frayssé et al. provide several equivalent ways to state Definition 2.16, which we will use throughout when convenient.

**Theorem 2.17** (Frayssé et al. 1996). *The following are equivalent:*

1.  $z \in \Lambda_\epsilon(A, B)$ .
2. There exists a unit vector  $u$  such that  $\|(A - zB)u\|_2 \leq \epsilon(1 + |z|)$ .
3.  $\|(A - zB)^{-1}\|_2 \geq \frac{1}{\epsilon(1 + |z|)}$ .
4.  $\sigma_n(A - zB) \leq \epsilon(1 + |z|)$ .

In the remainder of this section, we pursue bounds on  $\Lambda_\epsilon(A, B)$ . Recalling that  $(A, B)$  has an eigenvalue at infinity whenever  $B$  is singular, we first show that such a bound can only exist for  $\epsilon < \sigma_n(B)$ .

**Lemma 2.18.**  $\Lambda_\epsilon(A, B)$  is bounded if and only if  $\epsilon < \sigma_n(B)$ .

*Proof.* Let  $\epsilon < \sigma_n(B)$  and suppose  $\Lambda_\epsilon(A, B)$  is unbounded. By [Theorem 2.17](#), any nonzero  $z \in \Lambda_\epsilon(A, B)$  satisfies

$$\frac{1}{\epsilon(1+|z|)} \leq \|(A - zB)^{-1}\|_2 = \frac{1}{|z|} \left\| \left( \frac{1}{z}A - B \right)^{-1} \right\|_2 \implies \frac{|z|}{\epsilon(1+|z|)} \leq \left\| \left( \frac{1}{z}A - B \right)^{-1} \right\|_2. \quad (2.2.1)$$

Since  $\Lambda_\epsilon(A, B)$  is unbounded, we can take a limit  $z \rightarrow \infty$  in this inequality to obtain

$$\frac{1}{\epsilon} \leq \|(-B)^{-1}\|_2 = \frac{1}{\sigma_n(B)}, \quad (2.2.2)$$

which implies  $\epsilon \geq \sigma_n(B)$ , a contradiction.

To prove the converse, suppose now  $\epsilon \geq \sigma_n(B)$  and let  $U\Sigma V^T$  be the singular value decomposition of  $B$ . If  $D \in \mathbb{C}^{n \times n}$  is a diagonal matrix with  $D_{ii} = 0$  for  $1 \leq i \leq n-1$  and  $D_{nn} = -\sigma_n(B)$ , then  $\|UDV^T\|_2 = \sigma_n(B) \leq \epsilon$  and therefore eigenvalues of  $(A, B + UDV^T)$  belong to  $\Lambda_\epsilon(A, B)$ . But by construction  $B + UDV^T$  is singular, which means  $(A, B + UDV^T)$  has an eigenvalue at infinity and therefore  $\Lambda_\epsilon(A, B)$  must be unbounded.  $\square$

We next derive an upper bound on  $\Lambda_\epsilon(A, B)$  when it exists. Keeping in mind that we plan to perturb our matrices, and will therefore have access to a lower bound on  $\|B^{-1}\|_2 = \sigma_n(B)$  with high probability, we prove the following lemma.

**Lemma 2.19.** If  $B$  is invertible and  $\epsilon < \sigma_n(B)$  then any  $z \in \Lambda_\epsilon(A, B)$  satisfies

$$|z| \leq \frac{\epsilon\|B^{-1}\|_2 + \|B^{-1}A\|_2}{1 - \epsilon\|B^{-1}\|_2}.$$

*Proof.* Suppose  $|z| > \|B^{-1}A\|_2$  and consider  $\frac{B^{-1}A}{z} - I$ . For any vector  $x$ ,

$$\left\| \frac{B^{-1}A}{z}x \right\|_2 \leq \frac{\|B^{-1}A\|_2}{|z|} \|x\|_2 \quad (2.2.3)$$

by matrix/vector norm compatibility, so

$$\|x\|_2 - \left\| \frac{B^{-1}A}{z}x \right\|_2 \geq \|x\|_2 - \frac{\|B^{-1}A\|_2}{|z|} \|x\|_2 \geq 0, \quad (2.2.4)$$

where we know  $\|x\|_2 - (\|B^{-1}A\|_2/|z|)\|x\|_2$  is positive since  $|z| > \|B^{-1}A\|_2$ . Thus, applying this result and the reverse triangle inequality,

$$\sigma_n\left(\frac{B^{-1}A}{z} - I\right) = \min_{\|x\|_2=1} \left\| \left( \frac{B^{-1}A}{z} - I \right) x \right\|_2 \geq \min_{\|x\|_2=1} \left[ \|x\|_2 - \frac{\|B^{-1}A\|_2}{|z|} \|x\|_2 \right] = 1 - \frac{\|B^{-1}A\|_2}{|z|} \quad (2.2.5)$$

and therefore

$$\left\| \left( \frac{B^{-1}A}{z} - I \right)^{-1} \right\|_2 = \frac{1}{\sigma_n\left(\frac{B^{-1}A}{z} - I\right)} \leq \frac{1}{1 - \frac{\|B^{-1}A\|_2}{|z|}}. \quad (2.2.6)$$

If  $z \in \Lambda_\epsilon(A, B)$ , we then have

$$\frac{1}{\epsilon(1+|z|)} \leq \frac{\|B^{-1}\|_2}{|z|} \left\| \left( \frac{B^{-1}A}{z} - I \right)^{-1} \right\|_2 \leq \frac{\|B^{-1}\|_2}{|z|} \frac{1}{1 - \frac{\|B^{-1}A\|_2}{|z|}} = \frac{\|B^{-1}\|_2}{|z| - \|B^{-1}A\|_2}, \quad (2.2.7)$$

which, rearranging to solve for  $|z|$ , is equivalent to

$$|z| \leq \frac{\epsilon\|B^{-1}\|_2 + \|B^{-1}A\|_2}{1 - \epsilon\|B^{-1}\|_2}. \quad (2.2.8)$$

Since we assumed  $|z| > \|B^{-1}A\|_2$ , we have proved that  $z \in \Lambda_\epsilon(A, B)$  for  $\epsilon < \sigma_n(B)$  implies

$$|z| \leq \max \left\{ \|B^{-1}A\|_2, \frac{\epsilon \|B^{-1}\|_2 + \|B^{-1}A\|_2}{1 - \epsilon \|B^{-1}\|_2} \right\} = \frac{\epsilon \|B^{-1}\|_2 + \|B^{-1}A\|_2}{1 - \epsilon \|B^{-1}\|_2} \quad (2.2.9)$$

which finishes the proof.  $\square$

While this gives a nice upper bound for the pseudospectrum as a whole, the upper bound in Bauer-Fike is in terms of balls around the eigenvalues. If we add an assumption that  $B^{-1}A$  is diagonalizable, we can convert the bound just obtained to a similar result, obtaining our version of Bauer-Fike for matrix pencils.

**Theorem 2.20** (Bauer-Fike for Matrix Pencils). *If  $\epsilon < \sigma_n(B)$  and  $B^{-1}A$  is diagonalizable with eigenvector matrix  $V$ , then  $\Lambda_\epsilon(A, B)$  is contained in the union of balls around the eigenvalues of  $(A, B)$  of radius*

$$r_\epsilon = \epsilon \kappa(V) \|B^{-1}\|_2 \left( 1 + \frac{\epsilon \|B^{-1}\|_2 + \|B^{-1}A\|_2}{1 - \epsilon \|B^{-1}\|_2} \right).$$

*Proof.* By [Theorem 2.17](#), we know any  $z \in \Lambda_\epsilon(A, B)$  satisfies

$$\frac{1}{\epsilon(1+|z|)} \leq \|(A - zB)^{-1}\|_2 \leq \|B^{-1}\|_2 \|(B^{-1}A - zI)^{-1}\|_2. \quad (2.2.10)$$

Applying the fact that  $V$  diagonalizes  $B^{-1}A$ , meaning  $B^{-1}A = V\Lambda V^{-1}$  for a diagonal matrix  $\Lambda$ , this expression becomes

$$\frac{1}{\epsilon(1+|z|)} \leq \|B^{-1}\|_2 \|(V\Lambda V^{-1} - zI)^{-1}\|_2 \leq \kappa(V) \|B^{-1}\|_2 \|(\Lambda - zI)^{-1}\|_2. \quad (2.2.11)$$

Inverting and rearranging, we then have

$$\sigma_n(\Lambda - zI) \leq \epsilon \kappa(V) \|B^{-1}\|_2 (1 + |z|). \quad (2.2.12)$$

Recalling that  $\Lambda$  has on its diagonal the eigenvalues of  $(A, B)$ , we complete the proof by noting

$$\sigma_n(\Lambda - zI) = \min_{\lambda_i \in \Lambda(A, B)} |\lambda_i - z| \quad (2.2.13)$$

and replacing  $|z|$  in [\(2.2.12\)](#) with the upper bound provided by [Lemma 2.19](#).  $\square$

[Theorem 2.20](#) is not the only version of Bauer-Fike derived for the generalized eigenvalue problem (see [Appendix A](#)). Nevertheless, it is useful here since it leverages the assumptions we'll have available to us in the following sections. In particular, the perturbations applied to  $(A, B)$  to obtain  $(\tilde{A}, \tilde{B})$  guarantee with high probability that  $\tilde{B}$  is nonsingular (with a lower bound on  $\sigma_n(\tilde{B})$  known) and that  $\tilde{B}^{-1}\tilde{A}$  is diagonalizable. In the next section, we use our version of Bauer-Fike to prove pseudospectral shattering for perturbed pencils.

### 3 Pseudospectral Shattering for Matrix Pencils

Following the convention used by Banks et al. [\[9\]](#), define a grid on the complex plane as follows.

**Definition 3.1.** The grid  $g = \text{grid}(z_0, \omega, s_1, s_2)$  is the boundary of a  $s_1 \times s_2$  lattice in the complex plane consisting of  $\omega \times \omega$ -sized squares with lower left corner  $z_0 \in \mathbb{C}$ . The grid lines of  $g$  are parallel to either the real or the complex axis.

In this section, we show that with high probability the  $\epsilon$ -pseudospectrum of a scaled and perturbed matrix pencil is shattered with respect to a random grid  $g$  (constructed according to [Definition 3.1](#)) for sufficiently small  $\epsilon$ , where shattering is defined as follows.

**Definition 3.2.**  $\Lambda_\epsilon(A, B)$  is shattered with respect to a grid  $g$  if  $\Lambda_\epsilon(A, B) \cap g = \emptyset$  and each eigenvalue of  $(A, B)$  is contained in a unique box of  $g$ .

Throughout, we consider perturbations made by Ginibre random matrices and therefore make use of results from random matrix theory for this ensemble.

**Definition 3.3.** A random matrix  $G \in \mathbb{C}^{n \times n}$  is Ginibre if its entries are i.i.d. with distribution  $\mathcal{N}_{\mathbb{C}}(0, \frac{1}{n})$ .

Note that  $\mathcal{N}_{\mathbb{C}}(0, \frac{1}{n})$  in Definition 3.3 is a complex normal distribution. In practice, we can construct a Ginibre matrix by drawing a complex Gaussian matrix and normalizing by  $\frac{1}{\sqrt{n}}$ .

For the remainder of this section, let  $(\tilde{A}, \tilde{B}) = (A + \gamma G_1, B + \gamma G_2)$  for  $G_1, G_2$  two independent, complex Ginibre matrices,  $0 < \gamma < \frac{1}{2}$ , and  $A, B \in \mathbb{C}^{n \times n}$  with  $\|A\|_2, \|B\|_2 \leq 1$ . The norm requirement here is applied to simplify the analysis and can be assumed without loss of generality since our input matrices can be normalized if necessary. We are interested in showing shattering for the pseudospectra of the scaled pencil  $(\tilde{A}, n^\alpha \tilde{B})$ , where  $\alpha$  is a positive constant. As we will see, the choice to scale  $\tilde{B}$  is required to obtain usable bounds on the locations of the eigenvalues of  $(\tilde{A}, n^\alpha \tilde{B})$ . Later on, we will comment on how this choice of scaling affects the results.

### 3.1 Preliminaries

We begin by discussing some singular value bounds that will be useful later. The first of these is a bound on the norm (i.e., largest singular value) of a complex Ginibre matrix due to Banks et al. [10].

**Lemma 3.4** (Banks et al. 2021). *For  $G$  an  $n \times n$  complex Ginibre matrix,  $\mathbb{P}[\|G\|_2 \geq 2\sqrt{n} + t] \leq 2e^{-nt^2}$ .*

The same paper also provides a lower tail bound on the smallest singular value of a matrix after it is perturbed by a Ginibre matrix.

**Lemma 3.5** (Banks et al. 2021). *Let  $G$  be an  $n \times n$  complex Ginibre matrix. Then for any  $M \in \mathbb{C}^{n \times n}$  and any choice of  $\gamma$  and  $t$ ,  $\mathbb{P}[\sigma_n(M + \gamma G) < t] \leq n^2 \frac{t^2}{\gamma^2}$ .*

These are the main results from random matrix theory that we will use. Note that Lemma 3.5 implies that  $\tilde{B}$  is almost surely invertible, meaning with probability one we may assume that  $\tilde{B}^{-1}$  exists. Moreover, Lemma 3.4 and Lemma 3.5 allow us to control the location of the eigenvalues of  $(\tilde{A}, n^\alpha \tilde{B})$  as follows.

**Lemma 3.6.** *The eigenvalues of  $(\tilde{A}, n^\alpha \tilde{B})$  are contained in  $D(0, 3)$  – the disk of radius three centered at the origin – with probability at least  $1 - \frac{n^{2-2\alpha}}{\gamma^2} - 2e^{-n}$ .*

*Proof.* Consider  $X = n^{-\alpha} \tilde{B}^{-1} \tilde{A}$ . Since  $X$  and  $(\tilde{A}, n^\alpha \tilde{B})$  have the same eigenvalues, it is sufficient to bound the probability that  $\Lambda(X)$  is not contained in  $D(0, 3)$ . To do this, we note

$$\rho(X) \leq \|X\|_2 = n^{-\alpha} \|\tilde{B}^{-1} \tilde{A}\|_2 \leq \frac{1}{n^\alpha \sigma_n(\tilde{B})} \|\tilde{A}\|_2 \leq \frac{1}{n^\alpha \sigma_n(\tilde{B})} (\|A\|_2 + \gamma \|G_1\|_2). \quad (3.1.1)$$

Now  $\|A\|_2 \leq 1$  so, conditioning on the event  $\|G_1\|_2 \leq 4$ , we have  $\|A + \gamma G_1\|_2 \leq 3$ . Thus, if  $\Lambda(X) \not\subseteq D(0, 3)$  and therefore  $\rho(X) > 3$ , we obtain  $n^\alpha \sigma_n(\tilde{B}) < 1$ . Consequently,

$$\mathbb{P}[\Lambda(X) \not\subseteq D(0, 3) \mid \|G_1\|_2 \leq 4] \leq \mathbb{P}[n^\alpha \sigma_n(\tilde{B}) < 1] \leq \frac{n^{2-2\alpha}}{\gamma^2}, \quad (3.1.2)$$

where the last inequality comes from Lemma 3.5. By Bayes' Theorem, we therefore have

$$\mathbb{P}[\Lambda(X) \not\subseteq D(0, 3), \|G_1\|_2 \leq 4] \leq \frac{n^{2-2\alpha}}{\gamma^2}. \quad (3.1.3)$$

At the same time, applying Lemma 3.4, we have

$$\mathbb{P}[\Lambda(X) \not\subseteq D(0, 3), \|G_1\|_2 > 4] \leq \mathbb{P}[\|G_1\|_2 > 4] \leq 2e^{-n(4-2\sqrt{2})^2} \leq 2e^{-n}. \quad (3.1.4)$$

Putting these two results together, we conclude

$$\mathbb{P}[\Lambda(X) \not\subseteq D(0, 3)] \leq \frac{n^{2-2\alpha}}{\gamma^2} + 2e^{-n} \quad (3.1.5)$$

which completes the proof.  $\square$

With this in place, we can now consider building our random grid  $g$  over  $D(0, 3)$  which (with an appropriate choice of  $\alpha$  and  $\gamma$ ) will contain every eigenvalue of  $(\tilde{A}, n^\alpha \tilde{B})$  with high probability. Given a grid box size  $\omega$ , we define the random grid  $g = \text{grid}(z, \omega, \lceil 8/\omega \rceil, \lceil 8/\omega \rceil)$  for  $z$  a point chosen uniformly at random from the square cornered at  $-4 - 4i$  of side length  $\omega$ . The construction here is somewhat arbitrary; for convenience we choose  $g$  so that it roughly covers the smallest box with integer side length that contains  $D(0, 3)$  (with some buffer space).

### 3.2 Multi-Parameter Tail Bound

As in the proof of [Lemma 3.6](#), let  $X = n^{-\alpha} \tilde{B}^{-1} \tilde{A}$ . The bulk of the proof of shattering in the following section rests on a multi-parameter tail bound on  $\kappa_V(X)$  and  $\text{gap}(X)$ , which we derive here.

We start with two intermediate results. The first concerns the second to last singular value of  $yI - X$  for  $y \in \mathbb{C}$ .

**Lemma 3.7.** *For any  $t > 0$  and any  $y \in \mathbb{C}$ ,*

$$\mathbb{P}[\sigma_{n-1}(yI - X) < t \mid \|G_2\|_2 \leq 4] \leq 4 \left( \frac{t(1 + 4\gamma)n^{\alpha+1}}{\gamma} \right)^8$$

*Proof.* We begin by rewriting  $yI - X$  as

$$yI - X = n^{-\alpha} \tilde{B}^{-1} \left( n^\alpha y \tilde{B} - A - \gamma G_1 \right). \quad (3.2.1)$$

Using standard singular value inequalities, we then have

$$\sigma_{n-1}(yI - X) \geq \sigma_n \left( n^{-\alpha} \tilde{B}^{-1} \right) \sigma_{n-1} \left( n^\alpha y \tilde{B} - A - \gamma G_1 \right). \quad (3.2.2)$$

Now conditioning on  $\|G_2\|_2 \leq 4$ , we have  $\|\tilde{B}\|_2 \leq 1 + 4\gamma$ . Thus,  $\sigma_n(n^{-\alpha} \tilde{B}^{-1}) \geq \frac{1}{n^\alpha(1+4\gamma)}$  and therefore

$$\sigma_{n-1}(yI - X) \geq \frac{1}{n^\alpha(1+4\gamma)} \sigma_{n-1} \left( n^\alpha y \tilde{B} - A - \gamma G_1 \right). \quad (3.2.3)$$

Consequently, we observe

$$\mathbb{P}[\sigma_{n-1}(yI - X) < t \mid \|G_2\|_2 \leq 4] \leq \mathbb{P} \left[ \sigma_{n-1} \left( n^\alpha y \tilde{B} - A - \gamma G_1 \right) < tn^\alpha(1+4\gamma) \right]. \quad (3.2.4)$$

Setting  $M = n^\alpha y \tilde{B} - A$  and applying [\[9, Corollary 3.3\]](#) (noting that  $M$  is independent of  $G_1$  and that  $G_1$  and  $-G_1$  have the same distribution) we have

$$\mathbb{P}[\sigma_{n-1}(yI - X) < t \mid \|G_2\|_2 \leq 4] \leq 4 \left( \frac{t(1 + 4\gamma)n^{\alpha+1}}{\gamma} \right)^8 \quad (3.2.5)$$

for any  $t > 0$ . □

Next, we show that given any measurable set  $S \subset \mathbb{C}$ , we can bound the expected value of  $\sum_{\lambda_i \in S} \kappa(\lambda_i)^2$ , where the sum is taken over eigenvalues of  $X$ . This gives us some control over  $\kappa_V(X)$ ; in particular, taking  $V$  to be the eigenvector matrix of  $X$  scaled so that each column is a unit vector, we observe

$$\kappa_V(X) \leq \kappa(V) \leq \|V\|_F \|V^{-1}\|_F \leq \sqrt{n \sum_{i=1}^n \kappa(\lambda_i)^2}. \quad (3.2.6)$$

Note that with probability one  $X$  has a full set of distinct eigenvalues and is therefore diagonalizable. The proof of this result follows closely a proof of Banks et al. for the single matrix case [\[10, Theorem 1.5\]](#).



**Lemma 3.8.** *Let  $\lambda_1, \dots, \lambda_n$  be the eigenvalues of  $X$ . For any measurable set  $S \subset \mathbb{C}$ ,*

$$\mathbb{E} \left[ \sum_{\lambda_i \in S} \kappa(\lambda_i)^2 \mid \|G_2\|_2 \leq 4 \right] \leq \left( \frac{(1+4\gamma)n^{\alpha+1}}{\gamma} \right)^2 \frac{\text{vol}(S)}{\pi}.$$

*Proof.* By Definition 2.14, we know for any  $z \in \mathbb{C}$

$$\mathbb{P}[z \in \Lambda_\epsilon(X)] = \mathbb{P}[\sigma_n(zI - X) < \epsilon]. \quad (3.2.7)$$

Following the same argument made in Lemma 3.7, swapping [9, Corollary 3.3] for Lemma 3.5, we therefore have

$$\mathbb{P}[z \in \Lambda_\epsilon(X) \mid \|G_2\|_2 \leq 4] \leq \left( \frac{\epsilon(1+4\gamma)n^{\alpha+1}}{\gamma} \right)^2. \quad (3.2.8)$$

Consider now the measurable set  $S \subset \mathbb{C}$ . Using (3.2.8), we observe

$$\begin{aligned} \mathbb{E}[\text{vol}(\Lambda_\epsilon(X) \cap S) \mid \|G_2\|_2 \leq 4] &= \mathbb{E} \left[ \int_S \mathbb{1}_{z \in \Lambda_\epsilon(X) \mid \|G_2\|_2 \leq 4} dz \right] \\ &= \int_S \mathbb{P}[z \in \Lambda_\epsilon(X) \mid \|G_2\|_2 \leq 4] dz \\ &\leq \left( \frac{\epsilon(1+4\gamma)n^{\alpha+1}}{\gamma} \right)^2 \text{vol}(S). \end{aligned} \quad (3.2.9)$$

Applying this result alongside [10, Lemma 3.2] and Fatou's Lemma for conditional expectation, we conclude

$$\begin{aligned} \mathbb{E} \left[ \sum_{\lambda_i \in S} \kappa(\lambda_i)^2 \mid \|G_2\|_2 \leq 4 \right] &= \mathbb{E} \left[ \liminf_{\epsilon \rightarrow 0} \frac{\text{vol}(\Lambda_\epsilon(X) \cap S)}{\pi \epsilon^2} \mid \|G_2\|_2 \leq 4 \right] \\ &\leq \liminf_{\epsilon \rightarrow 0} \frac{\mathbb{E}[\text{vol}(\Lambda_\epsilon(X) \cap S \mid \|G_2\|_2 \leq 4)]}{\pi \epsilon^2} \\ &\leq \left( \frac{(1+4\gamma)n^{\alpha+1}}{\gamma} \right)^2 \frac{\text{vol}(S)}{\pi}, \end{aligned} \quad (3.2.10)$$

which completes the proof.  $\square$

With these in place, we are now ready to prove the main multi-parameter tail bound. In this result, as in the previous two,  $X = n^{-\alpha} \tilde{B}^{-1} \tilde{A}$  for our perturbed pencil  $(\tilde{A}, \tilde{B})$ . Again, this follows closely the proof of an equivalent tail bound of Banks et al. [9, Theorem 3.6].

**Theorem 3.9.** *For any  $t, \delta > 0$ ,*

$$\mathbb{P}[\kappa_V(X) < t, \text{gap}(X) > \delta] \geq \left[ 1 - \frac{9(1+4\gamma)^2 n^{2\alpha+3}}{t^2 \gamma^2} - 1296 \delta^6 \left( \frac{t(1+4\gamma)n^{\alpha+1}}{\gamma} \right)^8 \right] \left[ 1 - \frac{n^{2-2\alpha}}{\gamma^2} - 4e^{-n} \right].$$

*Proof.* We condition on the events  $\|G_2\|_2 \leq 4$  and  $\Lambda_\epsilon(X) \subseteq D(0, 3)$ . Combining Lemma 3.4 and Lemma 3.6, we know these occur with probability at least  $1 - \frac{n^{2-2\alpha}}{\gamma^2} - 4e^{-n}$ . Define now the events:

- $E_{\text{gap}} = \{\text{gap}(X) < \delta\}$
- $E_\kappa = \{\kappa_V(X) > t\}$ .

We are interested in bounding the probability of  $E_{\text{gap}} \cup E_\kappa$ . To do this, we construct a minimal  $\frac{\delta}{2}$ -net  $\mathcal{N}$  covering  $D(0, 3)$ , which exists with  $|\mathcal{N}| \leq \frac{324}{\delta^2}$  (see for example [55, Corollary 4.2.11]). By construction

$$E_{\text{gap}} \subset \{|D(y, \delta) \cap \Lambda(X)| \geq 2 \text{ for some } y \in \mathcal{N}\} \quad (3.2.11)$$

where  $D(y, \delta)$  is the ball of radius  $\delta$  centered at  $y$ . Now if  $D(y, \delta)$  contains two eigenvalues of  $X$ , [9, Lemma 3.5] implies  $\sigma_{n-1}(yI - X) < \delta \kappa_V(X)$ , where we note again that  $X$  is almost surely diagonalizable. Thus, if  $\text{gap}(X) < \delta$  either  $\sigma_{n-1}(yI - X) < \delta t$  for at least one  $y \in \mathcal{N}$  or  $\kappa_V(X) > t$ . In other words, defining the event  $E_y = \{\sigma_{n-1}(yI - X) < \delta t\}$  for  $y \in \mathcal{N}$ ,

$$E_{\text{gap}} \subset E_\kappa \cup \bigcup_{y \in \mathcal{N}} E_y \implies E_{\text{gap}} \cup E_\kappa \subset E_\kappa \cup \bigcup_{y \in \mathcal{N}} E_y. \quad (3.2.12)$$

By a union bound, we then have

$$\mathbb{P}[E_{\text{gap}} \cup E_\kappa] \leq \mathbb{P}[E_\kappa] + |\mathcal{N}| \max_{y \in \mathcal{N}} \mathbb{P}[E_y]. \quad (3.2.13)$$

To bound  $\mathbb{P}[E_\kappa]$ , we first use (3.2.6) to obtain

$$\mathbb{P}[E_\kappa] \leq \mathbb{P} \left[ t < \sqrt{n \sum_{i=1}^n \kappa(\lambda_i)^2} \right] = \mathbb{P} \left[ \sum_{i=1}^n \kappa(\lambda_i)^2 > \frac{t^2}{n} \right]. \quad (3.2.14)$$

Applying Markov's inequality and Lemma 3.8 (recalling that we've conditioned on  $\Lambda(X) \subseteq D(0, 3)$ ) we then have

$$\mathbb{P}[E_\kappa] \leq \frac{n}{t^2} \mathbb{E} \left[ \sum_{\lambda_i \in D(0, 3)} \kappa(\lambda_i)^2 \right] \leq \frac{9(1+4\gamma)^2 n^{2\alpha+3}}{t^2 \gamma^2}. \quad (3.2.15)$$

Similarly, Lemma 3.7 implies

$$\mathbb{P}[E_y] \leq 4 \left( \frac{\delta t(1+4\gamma)n^{\alpha+1}}{\gamma} \right)^8 \quad (3.2.16)$$

for all  $y \in \mathcal{N}$ . Putting everything together, we conclude

$$\mathbb{P}[E_{\text{gap}} \cup E_\kappa] \leq \frac{9(1+4\gamma)^2 n^{2\alpha+3}}{t^2 \gamma^2} + 4 \left( \frac{\delta t(1+4\gamma)n^{\alpha+1}}{\gamma} \right)^8 \frac{324}{\delta^2} \quad (3.2.17)$$

so we have shown

$$\mathbb{P}[\kappa_V(X) < t, \text{gap}(X) > \delta \mid \Lambda(X) \subseteq D(0, 3), \|G_2\|_2 \leq 4] \geq 1 - \frac{9(1+4\gamma)^2 n^{2\alpha+3}}{t^2 \gamma^2} - 1296\delta^6 \left( \frac{t(1+4\gamma)n^{\alpha+1}}{\gamma} \right)^8. \quad (3.2.18)$$

Noting

$$\mathbb{P}[\kappa_V(X) < t, \text{gap}(X) > \delta] \geq \mathbb{P}[\kappa_V(X) < t, \text{gap}(X) > \delta, \Lambda(X) \subseteq D(0, 3), \|G_2\|_2 \leq 4], \quad (3.2.19)$$

we obtain the final result by Bayes' Theorem.  $\square$

**Remark 3.10.** Note that we could replace  $\kappa_V(X)$  in Theorem 3.9 with  $\kappa(V)$  for any eigenvector matrix  $V$  satisfying (3.2.6). In particular, as was used to derive the inequality, this applies to the scaling where each column of  $V$  has unit length.

Informally, Theorem 3.9 says that for the right choice of  $t$  and  $\delta$  (i.e., polynomial in  $n$  and inverse polynomial in  $n$  respectively) the eigenvector condition number of  $X$  is not too large and its eigenvalue gap is not too small. Since the eigenvalues and eigenvectors of  $X$  and  $(\tilde{A}, n^\alpha \tilde{B})$  are the same, this eigenvector and eigenvalue stability is inherited by our perturbed and scaled pencil.

### 3.3 Shattering

We are now ready to prove shattering for a specific pseudospectrum of  $(\tilde{A}, n^\alpha \tilde{B})$ .

**Theorem 3.11.** Let  $A, B \in \mathbb{C}^{n \times n}$  with  $\|A\|_2 \leq 1$  and  $\|B\|_2 \leq 1$ . Let  $(\tilde{A}, \tilde{B}) = (A + \gamma G_1, B + \gamma G_2)$  for  $G_1, G_2$  two independent complex Ginibre matrices and  $0 < \gamma < \frac{1}{2}$ . Let  $g$  be the grid

$$g = \text{grid}(z, \omega, \lceil 8/\omega \rceil, \lceil 8/\omega \rceil) \quad \text{with} \quad \omega = \frac{\gamma^4}{4} n^{-\frac{8\alpha+13}{3}},$$

where  $z$  is chosen uniformly at random from the square cornered at  $-4-4i$  of side length  $\omega$ . Then  $\|\tilde{A}\|_2 \leq 3$ ,  $\|\tilde{B}\|_2 \leq 3$ , and  $\Lambda_\epsilon(\tilde{A}, n^\alpha \tilde{B})$  is shattered with respect to  $g$  for

$$\epsilon = \frac{\gamma^5}{64n^{\frac{11\alpha+25}{3}} + \gamma^5}$$

with probability at least  $\left[1 - \frac{82}{n} - \frac{531441}{16n^2}\right] \left[1 - \frac{n^{2-2\alpha}}{\gamma^2} - 4e^{-n}\right]$ .

*Proof.* As in the previous section, let  $X = n^{-\alpha} \tilde{B}^{-1} \tilde{A}$ . We condition on the following events:  $n^\alpha \sigma_n(\tilde{B}) \geq 1$ ,  $\|G_1\|_2 \leq 4$ , and  $\|G_2\|_2 \leq 4$ . As noted above, these events occur with probability at least  $1 - \frac{n^{2-2\alpha}}{\gamma^2} - 4e^{-n}$  and, following the argument made in [Lemma 3.6](#), guarantee that  $\Lambda(X) \subseteq D(0, 3)$ . Consequently, we know with probability one each eigenvalue of  $X$ , and therefore of  $(\tilde{A}, n^\alpha \tilde{B})$ , is contained in a box of  $g$ . At the same time,

$$\|\tilde{A}\|_2 = \|A + \gamma G_1\|_2 \leq \|A\|_2 + \gamma \|G_1\|_2 \leq 3 \quad (3.3.1)$$

and similarly  $\|\tilde{B}\|_2 \leq 3$ .

Suppose now  $\kappa_V(X) < \frac{n^{\alpha+2}}{\gamma}$ ,  $\text{gap}(X) > \gamma^4 n^{-\frac{8\alpha+13}{3}}$ , and

$$\min_{\lambda_i \in \Lambda(X)} \text{dist}_g(\lambda_i) > \frac{\omega}{4n^2}, \quad (3.3.2)$$

where  $\text{dist}_g(\lambda_i) = \min_{y \in g} |\lambda_i - y|$ . By [\(3.2.18\)](#), we know the first two of these occur under our assumptions with probability at least

$$1 - \frac{9(1+4\gamma)^2 n^{2\alpha+3}}{\left(\frac{n^{\alpha+2}}{\gamma}\right)^2 \gamma^2} - 1296 \left(\frac{\gamma^4}{n^{\frac{8\alpha+13}{3}}}\right)^6 \left(\frac{\left(\frac{n^{\alpha+2}}{\gamma}\right)(1+4\gamma)n^{\alpha+1}}{\gamma}\right)^8, \quad (3.3.3)$$

which, applying  $\gamma < \frac{1}{2}$ , simplifies to  $1 - \frac{81}{n} - \frac{531441}{16n^2}$ . Similarly, by a simple geometric argument (using the fact that the eigenvalues of  $X$  are uniformly distributed in their grid boxes),

$$\mathbb{P} \left[ \min_{\lambda_i \in \Lambda(X)} \text{dist}_g(\lambda_i) > \frac{\omega}{4n^2} \right] \geq 1 - \frac{1}{n}. \quad (3.3.4)$$

Thus, these events occur under our assumptions with probability at least  $1 - \frac{82}{n} - \frac{531441}{16n^2}$ , which means by Bayes' Theorem that we have  $n^\alpha \sigma_n(\tilde{B}) \geq 1$ ,  $\|G_1\|_2 \leq 4$ ,  $\|G_2\|_2 \leq 4$ ,  $\kappa_V(X) < \frac{n^{\alpha+2}}{\gamma}$ ,  $\text{gap}(X) > \gamma^4 n^{-\frac{8\alpha+13}{3}}$ , and [\(3.3.2\)](#) with probability at least  $\left[1 - \frac{82}{n} - \frac{531441}{16n^2}\right] \left[1 - \frac{n^{2-2\alpha}}{\gamma^2} - 4e^{-n}\right]$ .

To complete the proof, we now show that these events guarantee shattering. To do this, we first observe that if  $\text{gap}(X) > \gamma^4 n^{-\frac{8\alpha+13}{3}}$  then no two eigenvalues can share a grid box of  $g$ . At the same time, [\(3.3.2\)](#) implies that the ball of radius  $\frac{\omega}{4n^2}$  around each eigenvalue does not intersect  $g$ . Therefore, it is sufficient to show that  $\Lambda_\epsilon(\tilde{A}, n^\alpha \tilde{B})$  is contained in these balls, which we can do by appealing to [Theorem 2.20](#), our version of Bauer-Fike for matrix pencils. In particular, noting that we can replace  $\kappa(V)$  with  $\kappa_V(X)$  by taking an infimum, [Theorem 2.20](#) implies that  $(\tilde{A}, n^\alpha \tilde{B})$  is contained in balls of radius

$$r_\epsilon = \epsilon \kappa_V(X) \|n^{-\alpha} \tilde{B}^{-1}\|_2 \left( 1 + \frac{\epsilon \|n^{-\alpha} \tilde{B}^{-1}\|_2 + \|X\|_2}{1 - \epsilon \|n^{-\alpha} \tilde{B}^{-1}\|_2} \right). \quad (3.3.5)$$

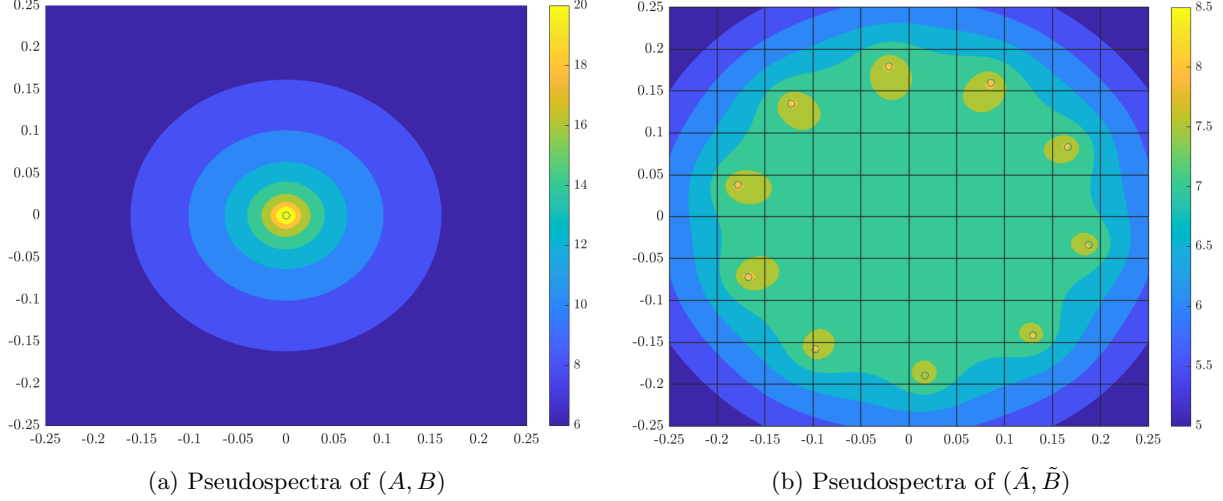


Figure 2: Pseudospectra of a pencil  $(A, B)$  before and after perturbation. Here,  $A$  is a  $10 \times 10$  Jordan block,  $B$  is the identity matrix, and the perturbed matrices are  $\tilde{A} = A + 10^{-7}G_1$  and  $\tilde{B} = B + 10^{-7}G_2$  for  $G_1$  and  $G_2$  two independent, complex Gaussian matrices. Once again eigenvalues are plotted with open circles. A grid that shatters the  $10^{-8}$ -pseudospectrum of  $(\tilde{A}, \tilde{B})$  is superimposed over figure (b).

Applying our bounds  $\|n^{-\alpha}\tilde{B}^{-1}\|_2 = \frac{1}{n^\alpha \sigma_n(\tilde{B})} \leq 1$ ,  $\|X\|_2 \leq 3$ , and  $\kappa_V(X) \leq \frac{n^{\alpha+2}}{\gamma}$ , we obtain shattering as long as

$$r_\epsilon \leq \epsilon \left( \frac{n^{\alpha+2}}{\gamma} \right) \left( \frac{4}{1-\epsilon} \right) \leq \frac{\omega}{4n^2} = \frac{\gamma^4}{16n^{\frac{8\alpha+19}{3}}} \quad (3.3.6)$$

or, equivalently,  $\epsilon \leq \frac{\gamma^5}{(64n^{\frac{11\alpha+25}{3}} + \gamma^5)}$ .  $\square$

This result clarifies the impact of the scaling  $n^\alpha$ . On one hand, increasing  $\alpha$  drives the term  $\frac{n^{2-2\alpha}}{\gamma^2}$  in our probability bound to zero, assuming  $\gamma$  is fixed. Said another way, a larger choice of  $\alpha$  allows us to take  $\gamma$  smaller without losing our guarantee of shattering. In particular, we need

$$\gamma > n^{1-\alpha} \quad (3.3.7)$$

to ensure that the probability in [Theorem 3.11](#) is not vacuous. This is important, as we'd like to perturb our matrices as little as possible. Nevertheless, we pay a penalty for increasing  $\alpha$  in  $\omega$  and  $\epsilon$ , both of which shrink as  $\alpha$  increases. This trade-off reflects a fundamental geometric reality: the more we scale by, the closer the eigenvalues of  $(\tilde{A}, n^\alpha \tilde{B})$  are driven to zero (and therefore to each other), meaning we'll need a finer grid and a smaller pseudospectrum to guarantee shattering.

[Figure 2](#) demonstrates pseudospectral shattering on a  $10 \times 10$  example. We observe here all of the same phenomena as in single-matrix shattering: small perturbations turn a pencil with a poorly conditioned eigenvalue problem (in this case only one eigenvalue repeated ten times) to one with a full set of distinct eigenvalues. Notice in particular how much faster the pseudospectra of  $(\tilde{A}, \tilde{B})$  coalesce around the eigenvalues as  $\epsilon \rightarrow 0$ .

In the remainder of this section, we develop two perturbation results: one for pseudospectral shattering ([Lemma 3.12](#)) and one for individual eigenvalues and eigenvectors ([Lemma 3.13](#)). These follow closely [[9](#), Lemmas 5.8 and 5.9] and will be useful in the next section.

**Lemma 3.12.** *Suppose  $(A, B)$  is regular and  $\Lambda_\epsilon(A, B)$  is shattered with respect to a finite grid  $g$ . If  $\|A - A'\|_2, \|B - B'\|_2 \leq \eta < \epsilon$  then each eigenvalue of  $(A', B')$  shares a grid box with exactly one eigenvalue of  $(A, B)$  and  $\Lambda_{\epsilon-\eta}(A', B')$  is also shattered with respect to  $g$ .*

*Proof.* If  $z \in \Lambda_{\epsilon-\eta}(A', B')$  then  $z$  is an eigenvalue of a pencil  $(C, D)$  with  $\|A' - C\|_2, \|B' - D\|_2 \leq \epsilon - \eta$ . In this case,

$$\|A - C\|_2 \leq \|A - A' + A' - C\|_2 \leq \|A - A'\|_2 + \|A' - C\|_2 \leq \eta + \epsilon - \eta = \epsilon \quad (3.3.8)$$

and similarly  $\|B - D\|_2 \leq \epsilon$ , which implies  $z \in \Lambda_\epsilon(A, B)$ . Thus,  $\Lambda_{\epsilon-\eta}(A', B') \subseteq \Lambda_\epsilon(A, B)$ , which guarantees that  $\Lambda_{\epsilon-\eta}(A', B')$  is also shattered with respect to  $g$ . To show that each eigenvalue of  $(A', B')$  shares a grid box with exactly one eigenvalue of  $(A, B)$ , consider  $A_t = A + t(A' - A)$  and  $B_t = B + t(B' - B)$  for  $t \in [0, 1]$ . Since  $(A, B)$  is regular (and moreover  $\epsilon < \sigma_n(B)$  since  $\Lambda_\epsilon(A, B)$  is bounded),  $(A_t, B_t)$  continuously deforms the eigenvalues of  $(A, B)$  to eigenvalues of  $(A', B')$  while staying within  $\Lambda_\eta(A, B) \subseteq \Lambda_\epsilon(A, B)$ . Since  $\Lambda_\epsilon(A, B)$  is shattered with respect to  $g$  and therefore no two eigenvalues of  $(A, B)$  share a grid box, this ensures that each eigenvalue of  $(A', B')$  belongs to a grid box with a unique eigenvalue of  $(A, B)$   $\square$

**Lemma 3.13.** *Suppose  $(A, B)$  is regular and  $\Lambda_\epsilon(A, B)$  is shattered with respect to a finite grid  $g$  with boxes of side length  $\omega$ . If  $\|A - A'\|_2, \|B - B'\|_2 \leq \eta < \epsilon$  then for any right unit eigenvector  $v'$  of  $(A', B')$  there exists a right unit eigenvector  $v$  of  $(A, B)$  such that*

1. *The eigenvalue of  $(A', B')$  corresponding to  $v'$  shares a grid box of  $g$  with the eigenvalue of  $(A, B)$  that corresponds to  $v$ .*

$$2. \|v' - v\| \leq \frac{\sqrt{8}\omega}{\pi} \frac{\eta}{\epsilon(\epsilon-\eta)} (1 + \|B^{-1}A\|_2) \|B\|_2.$$

*Proof.* Let  $\lambda'$  be the eigenvalue of  $(A', B')$  corresponding to  $v'$ . By Lemma 3.12,  $\lambda'$  shares a grid box of  $g$  with a unique eigenvalue of  $\lambda$  of  $(A, B)$ . Let  $v$  be the right unit eigenvector of  $(A, B)$  corresponding to  $\lambda$ . In addition, let  $w'$  and  $w$  be the left eigenvectors corresponding to  $v'$  and  $v$  respectively, normalized so that  $w^H v = (w')^H v' = 1$ . If  $\Gamma$  is the contour of the grid box containing both  $\lambda$  and  $\lambda'$ , then by (2.1.1)

$$\begin{aligned} v'(w')^H - vw^H &= \frac{1}{2\pi i} \oint_{\Gamma} (z - (B')^{-1}A')^{-1} dz - \frac{1}{2\pi i} \oint_{\Gamma} (z - B^{-1}A)^{-1} dz \\ &= \frac{1}{2\pi i} \oint_{\Gamma} (z - (B')^{-1}A')^{-1} - (z - B^{-1}A)^{-1} dz. \end{aligned} \quad (3.3.9)$$

By the resolvent identity

$$\begin{aligned} (z - (B')^{-1}A')^{-1} - (z - B^{-1}A)^{-1} &= (z - (B')^{-1}A')^{-1} ((B')^{-1}A' - B^{-1}A) (z - B^{-1}A)^{-1} \\ &= (zB' - A')^{-1} B' ((B')^{-1}A' - B^{-1}A) (zB - A)^{-1} B \\ &= (zB' - A')^{-1} (A' - B'B^{-1}A) (zB - A)^{-1} B, \end{aligned} \quad (3.3.10)$$

so, applying this along with the ML inequality above, we have

$$\|v'(w')^H - vw^H\|_2 \leq \frac{2\omega}{\pi} \sup_{z \in \Gamma} \|(zB' - A')^{-1} (A' - B'B^{-1}A) (zB - A)^{-1} B\|_2. \quad (3.3.11)$$

Now  $\Lambda_\epsilon(A, B)$  is shattered with respect to  $g$  and therefore does not intersect  $\Gamma$ , so we know  $\|(zB - A)^{-1}\|_2 \leq \frac{1}{\epsilon(1+|z|)} \leq \frac{1}{\epsilon}$  for all  $z \in \Gamma$ . Moreover, again by Lemma 3.12,  $\Lambda_{\epsilon-\eta}(A', B')$  is shattered with respect to  $g$ , so the same argument implies  $\|(zB' - A')^{-1}\|_2 \leq \frac{1}{\epsilon-\eta}$  for all  $z \in \Gamma$ . Applying this to the previous inequality, we conclude

$$\|v'(w')^H - vw^H\|_2 \leq \frac{2\omega}{\pi} \frac{1}{\epsilon(\epsilon-\eta)} \|A' - B'B^{-1}A\|_2 \|B\|_2. \quad (3.3.12)$$

Writing  $B' = B + E$  for some  $\|E\|_2 \leq \eta$  since  $\|B - B'\|_2 \leq \eta$ , we have

$$\|A' - B'B^{-1}A\|_2 = \|A' - (B + E)B^{-1}A\|_2 \leq \|A' - A\|_2 + \|EB^{-1}A\|_2 \leq \eta(1 + \|B^{-1}A\|_2) \quad (3.3.13)$$

which yields a final upper bound

$$\|v'(w')^H - vw^H\|_2 \leq \frac{2\omega}{\pi} \frac{\eta}{\epsilon(\epsilon-\eta)} (1 + \|B^{-1}A\|_2) \|B\|_2. \quad (3.3.14)$$

Since without loss of generality we can assume  $v^H v' \geq 0$  (if this is not true we can just rotate  $v$ ), and using the fact that  $\|v\| = \|v'\| = 1$ , we complete the proof by observing

$$\|v' - v\|_2 = \sqrt{2 - 2v^H v'} \leq \sqrt{2} \|v'(w')^H - vw^H\|_2. \quad (3.3.15)$$

This inequality is nontrivial (see the proof of [9, Lemma 5.8] for the details). Combining it with (3.3.14), we conclude that  $v$  is the desired eigenvector of  $(A, B)$  with  $\|v' - v\| \leq \frac{\sqrt{8}\omega}{\pi} \frac{\eta}{\epsilon(\epsilon-\eta)} (1 + \|B^{-1}A\|_2) \|B\|_2$ .  $\square$

## 4 Inverse-Free Divide-and-Conquer

In this section, we develop a divide-and-conquer eigensolver that, based on the pseudospectral shattering result proved in the previous section, produces approximations of the eigenvalues and eigenvectors of the perturbed and scaled pencil  $(\tilde{A}, n^\alpha \tilde{B})$ . We first provide motivation and background before stating the divide-and-conquer algorithm and proving convergence in exact arithmetic. In the next section, we use this divide-and-conquer routine to produce approximate diagonalizations for arbitrary pencils.

### 4.1 Motivation

Suppose we have a matrix pencil  $(A, B)$  that we want to split into two smaller problems with disjoint spectra. Let  $P_R$  be a rank- $k$  spectral projector onto the span of a set of right eigenvectors of  $(A, B)$  and let  $U_R \in \mathbb{C}^{n \times k}$  be a matrix whose orthonormal columns span  $\text{range}(P_R)$ . Similarly, let  $U_L \in \mathbb{C}^{n \times k}$  be a matrix whose orthonormal columns span the left deflating subspace of  $(A, B)$  corresponding to  $\text{range}(P_R)$ .

If  $v$  is a right eigenvector of  $(A, B)$  in  $\text{range}(P_R)$  then  $v = U_R w$  for some  $w \in \mathbb{C}^k$ . Moreover, if  $\lambda$  is the eigenvalue corresponding to  $v$ , then

$$U_L^H A U_R w = U_L^H A v = U_L^H \lambda B v = \lambda U_L^H B U_R w, \quad (4.1.1)$$

so  $(\lambda, w)$  is an eigenpair of the  $k \times k$  pencil  $(U_L^H A U_R, U_L^H B U_R)$ . Meanwhile, if  $(\lambda, w)$  is an eigenpair of  $(U_L^H A U_R, U_L^H B U_R)$  then  $U_L^H A v = \lambda U_L^H B v$  for  $v = U_R w$ , which subsequently implies  $A v = \lambda B v$  since both  $A v$  and  $B v$  belong to the left deflating subspace spanned by the columns of  $U_L$ .

In short,  $(\lambda, v)$  is an eigenpair of  $(A, B)$  if and only if  $(\lambda, w)$  is an eigenpair of  $(U_L^H A U_R, U_L^H B U_R)$  for  $v = U_R w$ . Thus, if we can compute  $U_L$  and  $U_R$  we can find eigenpairs of  $(A, B)$  by solving the smaller problem  $(U_L^H A U_R, U_L^H B U_R)$ , whose spectra is contained in  $\Lambda(A, B)$  and whose eigenvectors are in simple correspondence with those of  $(A, B)$ . The only potential drawback is that  $(U_L^H A U_R, U_L^H B U_R)$  can only provide  $k$  eigenpairs, but this can be easily remedied by repeating the process for the projector onto the remaining eigenvectors. These observations are the heart of divide-and-conquer, which proceeds as follows:

1. Locate a set of eigenvectors of  $(A, B)$  and compute the spectral projectors  $P_R$  and  $P_L$  onto the corresponding right and left deflating subspaces.
2. Apply a rank-revealing factorization to find matrices  $U_R$  and  $U_L$  consisting of orthonormal columns that span  $\text{range}(P_R)$  and  $\text{range}(P_L)$  respectively.
3. Reduce the problem  $(A, B)$  to  $(U_L^H A U_R, U_L^H B U_R)$  and repeat for the other set of eigenvectors, then recur.

The only remaining question concerns how to locate a set of eigenvectors to project onto. We plan to do this via pseudospectral shattering. If we have a grid that shatters the pseudospectrum of our perturbed and scaled problem  $(\tilde{A}, n^\alpha \tilde{B})$ , we can search for a grid line that significantly<sup>2</sup> splits the spectrum; applying a Möbius transformation that sends that grid line to the unit circle and then repeatedly squaring the pencil to drive one set of eigenvalues to zero, we obtain a projector onto the eigenvectors belonging to the surviving eigenvalues. In this approach, finding a grid line that produces a significant split ensures that divide-and-conquer will succeed in  $O(\log(n))$  steps.

For this to work without drawing a new grid at each step, we need shattering to be preserved as the problem shrinks in size. This is guaranteed by the following lemma.

**Lemma 4.1.** *Let  $P_R$  be a spectral projector for a regular matrix pencil  $(A, B)$  and let  $P_L$  be the projector onto the corresponding left deflating subspace. Let  $U_L, U_R \in \mathbb{C}^{n \times k}$  be matrices whose orthonormal columns span the ranges of  $P_L$  and  $P_R$  respectively. Then*

$$\Lambda_\epsilon(U_L^H A U_R, U_L^H B U_R) \subseteq \Lambda_\epsilon(A, B).$$

---

<sup>2</sup>Significant here means that at least a fifth of the eigenvalues lie on either side of the line.



*Proof.* If  $z \in \Lambda_\epsilon(U_L^H AU_R, U_L^H BU_R)$  then there exists a unit vector  $u \in \mathbb{C}^k$  such that

$$\|U_L^H(A - zB)U_R u\|_2 = \|(U_L^H AU_R - zU_L^H BU_R)u\|_2 \leq \epsilon(1 + |z|). \quad (4.1.2)$$

Let  $y = U_R u \in \mathbb{C}^n$ . Since  $U_R$  has orthonormal columns  $\|y\|_2 = \|U_R u\|_2 = \|u\|_2 = 1$ . Moreover,  $y$  is in the right deflating subspace  $\text{range}(P_R)$ , which means  $(A - zB)y$  belongs to the corresponding left deflating subspace  $\text{range}(P_L)$ . Since the columns of  $U_L$  are an orthonormal basis for this subspace, we conclude

$$\|(A - zB)y\|_2 = \|U_L^H(A - zB)y\|_2 \leq \epsilon(1 + |z|) \quad (4.1.3)$$

and therefore  $z \in \Lambda_\epsilon(A, B)$ .  $\square$

This result emphasizes the importance of the matrices  $U_L$  and  $U_R$ . While in principle many of the building blocks of divide-and-conquer hold for arbitrary matrices whose columns span deflating subspaces corresponding to eigenvectors (like (4.1.1) for example) the proof of [Lemma 4.1](#) requires properties of matrices with orthonormal columns, meaning it would not be sufficient to simply compute the projectors  $P_R$  and  $P_L$ . On top of this,  $U_L$  and  $U_R$  have the added benefit of ensuring that the norms of  $U_L^H AU_R$  and  $U_L BU_R$  don't grow, allowing us to carry over norm assumptions as we recur.

## 4.2 Numerical Building Blocks

In this section, we review the numerical building blocks that allow us to compute the projectors  $P_R$  and  $P_L$  and subsequently the orthonormal bases contained in  $U_L$  and  $U_R$ . Note that, as mentioned in the introduction, each of these uses only QR and matrix multiplication.

### 4.2.1 Implicit Repeated Squaring (IRS)

We begin with Implicit Repeated Squaring (**IRS**), a routine for repeatedly squaring a product  $A^{-1}B$  without forming it. **IRS** first appeared in the context of eigenvalue problems in initial explorations of inverse-free and parallel methods [\[5, 39\]](#). It was subsequently stated as it appears in [Algorithm 1](#) under the name **IRS** in a technical report of Ballard, Demmel, and Dumitriu [\[6\]](#).

---

**Algorithm 1** Implicit Repeated Squaring (**IRS**)

**Input:**  $A, B \in \mathbb{C}^{n \times n}$  and  $p$  a positive integer

**Output:**  $A_p, B_p \in \mathbb{C}^{n \times n}$  satisfying  $A_p^{-1}B_p = (A^{-1}B)^{2^p}$

---

```

1:  $A_0 = A$ 
2:  $B_0 = B$ 
3: for  $j = 0 : p - 1$  do
4:
```

$$\begin{pmatrix} B_j \\ -A_j \end{pmatrix} = \begin{pmatrix} Q_{11} & Q_{12} \\ Q_{21} & Q_{22} \end{pmatrix} \begin{pmatrix} R_j \\ 0 \end{pmatrix}$$

$$A_{j+1} = Q_{12}^H A_j$$

$$B_{j+1} = Q_{22}^H B_j$$

```

5: end for
6: return  $A_p, B_p$ 
```

---

We can verify the guarantee of [Algorithm 1](#) by noting that line 4 ensures  $Q_{12}^H B_j - Q_{22}^H A_j = 0$  and consequently  $B_j A_j^{-1} = Q_{12}^{-H} Q_{22}^H$ , which implies

$$A_{j+1}^{-1} B_{j+1} = A_j^{-1} Q_{12}^{-H} Q_{22}^H B_j = A_j^{-1} B_j A_j^{-1} B_j = (A_j^{-1} B_j)^2. \quad (4.2.1)$$

The connection to spectral projectors is fairly straightforward: if  $A$  is nonsingular,  $A^{-1}B$  and  $(A, B)$  have the same set of eigenvectors, with each finite eigenvalue  $\lambda$  of  $A^{-1}B$  corresponding to an eigenvalue  $\frac{1}{\lambda}$  of

Eigenvalue Correspondence in <b>IRS</b> (Algorithm 1)							
$(A, B)$	$A^{-1}B$	$A_p^{-1}B_p$	$(A_p + B_p)^{-1}A_p$	$(A^H, B^H)$	$A^{-H}B^H$	$\mathcal{A}_p^{-1}\mathcal{B}_p$	$\mathcal{A}_p^H(\mathcal{A}_p + \mathcal{B}_p)^{-H}$
$\lambda$	$\lambda^{-1}$	$\lambda^{-2^p}$	$(1 + \lambda^{-2^p})^{-1}$	$\bar{\lambda}$	$(\bar{\lambda})^{-1}$	$(\bar{\lambda})^{-2^p}$	$(1 + \bar{\lambda}^{-2^p})^{-1}$

Table 1: Correspondence between each eigenvalue  $\lambda$  of  $(A, B)$  and an eigenvalue of the matrices that appear when **IRS** is used to compute spectral projectors. Here,  $[A_p, B_p] = \mathbf{IRS}(A, B, p)$  while  $[\mathcal{A}_p, \mathcal{B}_p] = \mathbf{IRS}(A^H, B^H, p)$ .

$(A, B)$ . Repeatedly squaring  $A^{-1}B$  drives its eigenvalues to either zero or infinity, assuming  $(A, B)$  has no eigenvalues on the unit circle, without changing eigenvectors. Moreover, after  $p$  steps of repeated squaring we have

$$(A_p + B_p)^{-1}A_p = (I + A_p^{-1}B_p)^{-1} = (I + (A^{-1}B)^{2^p})^{-1}, \quad (4.2.2)$$

so the eigenvalues of  $(A_p + B_p)^{-1}A_p$  are close to either zero or one, corresponding to eigenvalues that were originally inside, respectively outside, the unit disk. For clarity, Table 1 shows the correspondence between eigenvalues of  $(A, B)$  and eigenvalues of the outputs of **IRS**.

Since  $(A_p + B_p)^{-1}A_p$  has the same set of eigenvectors as  $A^{-1}B$ , it is not hard to show that  $(A_p + B_p)^{-1}A_p$  approaches a projector  $P_{R,|z|>1}$  onto the right deflating subspace of  $(A, B)$  spanned by eigenvectors with eigenvalues outside the unit disk [5, §4]. Nevertheless, for divide-and-conquer to proceed we also need a projector onto the corresponding left deflating subspace. Luckily, this can be done by running **IRS** on  $(A^H, B^H)$  since taking a Hermitian transpose swaps right and left deflating spaces. In fact, if  $\mathcal{A}_p$  and  $\mathcal{B}_p$  are the outputs of  $p$  steps of repeated squaring on  $(A^H, B^H)$ , then

$$\mathcal{A}_p^H(\mathcal{A}_p + \mathcal{B}_p)^{-H} = (I + (A^{-H}B^H)^{2^p})^{-H} \quad (4.2.3)$$

approaches a projector  $P_{L,|z|>1}$  onto the left deflating subspace corresponding to  $P_{R,|z|>1}$ . And while taking a Hermitian transpose does change the eigenvalues, we can see from Table 1 that repeated squaring on  $(A^H, B^H)$  drives corresponding eigenvalues to the same destination (either zero or one).

As mentioned, **IRS** breaks down if the input pencil has an eigenvalue on the unit circle. Considering such a problem to be ill-posed, Bai, Demmel, and Gu introduce the following distance  $d_{(A,B)}$ , whose reciprocal can be thought of as a condition number for the procedure.

**Definition 4.2.** The distance from  $(A, B)$  to the nearest ill-posed problem is

$$d_{(A,B)} = \inf \{ \|E\| + \|F\| : (A + E) - z(B + F) \text{ is singular for some } |z| = 1 \}.$$

Using  $d_{(A,B)}$ , they prove quadratic convergence for exact arithmetic **IRS**. Informally, this result states that to reach accuracy  $\delta$  we need to take roughly  $O(\log_2(\frac{1}{\delta}))$  steps of repeated squaring.

**Theorem 4.3** (Bai-Demmel-Gu 1994). *Let  $A_p, B_p$  be the result of applying **IRS** to  $A, B$ . If*

$$p \geq \log_2 \left[ \frac{\|(A, B)\|_2 - d_{(A,B)}}{d_{(A,B)}} \right]$$

then

$$\|(A_p + B_p)^{-1}A_p - P_{R,|z|>1}\|_2 \leq \|P_{R,|z|>1}\|_2 \frac{2^{p+3} \left(1 - \frac{d_{(A,B)}}{\|(A,B)\|_2}\right)^{2^p}}{\max \left\{ 0, 1 - 2^{p+2} \left(1 - \frac{d_{(A,B)}}{\|(A,B)\|_2}\right)^{2^p} \right\}}.$$

Note that because  $d_{(A^H, B^H)} = d_{(A,B)}$  and  $\|(A, B)\|_2 = \|(A^H, B^H)\|_2$ , Theorem 4.3 can be applied to the left projector by swapping  $A, B$ ,  $(A_p + B_p)^{-1}A_p$ , and  $P_{R,|z|>1}$  for  $A^H, B^H$ ,  $\mathcal{A}_p^H(\mathcal{A}_p + \mathcal{B}_p)^{-H}$ , and  $P_{L,|z|>1}$  respectively.

#### 4.2.2 RURV and GRURV

Once we have our spectral projectors  $P_R$  and  $P_L$ , we next need to apply a rank-revealing factorization to locate an orthonormal basis for the corresponding right and left deflating subspaces. To do this, we produce a (random) URV factorization of the projectors.

**Definition 4.4.**  $A = URV$  is a URV factorization of the matrix  $A \in \mathbb{C}^{n \times n}$  if  $R$  is upper triangular and  $U, V \in \mathbb{C}^{n \times n}$  are unitary.

The URV factorization was first introduced by Stewart [50] as an alternative to the SVD with many of the same properties. Most important is its rank-revealing capability: when  $A$  has effective rank  $k$  (i.e., there is a significant gap between  $\sigma_k(A)$  and  $\sigma_{k+1}(A)$ ),  $A = URV$  is a rank-revealing factorization with

$$R = \begin{pmatrix} R_{11} & R_{21} \\ 0 & R_{22} \end{pmatrix} \quad (4.2.4)$$

for  $R_{11}$  a  $k \times k$  block if  $\sigma_k(R_{11})$  is a “good” approximation to  $\sigma_k(A)$  and  $\sigma_1(R_{22})$  is a “good” approximation of  $\sigma_{k+1}(A)$ . We will make the meaning of “good” precise in the guarantees to come.

While there are many ways to compute a rank-revealing URV factorization (see for example [24, §3]) we are interested in the **RURV** algorithm of Demmel, Dumitriu, and Holtz [17], which is stated below as Algorithm 2.

---

**Algorithm 2** Randomized Rank-Revealing Factorization (**RURV**)

---

**Input:**  $A \in \mathbb{C}^{n \times n}$

**Output:**  $U$  unitary matrix,  $R$  upper triangular matrix, and  $V$  Haar such that  $A = URV$  is a rank-revealing factorization of  $A$ .

---

- 1: Draw a random matrix  $B$  with i.i.d.  $\mathcal{N}_{\mathbb{C}}(0, 1)$  entries
  - 2:  $[V, \hat{R}] = \mathbf{QR}(B)$
  - 3:  $\hat{A} = A \cdot V^H$
  - 4:  $[U, R] = \mathbf{QR}(\hat{A})$
  - 5: **return**  $U, R, V$
- 

This randomized algorithm is simple to implement, backwards stable [7, Theorem 4.5], and capable of producing strongly rank-revealing factorizations (in the sense of Gu and Eisenstat [28]). In fact, Ballard et al. [7] prove the following, demonstrating that **RURV** matches the best-known guarantees for deterministic factorizations.

**Theorem 4.5** (Ballard et al. 2019). *Let  $A \in \mathbb{C}^{n \times n}$  with singular values  $\sigma_1, \sigma_2, \dots, \sigma_n$ . Let  $R$  be the matrix produced by applying exact arithmetic **RURV** to  $A$  as in (4.2.4). Assume that  $k, n - k > 30$ . Then with probability  $1 - \delta$  the following occur:*

$$\begin{aligned} \frac{\delta}{2.02} \frac{\sigma_k}{\sqrt{k(n-k)}} &\leq \sigma_k(R_{11}) \leq \sigma_k \\ \sigma_{k+1} &\leq \sigma_1(R_{22}) \leq 2.02 \frac{\sqrt{k(n-k)}}{\delta} \sigma_{k+1} \\ \|R_{11}^{-1} R_{12}\|_2 &\leq \frac{6.1 \sqrt{k(n-k)}}{\delta} + \frac{\sigma_{k+1}}{\sigma_k} \frac{50 \sqrt{k^3(n-k)^3}}{\delta^3}. \end{aligned}$$

The proof of Theorem 4.5 boils down to bounding the smallest singular value of a  $k \times k$  block of a Haar unitary matrix via [17, Theorem 5.2]. The requirement  $k, n - k > 30$  comes from the bound used by Ballard et al. [7, Corollary 3.4]. Banks et al. subsequently demonstrated that this can be relaxed [9, Proposition C.3], although the fundamental guarantees are the same: with high probability **RURV** produces a factorization such that  $\sigma_k(R_{11})$  and  $\sigma_1(R_{22})$  are at worst a multiplicative factor of  $O(\sqrt{k(n-k)})$  away from  $\sigma_k(A)$  and

---

**Algorithm 3** Generalized Randomized Rank-Revealing Factorization (**GRURV**)**Input:**  $k$  a positive integer,  $A_1, A_2, \dots, A_k \in \mathbb{C}^{n \times n}$ , and  $m_1, m_2, \dots, m_k \in \{1, -1\}$ **Output:**  $U$  unitary,  $R_1, R_2, \dots, R_k$  upper triangular, and  $V$  Haar such that  $UR_1^{m_1}R_2^{m_2}\dots R_k^{m_k}V$  is a rank-revealing factorization of  $A_1^{m_1}A_2^{m_2}\dots A_k^{m_k}$ 

---

```
1: if  $m_k = 1$  then
2:    $[U, R_k, V] = \mathbf{RURV}(A_k)$ 
3: else
4:    $[U, L_k, V] = \mathbf{RULV}(A_k^H)$ 
5:    $R_k = L_k^H$ 
6: end if
7:  $U_{\text{current}} = U$ 
8: for  $i = k - 1 : 1$  do
9:   if  $m_i = 1$  then
10:     $[U, R_i] = \mathbf{QR}(A_i \cdot U_{\text{current}})$ 
11:     $U_{\text{current}} = U$ 
12:   else
13:     $[U, R_i] = \mathbf{RQ}(U_{\text{current}}^H \cdot A_i)$ 
14:     $U_{\text{current}} = U^H$ 
15:   end if
16: end for
17: return  $U_{\text{current}}$ , optionally  $R_1, R_2, \dots, R_k, V$ 
```

---

$\sigma_{k+1}(A)$  respectively.

Of course, the projectors we would like to apply **RURV** to are not simple matrices but rather products of the form  $A^{-1}B$  or  $AB^{-1}$  (i.e., the approximate projectors  $(A_p + B_p)^{-1}A_p$  and  $\mathcal{A}_p^H(\mathcal{A}_p + \mathcal{B}_p)^{-H}$  from **IRS**). Since we avoid taking inverses, explicitly forming either of these products is not an option. Instead, a generalized version of **RURV** – referred to as **GRURV** and presented here as [Algorithm 3](#) – allows us to apply **RURV** to an arbitrary product of matrices and their inverses. Note that in this routine **RULV** is a version of **RURV** that replaces the QR factorization in line 4 of [Algorithm 2](#) with QL.

**GRURV** was first introduced in a technical report of Ballard, Demmel, and Dumitriu [\[6\]](#) specifically to apply **RURV** to spectral projectors found by **IRS**. Importantly, exact arithmetic **GRURV** is essentially equivalent to applying exact arithmetic **RURV** to the corresponding product [\[7, Theorem 5.2\]](#), which allows us to access guarantees like [Theorem 4.5](#) for **GRURV** in exact arithmetic without any additional effort.

#### 4.2.3 DEFLATE

We are now ready to state a routine that combines **IRS** and **GRURV** to accomplish items 1 and 2 from our outline of divide-and-conquer in [Section 4.1](#). Such a routine was first stated as **RGNEP** [\[6, Algorithm 4\]](#), albeit in a different form than what we present below. In particular, **RGNEP** assumes no knowledge of the number of eigenvalues of  $(A, B)$  inside/outside the unit circle (equivalently, the rank of the corresponding spectral projectors), instead multiplying by the full  $n \times n$  unitary matrices produced by **GRURV** and deciding where to split the problem to minimize certain matrix norms. Since we will have access to information about the rank of the projectors being computed (this is essentially how dividing grid lines are selected), we state an alternative **DEFLATE** ([Algorithm 4](#)), which simply takes the first  $k$  columns of the matrices computed by **GRURV**.

For **DEFLATE** to succeed, we need to know that the first  $k$  columns of the U-factor produced by **GRURV** span the range of the rank- $k$  product it is applied to with high probability. We would also like a guarantee that the result for an approximate projector is close to the corresponding result for a true spectral projector (since **IRS** can only produce approximations of  $P_R$  or  $P_L$ ).

If we apply **RURV** to a rank- $k$  matrix  $A$ , the first  $k$  columns of the U factor almost surely span  $\text{range}(A)$ . The intuition behind this is fairly simple: multiplying by the Haar matrix in line 3 of **RURV** “mixes” the columns of  $A$ , distributing information so that the first  $k$  columns of  $A$  – and therefore the first  $k$  columns of  $U$  – are likely to span  $\text{range}(A)$ . On top of this, we have the following perturbation result in exact arithmetic,

---

**Algorithm 4** Deflating Subspace Finder (**DEFLATE**)**Input:**  $A, B \in \mathbb{C}^{n \times n}$ , positive integers  $p$  and  $k$ **Requires:**  $k \leq n$ ;  $(A, B)$  has no eigenvalues on the unit circle and exactly  $k$  eigenvalues outside it.**Output:**  $U_R^{(k)}, U_L^{(k)} \in \mathbb{C}^{k \times n}$  with orthonormal columns that approximately span right and left deflating subspaces of  $(A, B)$ .

- 
- 1:  $[A_p, B_p] = \mathbf{IRS}(A, B, p)$
  - 2:  $U_R = \mathbf{GRURV}(2, A_p + B_p, A_p, -1, 1)$
  - 3:  $[A_p, B_p] = \mathbf{IRS}(A^H, B^H, p)$
  - 4:  $U_L = \mathbf{GRURV}(2, A_p^H, (A_p + B_p)^H, 1, -1)$
  - 5:  $U_R^{(k)} = U_R(:, 1 : k)$
  - 6:  $U_L^{(k)} = U_L(:, 1 : k)$
  - 7: **return**  $U_R^{(k)}, U_L^{(k)}$
- 

originally proved by Banks et al. [9, Proposition C.12].

**Theorem 4.6** (Banks et al. 2019). *Let  $A, A' \in \mathbb{C}^{n \times n}$  with  $\|A - A'\|_2 \leq \delta$  and  $\text{rank}(A) = \text{rank}(A^2) = k$ . Let  $T$  and  $S$  contain the first  $k$  columns of the  $U$  factors produced by applying exact arithmetic **RURV** to  $A$  and  $A'$  respectively. Then for any  $\theta \in (0, 1)$  with probability  $1 - \theta^2$  there exists a unitary  $W \in \mathbb{C}^{k \times k}$  such that*

$$\|S - TW^H\|_2 \leq \sqrt{\frac{8\sqrt{k(n-k)}}{\sigma_k(T^H AT)}} \cdot \sqrt{\frac{\delta}{\theta}}$$

Letting  $A$  be a rank- $k$  spectral projector (in which case  $\sigma_k(T^H AT) = 1$ ), [Theorem 4.6](#) says that the first  $k$  columns of the  $U$  factor of an approximation  $A'$  of  $A$  are close to a rotation/reflection of the first  $k$  columns of the  $U$ -factor of  $A$  as long as  $\|A - A'\|_2$  is sufficiently small.

Recalling that exact arithmetic **GRURV** is equivalent to exact arithmetic **RURV** on the corresponding product, these results generalize directly. Not only can we say that almost surely the first  $k$  columns of the  $U$ -factor produced by **GRURV** span the range of the product, but a perturbation result similar to [Theorem 4.6](#) holds. Combining these with our analysis of **IRS** yields the following exact arithmetic guarantee for **DEFLATE**.

**Theorem 4.7.** *Suppose  $(A, B)$ ,  $p$ , and  $k$  satisfy the requirements of **DEFLATE**, where  $p$  is large enough to ensure error in repeated squaring is at most  $\delta$  in lines 1 and 3. Let  $U_R^{(k)}$  and  $U_L^{(k)}$  be the outputs of running this algorithm in exact arithmetic. Then for any  $\nu \in (0, 1)$ , there exist  $U_R, U_L \in \mathbb{C}^{n \times k}$  with orthonormal columns spanning right and left deflating subspaces of  $(A, B)$  respectively such that*

1.  $\|U_R^{(k)} - U_R\|_2 \leq \sqrt{8\sqrt{k(n-k)}} \sqrt{\frac{\delta}{\nu}}$
2.  $\|U_L^{(k)} - U_L\|_2 \leq \sqrt{8\sqrt{k(n-k)}} \sqrt{\frac{\delta}{\nu}}$

with probability at least  $1 - 2\nu^2$ .

*Proof.* Consider first  $U_R^{(k)}$  and let  $A_p$  and  $B_p$  be the outputs of applying  $p$  steps of exact arithmetic repeated squaring to  $A$  and  $B$ . We know  $(A_p + B_p)^{-1}A_p$  approaches a projector  $P_{R,|z|>1}$  onto the right deflating subspace spanned by eigenvectors of  $(A, B)$  with eigenvalues outside the unit circle. Let  $URV = P_{R,|z|>1}$  be a rank-revealing factorization of  $P_{R,|z|>1}$  obtained via exact arithmetic **RURV** and let  $U^{(k)}$  contain the first  $k$  columns of  $U$ . Since  $k$  is the number of eigenvalues with modulus greater than one, we know  $k = \text{rank}(P_{R,|z|>1})$  and moreover  $\text{range}(U^{(k)}) = \text{range}(P_{R,|z|>1})$  almost surely. Thus, since  $p$  is large enough to ensure  $\|(A_p + B_p)^{-1}A_p - P_{R,|z|>1}\|_2 \leq \delta$  and exact arithmetic **GRURV** satisfies the same guarantees as exact **RURV**, we have by [Theorem 4.6](#) that with probability at least  $1 - \nu^2$  there exists a unitary  $W \in \mathbb{C}^{k \times k}$  such that

$$\|U_R^{(k)} - U^{(k)}W^H\|_2 \leq \sqrt{8\sqrt{k(n-k)}} \sqrt{\frac{\delta}{\nu}}. \quad (4.2.5)$$

Setting  $U_R = U^{(k)}W^H$ , we have inequality 1 with probability at least  $1 - \nu^2$ . Repeating the same argument for  $U_L^{(k)}$ , using this time the fact that  $[A_p, B_p] = \mathbf{IRS}(A^H, B^H, p)$  implies  $\|A_p^H(A_p + B_p)^{-H} - P_{L,|z|>1}\|_2 \leq \delta$  for  $P_{L,|z|>1}$  a projector onto the left deflating subspace corresponding to  $P_{R,|z|>1}$ , we obtain result 2 also with probability at least  $1 - \nu^2$ . Taking a union bound, we have both 1 and 2 with probability at least  $1 - 2\nu^2$ .  $\square$

### 4.3 Divide-and-Conquer Routine

With **IRS**, **GRURV**, and **DEFLATE** (and their exact arithmetic guarantees discussed above) we can now state our divide-and-conquer eigensolver, presented below as **EIG** (Algorithm 5). The main inputs for this routine are a pencil  $(A, B)$  and a grid  $g$  that shatters  $\Lambda_\epsilon(A, B)$  for some  $\epsilon > 0$ . In practice, this will be our perturbed and scaled pencil  $(\tilde{A}, n^\alpha \tilde{B})$  (hence the norm assumption on  $B$  has a factor of  $n^\alpha$  attached) and the shattering grid guaranteed by Theorem 3.11. Recall that shattering implies that  $(A, B)$  is both regular and diagonalizable.

Before proving exact arithmetic guarantees for **EIG**, we first provide a high-level overview of the algorithm to motivate why it works. Throughout, we rely on the analysis of each of the building blocks from the previous section as well as the requirements listed in Algorithm 5.

1. Since **EIG** calls itself recursively, the first three lines check for our stopping criteria. We choose to continue divide-and-conquer until the pencil is  $1 \times 1$ , though as mentioned in the introduction we could choose instead to stop once the pencil is small enough to be handled by another method.
2. The next four lines (4-7) set parameters for the algorithm. Most importantly, they determine how many steps of repeated squaring need to be taken to achieve the desired accuracy (i.e., the value of  $p$  in line 7).
3. Lines 8-15 execute a search over  $g$  for a grid line that sufficiently splits the spectrum, which in our case means separating at least a fifth of the eigenvalues on each side. Since  $g$  shatters  $\Lambda_\epsilon(A, B)$ , a grid line that sufficiently splits the spectrum always exists.
4. We check a line  $\text{Re}(z) = h$  of the grid by applying the Möbius transformation  $S(z) = \frac{z-(h-1)}{z-(h+1)}$  to  $(A, B)$  (line 9).  $S$  maps the grid line to the unit circle while sending the half plane  $\{\text{Re}(z) < h\}$  inside the unit disk. Applying this transformation to  $(A, B)$  sends eigenvalues to the left/right of the dividing line inside/outside the unit circle respectively without changing eigenvectors.
5. Lines 10 and 11 apply **IRS** and **GRURV** to the transformed pencil  $(\mathcal{A}, \mathcal{B})$ . This produces a rank-revealing factorization  $UR_1^{-1}R_2V$  of the approximate projector onto the right deflating subspace corresponding to eigenvectors of  $(\mathcal{A}, \mathcal{B})$  with eigenvalues outside the unit disk (equivalently eigenvectors of  $(A, B)$  with eigenvalues to the right of the selected grid line).
6. In line 12, we leverage the rank-revealing guarantees of **RURV**, and by extension **GRURV**, to read off the rank of the approximate projector. Note that we do this without forming  $R_1^{-1}R_2$ . The grid line is selected if this rank is between  $\frac{1}{5}m$  and  $\frac{4}{5}m$ , where  $m$  is the size of the pencil (which shrinks as we recur).
7. In line 8 we assume that the grid line is vertical, however it is possible that only a horizontal grid line sufficiently splits the spectrum. This is covered in line 14. The remainder of the algorithm similarly assumes the split is vertical, though we note in lines 17, 20, and 22 the adjustments that need to be made if we split by  $\text{Im}(z) = h$  instead of  $\text{Re}(z) = h$ .
8. Once a dividing line is identified, we call **DEFLATE** twice to compute orthonormal bases for both sets of spectral projectors. To recover eigenvectors corresponding to eigenvalues to the left of the line, we apply the alternative Möbius transformation  $S(z) = \frac{z-(h+1)}{z-(h-1)}$ .
9. In line 19 we compute the next pair of subproblems. We then pass these to **EIG** along with pieces of the grid  $g$  and slightly adjusted parameters. In particular, note that the  $\epsilon$  for which  $\Lambda_\epsilon(A, B)$  is shattered shrinks by a factor of  $\frac{4}{5}$  at each step. As we will see, this is necessary to guarantee shattering since  $U_R^{(k)}$ ,  $U_L^{(k)}$ ,  $U_R^{(m-k)}$  and  $U_L^{(m-k)}$  are only approximations of the matrices used in Lemma 4.1.



---

**Algorithm 5** Divide-and-Conquer Eigensolver (**EIG**)

**Input:**  $n \in \mathbb{N}_+$ ,  $A, B \in \mathbb{C}^{m \times m}$ ,  $\epsilon > 0$ ,  $\alpha > 1$ ,  $g$  an  $s_1 \times s_2$  grid with box size  $\omega$ ,  $\beta > 0$  a desired eigenvector accuracy, and  $\theta \in (0, 1)$  a failure probability.

**Requires:**  $m \leq n$ ,  $\|A\|_2 \leq 3$ ,  $\|B\|_2 \leq 3n^\alpha$ ,  $g \subset \{z : |\operatorname{Re}(z)|, |\operatorname{Im}(z)| < 5\}$ , and  $\Lambda_\epsilon(A, B)$  shattered w.r.t.  $g$ .

**Output:**  $T$  an invertible matrix and  $(D_1, D_2)$  a diagonal pencil. The eigenvalues of  $(D_1, D_2)$  each share a grid box of  $g$  with a unique eigenvalue of  $(A, B)$  and each column of  $T$  is an approximate right unit eigenvector of  $(A, B)$ .

---

```
1: if  $m = 1$  then
2:    $T = 1$ ;  $D_1 = A$ ;  $D_2 = B$ 
3: else
4:    $\zeta = 2(\lfloor \log_2(\max\{s_1, s_2\}) + 1 \rfloor)$ 
5:    $\eta = \min \left\{ \frac{4\pi}{315\sqrt{8}} \frac{\beta\epsilon^2}{\omega n^\alpha}, \frac{1}{2 \log_{5/4}(n)} \right\}$ 
6:    $\delta = \min \left\{ \sqrt{\frac{\theta}{10}} \frac{\epsilon^2}{7200n^{2\alpha+3}}, \frac{\theta}{2(\theta+10n^6\zeta)}, \sqrt{\frac{\theta}{10}} \frac{\eta^2}{288n^{2\alpha+3}} \right\}$ 
7:    $p = \left\lceil \max \left\{ 7, \log_2 \left( \frac{105n^\alpha}{\epsilon} - 1 \right), -2 \log_2 \left( -\frac{1}{2} \log_2 \left( 1 - \frac{\epsilon}{105n^\alpha} \right) \right), 1 + \log_2 \left[ \frac{\log_2 \left( \frac{\delta\pi\epsilon}{12n^\alpha m\omega + \delta\pi\epsilon} \right)}{\log_2 \left( 1 - \frac{\epsilon}{105n^\alpha} \right)} \right] \right\} \right\rceil$ 
8:   Choose a grid line  $\operatorname{Re}(z) = h$  of  $g$ 
9:    $(\mathcal{A}, \mathcal{B}) = (A - (h-1)B, A - (h+1)B)$ 
10:   $[A_p, B_p] = \mathbf{IRS}(\mathcal{A}, \mathcal{B}, p)$ 
11:   $[U, R_1, R_2, V] = \mathbf{GRURV}(2, A_p + B_p, A_p, -1, 1)$ 
12:   $k = \# \left\{ i : \left| \frac{R_2(i, i)}{R_1(i, i)} \right| \geq \sqrt{\frac{\theta}{10\zeta}} \frac{1-\delta}{n^3} \right\}$ 
13:  if  $k < \frac{1}{5}m$  or  $k > \frac{4}{5}m$  then
14:    Return to step 7 and choose a new grid line, executing a binary search if necessary. If this fails,
    search over horizontal grid lines  $\operatorname{Im}(z) = h$ , this time setting  $(\mathcal{A}, \mathcal{B}) = (A - i(h-1)B, A - i(h+1)B)$ .
15:  else
16:     $[U_R^{(k)}, U_L^{(k)}] = \mathbf{DEFLATE}(\mathcal{A}, \mathcal{B}, p, k)$ 
17:     $(\mathcal{A}, \mathcal{B}) = (A - (h+1)B, A - (h-1)B)$   $\triangleright$  or  $(\mathcal{A}, \mathcal{B}) = (A - i(h+1)B, A - i(h-1)B)$ 
18:     $[U_R^{(m-k)}, U_L^{(m-k)}] = \mathbf{DEFLATE}(\mathcal{A}, \mathcal{B}, p, m-k)$ 
19:
    
$$(A_{11}, B_{11}) = \left( (U_L^{(k)})^H A U_R^{(k)}, (U_L^{(k)})^H B U_R^{(k)} \right)$$


$$(A_{22}, B_{22}) = \left( (U_L^{(m-k)})^H A U_R^{(m-k)}, (U_L^{(m-k)})^H B U_R^{(m-k)} \right)$$

20:     $g_R = \{z \in g : \operatorname{Re}(z) > h\}$   $\triangleright$  or  $g_R = \{z \in g : \operatorname{Im}(z) > h\}$ 
21:     $[\hat{T}, \hat{D}_1, \hat{D}_2] = \mathbf{EIG}(n, A_{11}, B_{11}, \frac{4}{5}\epsilon, \alpha, g_R, \frac{1}{3}\beta, \theta)$ 
22:     $g_L = \{z \in g : \operatorname{Re}(z) < h\}$   $\triangleright$  or  $g_L = \{z \in g : \operatorname{Im}(z) < h\}$ 
23:     $[\tilde{T}, \tilde{D}_1, \tilde{D}_2] = \mathbf{EIG}(n, A_{22}, B_{22}, \frac{4}{5}\epsilon, \alpha, g_L, \frac{1}{3}\beta, \theta)$ 
24:
    
$$T = \begin{pmatrix} U_R^{(k)} & U_R^{(m-k)} \end{pmatrix} \begin{pmatrix} \hat{T} & 0 \\ 0 & \tilde{T} \end{pmatrix}$$


$$D_1 = \begin{pmatrix} \hat{D}_1 & 0 \\ 0 & \tilde{D}_1 \end{pmatrix}$$


$$D_2 = \begin{pmatrix} \hat{D}_2 & 0 \\ 0 & \tilde{D}_2 \end{pmatrix}$$

25:  end if
26: end if
27: return  $T, D_1, D_2$ 
```

---

10. Once the recursion finishes, **EIG** reconstructs a diagonal pencil  $(D_1, D_2)$  and a set of approximate right eigenvectors  $T$  (line 24).

With this outline in mind, we are now ready to state and prove our main guarantee for **EIG**.

**Theorem 4.8.** *Let  $(A, B)$  and  $g$  be a pencil and grid satisfying the requirements of **EIG**. Then for any choice of  $\theta \in (0, 1)$  and  $\beta > 0$ , exact arithmetic **EIG** applied to  $(A, B)$  and  $g$  satisfies the following with probability at least  $1 - \theta$ .*

1. *The recursive procedure converges and each eigenvalue of the diagonal pencil  $(D_1, D_2)$  shares a grid box with a unique eigenvalue of  $(A, B)$ .*
2. *If  $\sigma_n(B) \geq 1$ , each column  $t_i$  of  $T$  satisfies  $\|t_i - v_i\|_2 \leq \beta$  for some right unit eigenvector  $v_i$  of  $(A, B)$ .*

*Proof.* We start by bounding the probability that the first guarantee does not hold. Since **EIG** calls itself recursively, we do this by bounding the probability of failure for one step of divide and conquer. In this context, success requires two events: first, a dividing line that sufficiently splits the spectrum must be found; second, the subsequent calls to **EIG** must be valid, meaning the inputs satisfy the listed properties.

Computing the probabilities that these occur is fairly lengthy, so to improve readability we number the steps in the proof and provide in bold a description of what each step accomplishes. Throughout, we use the assumptions on the inputs – i.e.  $A, B \in \mathbb{C}^{m \times m}$  with  $m \leq n$ ,  $\|A\|_2 \leq 3$ ,  $\|B\|_2 \leq 3n^\alpha$ , and  $\Lambda_\epsilon(A, B)$  is shattered with respect to the grid  $g$ , which is  $s_1 \times s_2$  consisting of boxes of size  $\omega$ .

**1. Any transformed pencil  $(\mathcal{A}, \mathcal{B})$  in **EIG** satisfies  $d_{(\mathcal{A}, \mathcal{B})} \geq \frac{2}{5}\epsilon$ .**

Consider first a vertical grid line  $\text{Re}(z) = h$  and  $(\mathcal{A}, \mathcal{B}) = (A - (h - 1)B, A - (h + 1)B)$  as in line 9. Suppose  $z \in \Lambda_{\epsilon'}(\mathcal{A}, \mathcal{B})$  for some  $\epsilon' > 0$ . In this case, there exist matrices  $E$  and  $F$  with  $\|E\|_2, \|F\|_2 \leq \epsilon'$  such that  $z$  is an eigenvalue of  $(\mathcal{A} + E, \mathcal{B} + F)$ . If we apply the Möbius transformation  $S(z) = \frac{(h+1)z - (h-1)}{z-1}$  to this pencil, we observe that  $S(z)$  is an eigenvalue of

$$((h+1)(\mathcal{A} + E) - (h-1)(\mathcal{B} + F), (\mathcal{A} + E) - (\mathcal{B} + F)), \quad (4.3.1)$$

or, equivalently,

$$(2A + (h+1)E - (h-1)F, 2B + E - F). \quad (4.3.2)$$

Dividing by two, we conclude that  $S(z)$  is an eigenvalue of  $(A + \frac{h+1}{2}E - \frac{h-1}{2}F, B + \frac{1}{2}E - \frac{1}{2}F)$ , where

$$\left\| \frac{h+1}{2}E - \frac{h-1}{2}F \right\|_2 \leq \frac{|h+1|}{2}\|E\|_2 + \frac{|h-1|}{2}\|F\|_2 \leq \frac{\epsilon'}{2}(|h+1| + |h-1|) \quad (4.3.3)$$

and

$$\left\| \frac{1}{2}E - \frac{1}{2}F \right\|_2 \leq \frac{1}{2}(\|E\|_2 + \|F\|_2) \leq \epsilon'. \quad (4.3.4)$$

Thus,  $S(z)$  belongs to  $\Lambda_{\epsilon''}(A, B)$  for

$$\epsilon'' = \max \left\{ \epsilon', \frac{\epsilon'}{2}(|h+1| + |h-1|) \right\} \leq 5\epsilon', \quad (4.3.5)$$

which means the preimage of  $\Lambda_{\epsilon/5}(\mathcal{A}, \mathcal{B})$  under  $S^{-1}$  is contained in  $\Lambda_\epsilon(A, B)$ . Since  $\Lambda_\epsilon(A, B)$  is shattered with respect to  $g$  and therefore does not intersect the dividing line  $\text{Re}(z) = h$ , we conclude that  $\Lambda_{\epsilon/5}(\mathcal{A}, \mathcal{B})$  does not intersect the unit circle. By [Definition 4.2](#), we obtain  $d_{(\mathcal{A}, \mathcal{B})} \geq \frac{2}{5}\epsilon$ . Making a similar argument for the transformed pencil in line 17 or in the case of a horizontal dividing line  $\text{Im}(z) = h$  yields  $d_{(\mathcal{A}, \mathcal{B})} \geq \frac{2}{5}\epsilon$  for any  $(\mathcal{A}, \mathcal{B})$  appearing in **EIG**. In the next step, we will use this lower bound to control the error in repeated squaring.

**2. The choice of  $p$  guarantees that the error in repeated squaring is at most  $\delta$ .**

Consider the first call to **IRS**, which applies repeated squaring to the transformed pencil  $(\mathcal{A}, \mathcal{B})$ . By

[Theorem 4.3](#), we know that as long as  $p \geq \log_2 \left[ \frac{\|(\mathcal{A}, \mathcal{B})\|_2 - d_{(\mathcal{A}, \mathcal{B})}}{d_{(\mathcal{A}, \mathcal{B})}} \right]$  then

$$\|(A_p + B_p)^{-1}A_p - P_{R,|z|>1}\|_2 \leq \|P_{R,|z|>1}\|_2 \frac{2^{p+3} \left(1 - \frac{d_{(\mathcal{A}, \mathcal{B})}}{\|(\mathcal{A}, \mathcal{B})\|_2}\right)^{2^p}}{\max \left\{0, 1 - 2^{p+2} \left(1 - \frac{d_{(\mathcal{A}, \mathcal{B})}}{\|(\mathcal{A}, \mathcal{B})\|_2}\right)^{2^p}\right\}}. \quad (4.3.6)$$

We just showed  $d_{(\mathcal{A}, \mathcal{B})} \geq \frac{2}{5}\epsilon$  and

$$\|(\mathcal{A}, \mathcal{B})\|_2 \leq \|\mathcal{A}\|_2 + \|\mathcal{B}\|_2 \leq 2\|A\|_2 + (|h-1| + |h+1|)\|B\|_2 \leq 42n^\alpha, \quad (4.3.7)$$

so to satisfy  $p \geq \log_2 \left[ \frac{\|(\mathcal{A}, \mathcal{B})\|_2 - d_{(\mathcal{A}, \mathcal{B})}}{d_{(\mathcal{A}, \mathcal{B})}} \right]$  it is sufficient to take  $p \geq \log_2 \left( \frac{105n^\alpha}{\epsilon} - 1 \right)$ . Similarly, to eliminate the maximum from the denominator of (4.3.6) it is sufficient to take  $p \geq -2 \log_2 \left( \log_2 \left( \frac{105n^\alpha}{105n^\alpha - \epsilon} \right) \right)$  provided  $p > 6$  (which allows us to simplify the bounds by assuming  $\log_2(p+2) < \frac{1}{2}p$ ).

With this, we can now turn to bounding the right hand side of (4.3.6). First, we upper bound  $\|P_{R,|z|>1}\|_2$ . Recall,

$$P_{R,|z|>1} = V \begin{pmatrix} 0 & 0 \\ 0 & I_r \end{pmatrix} V^{-1} = \sum_{j=m-r+1}^m v_j w_j^H \quad (4.3.8)$$

for  $r = \text{rank}(P_{R,|z|>1})$  and  $V$  a matrix that diagonalizes  $B^{-1}A$ .  $v_i$  and  $w_i^H$  are the columns of  $V$  and rows of  $V^{-1}$  respectively, scaled so that  $w_i^H v_i = 1$  with  $v_{m-r+1}, \dots, v_m$  corresponding to eigenvalues of  $(A, B)$  to the right of  $\text{Re}(z) = h$ . Since  $\Lambda_\epsilon(A, B)$  is shattered with respect to  $g$ , each of these eigenvalues  $\lambda_{m-r+1}, \dots, \lambda_m$  is contained in a separate grid box of  $g$ . If  $\Gamma_i$  is the contour of the grid box containing  $\lambda_i$ , this means

$$v_j w_j^H = \frac{1}{2\pi i} \oint_{\Gamma_j} (z - B^{-1}A)^{-1} dz \quad (4.3.9)$$

and therefore

$$P_{R,|z|>1} = \frac{1}{2\pi i} \sum_{j=m-r+1}^m \oint_{\Gamma_j} (z - B^{-1}A)^{-1} dz = \frac{1}{2\pi i} \sum_{j=m-r+1}^m \oint_{\Gamma_j} (zB - A)^{-1} B dz. \quad (4.3.10)$$

Thus, by the triangle inequality,

$$\|P_{R,|z|>1}\|_2 \leq \frac{1}{2\pi} \sum_{j=m-r+1}^m \left\| \oint_{\Gamma_j} (zB - A)^{-1} B dz \right\|_2. \quad (4.3.11)$$

Moreover, applying the ML inequality to each term in this sum, we have

$$\|P_{R,|z|>1}\|_2 \leq \frac{1}{2\pi} \sum_{j=m-r+1}^m 4\omega \sup_{z \in \Gamma_j} \|(zB - A)^{-1} B\|_2 \leq \frac{2\omega \|B\|_2}{\pi} \sum_{j=m-r+1}^m \sup_{z \in \Gamma_j} \|(A - zB)^{-1}\|_2. \quad (4.3.12)$$

Since shattering guarantees  $\Lambda_\epsilon(A, B) \cap \Gamma_j = \emptyset$  and therefore  $\|(A - zB)^{-1}\|_2 \leq \frac{1}{\epsilon(1+|z|)} \leq \frac{1}{\epsilon}$  for all  $z \in \Gamma_j$ , we conclude  $\|P_{R,|z|>1}\|_2 \leq \frac{2\omega r \|B\|_2}{\pi \epsilon}$ . Finally using the fact that  $\|B\|_2 \leq 3n^\alpha$  and  $r \leq m$ , we have a final upper bound  $\|P_{R,|z|>1}\|_2 \leq \frac{6n^\alpha m \omega}{\pi \epsilon}$ .

Combining this bound with  $d_{(\mathcal{A}, \mathcal{B})} \geq \frac{2}{5}\epsilon$  and  $\|(\mathcal{A}, \mathcal{B})\|_2 \leq 42n^\alpha$ , (4.3.6) becomes

$$\|(A_p + B_p)^{-1}A_p - P_{R,|z|>1}\|_2 \leq \frac{6n^\alpha m \omega}{\pi \epsilon} \cdot \frac{2^{p+3} \left(1 - \frac{\epsilon}{105n^\alpha}\right)^{2^p}}{1 - 2^{p+2} \left(1 - \frac{\epsilon}{105n^\alpha}\right)^{2^p}} \quad (4.3.13)$$

for  $p$  sufficiently large (i.e., following the bounds derived above). Thus, we obtain  $\|(A_p + B_p)^{-1}A_p - P_{R,|z|>1}\|_2 \leq \delta$  by taking

$$\frac{6n^\alpha m \omega}{\pi \epsilon} \cdot \frac{2^{p+3} \left(1 - \frac{\epsilon}{105n^\alpha}\right)^{2^p}}{1 - 2^{p+2} \left(1 - \frac{\epsilon}{105n^\alpha}\right)^{2^p}} \leq \delta \quad (4.3.14)$$

which is equivalent to

$$2^p \left[ \frac{p+2}{2^p} + \log_2 \left(1 - \frac{\epsilon}{105n^\alpha}\right) \right] \leq \log_2 \left( \frac{\delta \pi \epsilon}{12n^\alpha m \omega + \delta \pi \epsilon} \right). \quad (4.3.15)$$

Using again the assumption that  $p > 6$  and further taking  $p \geq -2 \log_2 \left(-\frac{1}{2} \log_2 \left(1 - \frac{\epsilon}{105n^\alpha}\right)\right)$  to ensure  $\frac{p+2}{2^p} \leq -\frac{1}{2} \log_2 \left(1 - \frac{\epsilon}{105n^\alpha}\right)$ , we get the desired accuracy as long as

$$2^{p-1} \log_2 \left(1 - \frac{\epsilon}{105n^\alpha}\right) \leq \log_2 \left( \frac{\delta \pi \epsilon}{12n^\alpha m \omega + \delta \pi \epsilon} \right) \quad (4.3.16)$$

which yields a final bound  $p \geq 1 + \log_2 \left[ \log_2 \left( \frac{\delta \pi \epsilon}{12n^\alpha m \omega + \delta \pi \epsilon} \right) / \log_2 \left(1 - \frac{\epsilon}{105n^\alpha}\right) \right]$ .

In the preceding analysis, we derived the following four bounds on  $p$ :

- $p \geq \log_2 \left( \frac{105n^\alpha}{\epsilon} - 1 \right)$  (to allow us to apply [Theorem 4.3](#)).
- $p \geq -2 \log_2 \left( \log_2 \left( \frac{105n^\alpha}{105n^\alpha - \epsilon} \right) \right)$  (to eliminate the maximum from the error bound).
- $p \geq -2 \log_2 \left( -\frac{1}{2} \log_2 \left(1 - \frac{\epsilon}{105n^\alpha}\right) \right)$  (to simplify the upper bound in [\(4.3.6\)](#)).
- $p \geq 1 + \log_2 \left[ \log_2 \left( \frac{\delta \pi \epsilon}{12n^\alpha m \omega + \delta \pi \epsilon} \right) / \log_2 \left(1 - \frac{\epsilon}{105n^\alpha}\right) \right]$  (to ensure an error of at most  $\delta$  given the other three bounds).

Since the third bound is always at least as large as the second and since we also assumed  $p > 6$ , we conclude that  $\|(A_p + B_p)^{-1}A_p - P_{R,|z|>1}\|_2 \leq \delta$  for the  $p$  chosen in line 7 of **EIG**. Note that since  $\|\mathcal{A}^H\|_2 = \|\mathcal{A}\|_2$ ,  $\|\mathcal{B}^H\|_2 = \|\mathcal{B}\|_2$ ,  $d_{(\mathcal{A}^H, \mathcal{B}^H)} = d_{(\mathcal{A}, \mathcal{B})}$ , and  $\Lambda_\epsilon(\mathcal{A}^H, \mathcal{B}^H)$  is shattered with respect to the grid  $g^H = \{\bar{z} : z \in g\}$ , the same argument guarantees that running repeated squaring on  $\mathcal{A}^H$ , and  $\mathcal{B}^H$  has error at most  $\delta$ . Similarly, the same results hold for the other transformed pencils in lines 14 and 17 since in all cases  $\|(\mathcal{A}, \mathcal{B})\|_2 \leq 42n^\alpha$  and  $d_{(\mathcal{A}, \mathcal{B})} \geq \frac{2}{5}\epsilon$ .

### 3. A dividing line that sufficiently splits the spectrum exists.

A dividing line sufficiently splits the spectrum if it separates at least  $\frac{1}{5}m$  of the  $m$  eigenvalues of  $(A, B)$ . Suppose that no vertical line of  $g$  does this. In this case, there exists adjacent vertical lines between which more than  $\frac{3}{5}m$  eigenvalues lie. Since no eigenvalues share the same grid box, this implies that a horizontal grid line must sufficiently split the spectrum.

### 4. With probability at least $1 - \frac{\theta}{10n^4}$ , **EIG** finds a dividing line that separates exactly $k$ eigenvalues to the right such that $\frac{1}{5}m \leq k \leq \frac{4}{5}m$ .

To obtain a lower bound on this probability, we first compute the probability that for any grid line  $\text{Re}(z) = h$  the value of  $k$  at line 12 is equal to the number of eigenvalues of  $(A, B)$  to the right of the line.

Suppose  $(A, B)$  has  $r$  eigenvalues to the right of  $\text{Re}(z) = h$ . In this case, we know in line 10 that  $(A_p + B_p)^{-1}A_p$  approaches a rank- $r$  projector  $P_{R,|z|>1}$ . Now  $k$  is obtained by computing a rank-revealing factorization  $U_R R_1^{-1} R_2 V = (A_p + B_p)^{-1}A_p$  via **GRURV** and then counting the diagonal entries of  $R_1^{-1}R_2$  that have modulus above a certain threshold. With this in mind, write

$$R_1^{-1}R_2 = \begin{bmatrix} R_{11} & R_{12} \\ 0 & R_{22} \end{bmatrix} \quad (4.3.17)$$

for  $R_{11}$  an  $r \times r$  matrix. Since we are working in exact arithmetic, **GRURV** satisfies all of the guarantees of exact arithmetic **RURV**. In particular, extending [17, Theorem 5.2] to complex matrices,

$$\sigma_r(R_{11}) \geq \sigma_r((A_p + B_p)^{-1}A_p)\sigma_r(X_{11}) \quad (4.3.18)$$

where  $X_{11}$  is the upper left  $r \times r$  block of  $X = Q^H V^H$  for the SVD  $(A_p + B_p)^{-1}A_p = P\Sigma Q^H$ . Similarly, by [7, Lemma 4.1],

$$\|R_{22}\|_2 \leq \frac{\sigma_{r+1}((A_p + B_p)^{-1}A_p)}{\sigma_r(X_{11})}. \quad (4.3.19)$$

Now  $\|(A_p + B_p)^{-1}A_p - P_{R,|z|>1}\|_2 \leq \delta$  as shown in step two above, so since the rank- $r$  projector  $P_{R,|z|>1}$  satisfies  $\sigma_r(P_{R,|z|>1}) = 1$  and  $\sigma_{r+1}(P_{R,|z|>1}) = 0$ , we have by the stability of singular values  $\sigma_r((A_p + B_p)^{-1}A_p) \geq 1 - \delta$  and  $\sigma_{r+1}((A_p + B_p)^{-1}A_p) \leq \delta$ . Moreover, since  $X$  is Haar unitary, we have by [9, Proposition C.3]

$$\mathbb{P}\left[\frac{1}{\sigma_r(X_{11})} \leq \frac{\sqrt{r(m-r)}}{\nu}\right] \geq 1 - \nu^2 \quad (4.3.20)$$

for any  $\nu \in (0, 1]$ . Applying these to (4.3.18) and (4.3.19) with  $\nu = \sqrt{\frac{\theta}{10\zeta}} \frac{1}{n^2}$  for  $\zeta = 2(\lfloor \log_2(s) + 1 \rfloor)$  and  $s = \max\{s_1, s_2\}$ , we have

$$\sigma_r(R_{11}) \geq (1 - \delta) \sqrt{\frac{\theta}{10\zeta}} \frac{1}{n^2 \sqrt{r(m-r)}} \geq \sqrt{\frac{\theta}{10\zeta}} \frac{1 - \delta}{n^3} \quad (4.3.21)$$

and

$$\|R_{22}\|_2 \leq \delta \sqrt{r(m-r)} n^2 \sqrt{\frac{10\zeta}{\theta}} \leq \delta n^3 \sqrt{\frac{10\zeta}{\theta}} \quad (4.3.22)$$

with probability at least  $1 - \frac{\theta}{10\zeta n^4}$ . Since the eigenvalues of any matrix are bounded in modulus above and below by its singular values and the eigenvalues of  $R_{11}$  and  $R_{22}$  are their diagonal entries, we conclude  $|R_{11}(i, i)| \geq \sqrt{\frac{\theta}{10\zeta}} \frac{1 - \delta}{n^3}$  for all  $1 \leq i \leq r$  while  $|R_{22}(j, j)| \leq \delta n^3 \sqrt{\frac{10\zeta}{\theta}}$  for all  $1 \leq j \leq m - r$  with probability at least  $1 - \frac{\theta}{10\zeta n^4}$ . Since the requirement in line 6 that  $\delta \leq \frac{\theta}{2(\theta + 10n^6\zeta)}$  guarantees  $\sqrt{\frac{\theta}{10\zeta}} \frac{1 - \delta}{n^3} > \delta n^3 \sqrt{\frac{10\zeta}{\theta}}$ , this implies that  $k = r$  with probability at least  $1 - \frac{\theta}{10\zeta n^4}$ .

We have shown so far that with high probability the value of  $k$  at line 12 is equal to the number of eigenvalues to the right of the vertical dividing line selected four lines earlier. Since repeating this argument yields the same probability of success when checking a horizontal grid line and we know a dividing line that separates at least  $\frac{1}{5}m$  eigenvalues must exist, we can therefore lower bound the probability that **EIG** finds a suitable line by requiring that the value of  $k$  is accurate for all lines that are checked. Since we do at most two binary searches to find a good enough grid line, we check at most  $\zeta$  lines. By a union bound, we conclude that a suitable line is found, and  $k$  is computed accurately for that line, with probability at least  $1 - \frac{\theta}{10n^4}$ .

5. Assuming  $k$  is computed correctly in line 12, there exists matrices  $\hat{U}_R^{(k)}, \hat{U}_L^{(k)} \in \mathbb{C}^{k \times m}$  and  $\hat{U}_R^{(m-k)}, \hat{U}_L^{(m-k)} \in \mathbb{C}^{(m-k) \times m}$  with orthonormal columns spanning corresponding right and left deflating subspaces of  $(A, B)$  such that

$$(a) \ \|U_R^{(k)} - \hat{U}_R^{(k)}\|_2 \leq \sqrt{\sqrt{\frac{10}{\theta}} 8n^3 \delta}$$

$$(b) \ \|U_L^{(k)} - \hat{U}_L^{(k)}\|_2 \leq \sqrt{\sqrt{\frac{10}{\theta}} 8n^3 \delta}$$

$$(c) \ \|U_R^{(m-k)} - \hat{U}_R^{(m-k)}\|_2 \leq \sqrt{\sqrt{\frac{10}{\theta}} 8n^3 \delta}$$

$$(d) \quad \|U_L^{(m-k)} - \hat{U}_L^{(m-k)}\|_2 \leq \sqrt{\sqrt{\frac{10}{\theta}} 8n^3 \delta}$$

With probability at least  $1 - \frac{2\theta}{5n^4}$ .

This result comes from applying [Theorem 4.7](#) twice with  $\nu = \sqrt{\frac{\theta}{10n^4}}$  and taking a union bound. In both cases, we use the fact that  $p$  is large enough to guarantee error in repeated squaring is at most  $\delta$  and consequently

$$\sqrt{8\sqrt{k(m-k)}} \sqrt{\frac{\delta}{\nu}} \leq \sqrt{8n\sqrt{\frac{10n^4}{\theta}} \delta} = \sqrt{\sqrt{\frac{10}{\theta}} 8n^3 \delta}. \quad (4.3.23)$$

## 6. Union bound on events that guarantee success for one step.

Let  $E_a, E_b, E_c$ , and  $E_d$  be events that correspond to the results (a), (b), (c), and (d) from step 5 and let  $E_k$  be the event that a sufficient dividing line is found and  $k$  computed accurately. We have just shown

$$\mathbb{P}(E_a \cap E_b \cap E_c \cap E_d \mid E_k) \geq 1 - \frac{2\theta}{5n^4}. \quad (4.3.24)$$

Since we also know  $\mathbb{P}(E_k) \geq 1 - \frac{\theta}{10n^4}$ , we conclude

$$\begin{aligned} \mathbb{P}(E_a \cap E_b \cap E_c \cap E_d \cap E_k) &= \mathbb{P}(E_a \cap E_b \cap E_c \cap E_d \mid E_k) \mathbb{P}(E_k) \\ &\geq \left(1 - \frac{2\theta}{5n^4}\right) \left(1 - \frac{\theta}{10n^4}\right) \\ &\geq 1 - \frac{\theta}{2n^4}. \end{aligned} \quad (4.3.25)$$

In the remainder of the proof, we will show that conditioning on these events guarantees success for one step of **FIG**.

## 7. If $E_a, E_b, E_c$ , and $E_d$ hold, then $\Lambda_{4\epsilon/5}(A_{11}, B_{11})$ and $\Lambda_{4\epsilon/5}(A_{22}, B_{22})$ are both shattered with respect to $g$ .

Let  $\hat{U}_R^{(k)}, \hat{U}_L^{(k)}, \hat{U}_R^{(m-k)}$ , and  $\hat{U}_L^{(m-k)}$  be the matrices such that  $\|U_R^{(k)} - \hat{U}_R^{(k)}\|_2, \|U_L^{(k)} - \hat{U}_L^{(k)}\|_2, \|U_R^{(m-k)} - \hat{U}_R^{(m-k)}\|_2$ , and  $\|U_L^{(m-k)} - \hat{U}_L^{(m-k)}\|_2$  are all bounded above by  $\sqrt{\sqrt{\frac{10}{\theta}} 8n^3 \delta}$  as in step five. Since  $\delta \leq \sqrt{\frac{\theta}{10}} \frac{\epsilon^2}{7200n^{2\alpha+3}}$ , we can replace this upper bound with  $\frac{\epsilon}{30n^\alpha}$ . With this in mind, let

$$\begin{aligned} (\hat{A}_{11}, \hat{B}_{11}) &= \left( (\hat{U}_L^{(k)})^H A \hat{U}_R^{(k)}, (\hat{U}_L^{(k)})^H B \hat{U}_R^{(k)} \right) \\ (\hat{A}_{22}, \hat{B}_{22}) &= \left( (\hat{U}_L^{(m-k)})^H A \hat{U}_R^{(m-k)}, (\hat{U}_L^{(m-k)})^H B \hat{U}_R^{(m-k)} \right). \end{aligned} \quad (4.3.26)$$

Note that by [Lemma 4.1](#),  $\Lambda_\epsilon(\hat{A}_{11}, \hat{B}_{11})$  and  $\Lambda_\epsilon(\hat{A}_{22}, \hat{B}_{22})$  are both contained in  $\Lambda_\epsilon(A, B)$  and therefore shattered with respect to  $g$ . At the same time,

$$\begin{aligned} \|A_{11} - \hat{A}_{11}\|_2 &= \|(U_L^{(k)})^H A U_R^{(k)} - (\hat{U}_L^{(k)})^H A \hat{U}_R^{(k)}\|_2 \\ &= \|(U_L^{(k)})^H A U_R^{(k)} - (\hat{U}_L^{(k)})^H A U_R^{(k)} + (\hat{U}_L^{(k)})^H A U_R^{(k)} - (\hat{U}_L^{(k)})^H A \hat{U}_R^{(k)}\|_2 \\ &\leq \|(U_L^{(k)} - \hat{U}_L^{(k)})^H A U_R^{(k)}\|_2 + \|(\hat{U}_L^{(k)})^H A (U_R^{(k)} - \hat{U}_R^{(k)})\|_2 \\ &\leq \|U_L^{(k)} - \hat{U}_L^{(k)}\|_2 \|A\|_2 + \|A\|_2 \|U_R^{(k)} - \hat{U}_R^{(k)}\|_2 \\ &\leq 6n^\alpha \frac{\epsilon}{30n^\alpha} \\ &= \frac{\epsilon}{5} \end{aligned} \quad (4.3.27)$$

and similarly  $\|B_{11} - \hat{B}_{11}\|_1 \leq \frac{\epsilon}{5}$ . Thus, by [Lemma 3.12](#),  $\Lambda_{4\epsilon/5}(A_{11}, B_{11})$  is shattered with respect to  $g$ . Repeating this argument for  $(A_{22}, B_{22})$  and  $(\hat{A}_{22}, \hat{B}_{22})$ , we conclude  $\Lambda_{4\epsilon/5}(A_{22}, B_{22})$  is also shattered with respect to  $g$ .

In the preceding analysis, we showed that for one step of recursion in **FIG**, a sufficient dividing line is found,  $k$  is computed correctly, and  $\Lambda_{4\epsilon/5}(A_{11}, B_{11})$  and  $\Lambda_{4\epsilon/5}(A_{22}, B_{22})$  are both shattered with respect to  $g$ , and therefore also with respect to the half grids  $g_R$  and  $g_L$ , with probability at least  $1 - \frac{\theta}{2n^4}$ . Since multiplying by matrices with orthonormal columns will preserve the norm requirements, we conclude that the subsequent calls to **FIG** in lines 21 and 23 are valid when these events occur. Hence, each recursive step succeeds with probability at least  $1 - \frac{\theta}{2n^4}$ . Since the recursive tree of **FIG** has depth at most  $\log_{5/4}(n)$  and each step calls **FIG** twice, a union bound implies that the first guarantee of **FIG** fails with probability at most

$$2 \cdot 2^{\log_{5/4}(n)} \frac{\theta}{2n^4} \leq 2n^4 \frac{\theta}{2n^4} = \theta. \quad (4.3.28)$$

We turn now to the second guarantee when  $\sigma_n(B) \geq 1$ . In this case, we will show that conditioning on the same events that ensure the first guarantee also imply the second. Since **FIG** builds the approximate eigenvectors recursively, we do this inductively.

The base case here corresponds to  $m = 1$ , in which case **FIG** gets the one right unit eigenvector ( $v = 1$ ) exactly correct. Suppose now we are reconstructing the eigenvectors of  $(A', B')$  from the two sub-problems  $(A_{11}, B_{11})$  and  $(A_{22}, B_{22})$  it is split into.  $(A', B')$  here is any pencil obtained in the divide and conquer process.

Let  $\hat{T}$  and  $\tilde{T}$  be the invertible matrices obtained from applying **FIG** to  $(A_{11}, B_{11})$  and  $(A_{22}, B_{22})$  as in lines 21 and 23 of the algorithm. Since these calls to **FIG** pass the parameter  $\frac{\beta}{3}$ , we can assume each column of  $\hat{T}$  or  $\tilde{T}$  is at most  $\frac{\beta}{3}$  away from a true unit right eigenvector of  $(A_{11}, B_{11})$  or  $(A_{22}, B_{22})$ . In addition, let

$$T = \begin{pmatrix} U_R^{(k)} & U_R^{(m-k)} \end{pmatrix} \begin{pmatrix} \hat{T} & 0 \\ 0 & \tilde{T} \end{pmatrix} \quad (4.3.29)$$

be the matrix of approximate eigenvectors of  $(A', B')$  computed in line 24. Finally let  $\hat{U}_R^{(k)}$  and  $\hat{U}_R^{(m-k)}$  be the true matrices approximated by  $U_R^{(k)}$  and  $U_R^{(m-k)}$ , as in step 5 above.

Consider now a column  $t_i$  of  $T$ . It suffices to handle the case where  $t_i = U_R^{(k)} \hat{t}_i$  for a column  $\hat{t}_i$  of  $\hat{T}$ , as the same argument applies exactly if  $t_i = U_R^{(m-k)} \tilde{t}_i$  for  $\tilde{t}_i$  a column of  $\tilde{T}$ . By our induction hypothesis, we know there exists a true right unit eigenvector  $\hat{v}_i$  of  $(A_{11}, B_{11})$  such that

$$\|\hat{t}_i - \hat{v}_i\|_2 \leq \frac{\beta}{3}. \quad (4.3.30)$$

Now let  $(\hat{A}_{11}, \hat{B}_{11})$  be the true problem approximated by  $(A_{11}, B_{11})$ . Conditioning on the same events used above, we know (following the same arguments as in steps 5 and 7)

$$\|A_{11} - \hat{A}_{11}\|_2, \|B_{11} - \hat{B}_{11}\|_2 \leq 6n^\alpha \|U_R^{(k)} - \hat{U}_R^{(k)}\|_2 \leq 6n^\alpha \sqrt{\sqrt{\frac{10}{\theta}} 8n^3 \delta}, \quad (4.3.31)$$

which, applying the bound  $\delta \leq \sqrt{\frac{\theta}{10} \frac{\eta^2}{288n^{2\alpha+3}}}$ , becomes

$$\|A_{11} - \hat{A}_{11}\|_2, \|B_{11} - \hat{B}_{11}\|_2 \leq 6n^\alpha \sqrt{\sqrt{\frac{10}{\theta}} 8n^3 \sqrt{\frac{\theta}{10} \frac{\eta^2}{288n^{2\alpha+3}}}} = \eta. \quad (4.3.32)$$

Thus, by [Lemma 3.13](#), there exists a right unit eigenvector  $\bar{v}_i$  of  $(\hat{A}_{11}, \hat{B}_{11})$  such that

$$\|\hat{v}_i - \bar{v}_i\|_2 \leq \frac{\sqrt{8}\omega}{\pi} \frac{\eta}{\epsilon(\epsilon - \eta)} (1 + \|\hat{B}_{11}^{-1} \hat{A}_{11}\|_2) \|\hat{B}_{11}\|_2. \quad (4.3.33)$$

To simplify this bound, we first observe that (again by the argument made in step 7 above) we can assume  $\epsilon - \eta \geq \frac{4}{5}\epsilon$ . In addition,  $\|\hat{A}_{11}\|_2 \leq 3$  and  $\|\hat{B}_{11}\|_2 \leq 3n^\alpha$ . Finally, since  $\sigma_n(B) \geq 1$  and any split of divide



and conquer can decrease the smallest singular value by at most  $\eta$  (by the stability of singular values), and since the decision tree of **EIG** has depth at most  $\log_{5/4}(n)$ , the bound  $\eta \leq \frac{1}{2 \log_{5/4}(n)}$  ensures

$$\sigma_n(\hat{B}_{11}) \geq 1 - \log_{5/4}(n)\eta \geq \frac{1}{2}. \quad (4.3.34)$$

Putting everything together, we have

$$\|\hat{v}_i - \bar{v}_i\|_2 \leq \frac{\sqrt{8}\omega}{\pi} \frac{\eta}{\frac{4}{5}\epsilon^2} \left(1 + \frac{\|\hat{A}_{11}\|_2}{\sigma_n(\hat{B}_{11})}\right) \|\hat{B}_{11}\|_2 \leq \frac{105\sqrt{8}}{4\pi} \frac{\omega n^\alpha}{\epsilon^2} \eta \leq \frac{\beta}{3}. \quad (4.3.35)$$

since  $\eta \leq \frac{4\pi}{315\sqrt{8}} \frac{\beta\epsilon^2}{\omega n^\alpha}$ . Now let  $v_i = \hat{U}_R^{(k)} \bar{v}_i$ , which is a true right unit eigenvector of  $(A', B')$ . By construction, we have

$$\begin{aligned} \|t_i - v_i\|_2 &= \|U_R^{(k)} \hat{t}_i - \hat{U}_R^{(k)} \bar{v}_i\|_2 \\ &= \|U_R^{(k)} \hat{t}_i - U_R^{(k)} \hat{v}_i + U_R^{(k)} \hat{v}_i - \hat{U}_R^{(k)} \hat{v}_i + \hat{U}_R^{(k)} \hat{v}_i - \hat{U}_R^{(k)} \bar{v}_i\|_2 \\ &\leq \|U_R^{(k)} (\hat{t}_i - \hat{v}_i)\|_2 + \|(U_R^{(k)} - \hat{U}_R^{(k)}) \hat{v}_i\|_2 + \|\hat{U}_R^{(k)} (\hat{v}_i - \bar{v}_i)\|_2. \\ &\leq \|\hat{t}_i - \hat{v}_i\|_2 + \|U_R^{(k)} - \hat{U}_R^{(k)}\|_2 + \|\hat{v}_i - \bar{v}_i\|_2. \end{aligned} \quad (4.3.36)$$

Applying (4.3.30) and (4.3.35) to this and using the fact that  $\|U_R^{(k)} - \hat{U}_R^{(k)}\|_2 \leq \frac{\beta}{3}$ , we conclude

$$\|t_i - v_i\|_2 \leq \frac{\beta}{3} + \frac{\beta}{3} + \frac{\beta}{3} = \beta. \quad (4.3.37)$$

By induction, we obtain the same bound for the approximate and true eigenvectors of  $(A, B)$ .  $\square$

The condition on the eigenvector guarantee in Theorem 4.8 (i.e., that  $\sigma_n(B) \geq 1$ ) may seem restrictive, but it reflects the use-case in the following section. That is, while it is possible to adjust the parameters of **EIG** to allow for less strict lower bounds on  $\sigma_n(B)$ , we plan to apply **EIG** to the perturbed and scaled  $(\tilde{A}, n^\alpha \tilde{B})$ , where by construction  $\sigma_n(n^\alpha \tilde{B}) \geq 1$  with high probability.

## 5 Randomized Pencil Diagonalization

We can now prove our main result, presented in the introduction as Theorem 1.1. First, we state our algorithm for producing an approximate diagonalization and show it succeeds in exact arithmetic with high probability. We follow that with corresponding forward error guarantees and an evaluation of the complexity of the routine.

### 5.1 Diagonalization Routine

In the previous section, we constructed an eigensolver that produces approximations of the eigenvalues and eigenvectors of  $(\tilde{A}, n^\alpha \tilde{B})$ , contained in the outputs  $(D_1, D_2)$  and  $T$  respectively. Since the  $n^\alpha$  scaling only changes eigenvalues and can be easily undone, this effectively yields eigenvalues/eigenvectors for  $(\tilde{A}, \tilde{B})$ . That is,  $T$  contains approximate eigenvectors of  $(\tilde{A}, \tilde{B})$  while the corresponding eigenvalues belong to  $(n^\alpha D_1, D_2)$  or equivalently  $(D_1, n^{-\alpha} D_2)$ . This prompts the question: how accurate are these approximations?

Unfortunately, as noted earlier, little can be said. While perturbation results do exist for the simple eigenvalues of a regular pencil or for the eigenvalues of a regular pencil obtained by perturbing a diagonalizable one [51, §VI Theorems 2.2 and 2.6], these are typically stated in terms of a chordal metric on the Riemann sphere. Our version of Bauer-Fike (Theorem 2.20) provides a route to some Euclidean norm bounds, which we state below, but its dependence on the smallest singular value of  $B$  means it is only useful if  $B$  is far from singular. This reflects a reality of our algorithm: **EIG** always produces a set of finite eigenvalues, and we cannot identify which ones are close to true finite eigenvalues of  $(A, B)$  and which ones are meant to be infinite.

Instead, we leverage **EIG** to produce an approximate diagonalization of  $(A, B)$ . Recall from Section 2

that if  $B$  is invertible and  $T$  contains right eigenvectors of  $(A, B)$  then  $S = BT$  produces a diagonalization of the pencil such that  $S^{-1}AT = D_1$  and  $S^{-1}BT = I$ . Using again the fact that  $\tilde{B}$  is invertible with high probability, we conclude that if  $T$  is the output of **EIG** then it and  $\tilde{B}T$  should approximately diagonalize  $(\tilde{A}, \tilde{B})$ . Assuming  $\|A - \tilde{A}\|_2$  and  $\|B - \tilde{B}\|_2$  are small, this produces an approximate diagonalization of  $(A, B)$ . We state **RPD**, a routine that wraps around **EIG** to produce this diagonalization, as [Algorithm 6](#) below.

---

**Algorithm 6** Randomized Pencil Diagonalization (**RPD**)

---

**Input:**  $A, B \in \mathbb{C}^{n \times n}$  and  $\varepsilon < 1$  a desired accuracy.

**Requires:**  $\|A\|_2, \|B\|_2 \leq 1$

**Output:** Nonsingular  $S, T$  and diagonal  $D$  such that  $\|A - SDT^{-1}\|_2, \|B - SIT^{-1}\|_2 \leq \varepsilon$  with high probability.

---

```

1:  $\gamma = \frac{\varepsilon}{16}$ 
2:  $\alpha = \frac{2 \lceil 2 \log_n(1/\gamma) + 3 \rceil}{2}$ 
3:  $\epsilon = \gamma^5 / (64n^{\frac{11\alpha+25}{3}} + \gamma^5)$ 
4:  $\beta = \frac{\varepsilon \gamma^2}{24(1+4\gamma)} n^{-3\alpha-5}$ 
5:  $\omega = \frac{\gamma^4}{4} n^{-\frac{8\alpha+13}{3}}$ 
6: Draw two independent Ginibre matrices  $G_1, G_2 \in \mathbb{C}^{n \times n}$ 
7:  $(\tilde{A}, \tilde{B}) = (A + \gamma G_1, B + \gamma G_2)$ 
8: Draw  $z$  uniformly from the box of side length  $\omega$  cornered at  $-4 - 4i$ 
9:  $g = \text{grid}(z, \omega, \lceil 8/\omega \rceil, \lceil 8/\omega \rceil)$ 
10:  $[T, D_1, D_2] = \mathbf{EIG}(n, \tilde{A}, n^\alpha \tilde{B}, \epsilon, \alpha, g, \beta, 1/n)$ 
11: for  $i = 1 : n$  do
12:    $D(i, i) = n^\alpha \frac{D_1(i, i)}{D_2(i, i)}$ 
13: end for
14:  $S = \tilde{B}T$ 
15: return  $S, T, D$ 

```

---

Note that the assumption  $\|A\|_2, \|B\|_2 \leq 1$  is essentially made for convenience; we can obtain a diagonalization of any pencil  $(A, B)$  via **RPD** by first normalizing the matrices accordingly. In [Theorem 5.1](#), we show that **RPD** produces an approximate diagonalization with the given accuracy in exact arithmetic, thereby proving the bulk of our main result, [Theorem 1.1](#). For reference, [Figure 3](#) provides a high level overview of **RPD**, including the details of its call to **EIG**.

**Theorem 5.1.** *For any  $A, B \in \mathbb{C}^{n \times n}$  with  $\|A\|_2, \|B\|_2 \leq 1$ , the outputs of exact arithmetic **RPD** satisfy*

$$\|A - SDT^{-1}\|_2, \|B - SIT^{-1}\|_2 \leq \varepsilon$$

*with probability at least*

$$\left[1 - \frac{82}{n} - \frac{531441}{16n^2}\right] \left[1 - \frac{1}{n} - 4e^{-n}\right] \left[1 - \frac{1}{n}\right].$$

*Proof.* Consider the perturbed and scaled pencil  $(\tilde{A}, n^\alpha \tilde{B})$ . By [Theorem 3.11](#) and its proof, with probability at least  $\left(1 - \frac{82}{n} - \frac{531441}{16n^2}\right) \left(1 - \frac{n^{2-2\alpha}}{\gamma^2} - 4e^{-n}\right)$  we have the following:

1.  $\|G_1\|_2, \|G_2\|_2 \leq 4$ ,
2.  $\|\tilde{A}\|_2 \leq 3$ ,
3.  $\|n^\alpha \tilde{B}\|_2 \leq 3n^\alpha$ ,
4.  $\sigma_n(n^\alpha \tilde{B}) \geq 1$ ,
5.  $\Lambda(\tilde{A}, n^\alpha \tilde{B}) \subseteq D(0, 3)$ ,
6.  $\kappa_V(n^{-\alpha} \tilde{B}^{-1} \tilde{A}) \leq \frac{n^{\alpha+2}}{\gamma}$ ,

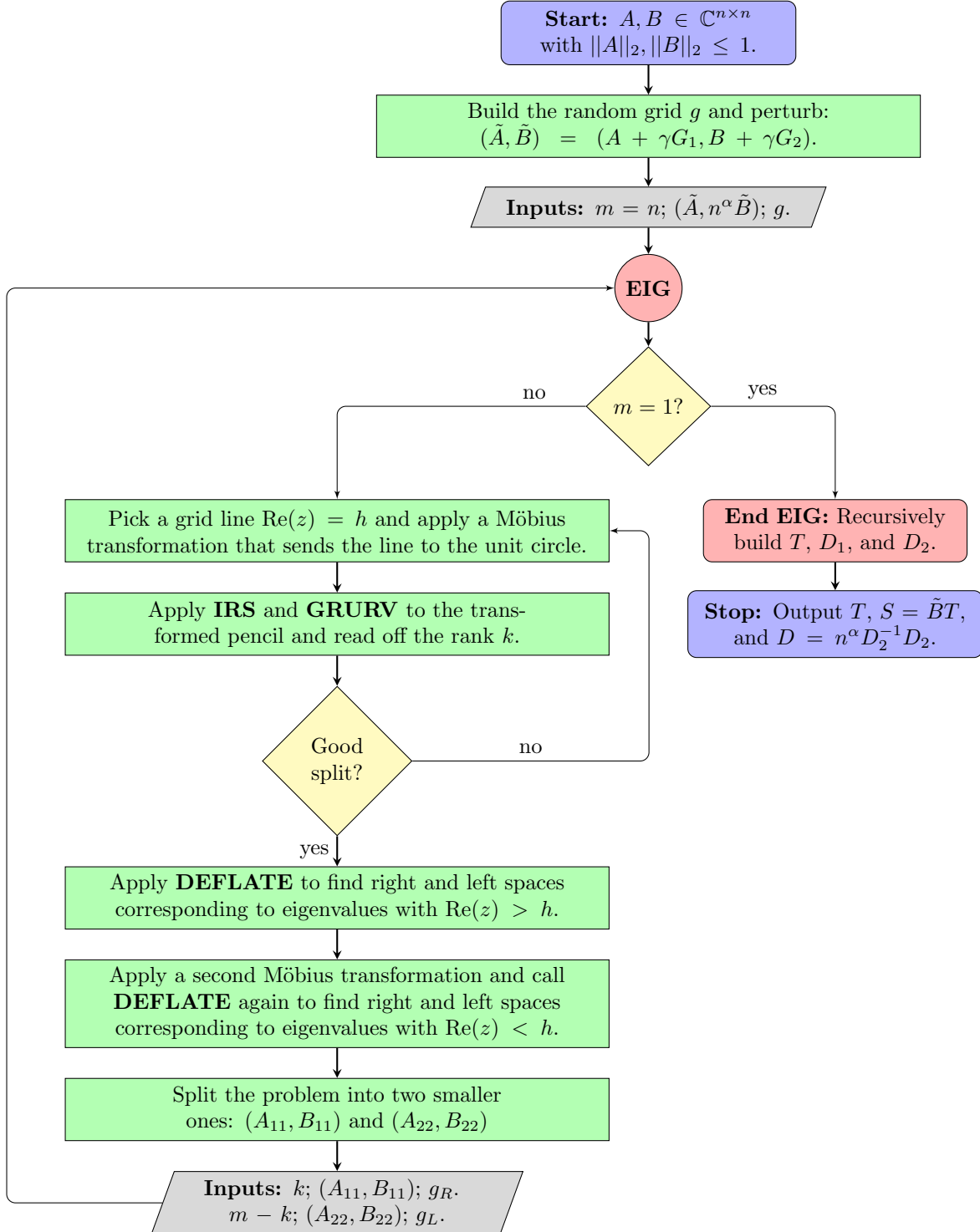


Figure 3: A diagram of **RPD** (Algorithm 6) for producing an approximate diagonalization of  $(A, B)$ . As in the pseudocode, we assume for simplicity that each split in **EIG** is made by a vertical grid line.

7.  $\Lambda_\epsilon(\tilde{A}, n^\alpha \tilde{B})$  is shattered with respect to the grid  $g$  (for  $\epsilon$  as in line 3).

Conditioning on these events, we observe that 2, 3, and 7 ensure that the call to **EIG** in line 10 is valid, meaning with probability at least  $1 - \frac{1}{n}$  we can add the guarantees of [Theorem 4.8](#) to our list:

8. Each eigenvalue of  $(D_1, D_2)$  shares a grid box of  $g$  with a true eigenvalue of  $(\tilde{A}, n^\alpha \tilde{B})$ .

9. Since  $\sigma_n(n^\alpha \tilde{B}) \geq 1$  (item 4) each column  $t_i$  of  $T$  satisfies  $\|t_i - v_i\|_2 \leq \beta$  for  $v_i$  a true unit right eigenvector of  $(\tilde{A}, n^\alpha \tilde{B})$ .

By the definition of conditional probability, all nine of these events occur simultaneously with probability at least

$$\left[1 - \frac{82}{n} - \frac{531441}{16n^2}\right] \left[1 - \frac{n^{2-2\alpha}}{\gamma^2} - 4e^{-n}\right] \left[1 - \frac{1}{n}\right]. \quad (5.1.1)$$

Since the choice of  $\alpha$  in line 2 guarantees

$$\frac{n^{2-2\alpha}}{\gamma^2} \leq \frac{1}{n} \quad (5.1.2)$$

(5.1.1) can be bounded from below by

$$\left[1 - \frac{82}{n} - \frac{531441}{16n^2}\right] \left[1 - \frac{1}{n} - 4e^{-n}\right] \left[1 - \frac{1}{n}\right]. \quad (5.1.3)$$

To complete the proof we show that the nine items listed above guarantee both  $\|A - SDT^{-1}\|_2 \leq \epsilon$  and  $\|B - SIT^{-1}\|_2 \leq \epsilon$ . The second of these is trivial: since  $\gamma = \frac{\epsilon}{16}$  and  $SIT^{-1} = \tilde{B}$  we have

$$\|B - SIT^{-1}\|_2 = \|B - \tilde{B}\|_2 = \|\gamma G_2\|_2 \leq 4\gamma = \frac{\epsilon}{4} < \epsilon. \quad (5.1.4)$$

To show the same for  $A$  and  $SDT^{-1}$  we use the following key fact. Let  $V$  be the matrix whose columns contain, in order, the true right unit eigenvectors of  $(\tilde{A}, n^\alpha \tilde{B})$  guaranteed by item 9. Since  $\tilde{B}$  is invertible with probability one and  $(\tilde{A}, \tilde{B})$  and  $(\tilde{A}, n^\alpha \tilde{B})$  have the same set of eigenvectors,  $V$  diagonalizes  $\tilde{B}^{-1}\tilde{A}$ . Thus, there exists a diagonal matrix  $\Lambda$  such that  $\tilde{B}^{-1}\tilde{A} = V\Lambda V^{-1}$ . Moreover, since the eigenvalue of  $(\tilde{A}, n^\alpha \tilde{B})$  corresponding to  $v_i$  shares a grid box of  $g$  with the eigenvalue of  $(D_1, D_2)$  corresponding to  $t_i$  (this was how  $v_i$  was found in the proof of [Theorem 4.8](#)), each diagonal entry of  $\Lambda$  is at most  $\sqrt{2}n^\alpha\omega$  away from the corresponding diagonal entry of  $D = n^\alpha D_2^{-1}D_1$ . Note that the eigenvalues of  $(D_1, D_2)$  are all contained in  $g$ , which guarantees that  $D_2$  is invertible. With all of this in mind, expand  $\|A - SDT^{-1}\|_2$  as follows:

$$\begin{aligned} \|A - SDT^{-1}\|_2 &= \|A - \tilde{A} + \tilde{A} - SDT^{-1}\|_2 \\ &\leq \|A - \tilde{A}\|_2 + \|\tilde{A} - SDT^{-1}\|_2 \\ &\leq \|A - \tilde{A}\|_2 + \|\tilde{B}\|_2 \|\tilde{B}^{-1}\tilde{A} - TDT^{-1}\|_2 \\ &\leq 4\gamma + (1 + 4\gamma) \|V\Lambda V^{-1} - TDT^{-1}\|_2 \\ &\leq 4\gamma + (1 + 4\gamma) [\|(V - T)\Lambda V^{-1}\|_2 + \|T(\Lambda - D)V^{-1}\|_2 + \|TD(V^{-1} - T^{-1})\|_2]. \end{aligned} \quad (5.1.5)$$

To simplify this bound in terms of our parameters, we observe the following.

- Since the columns of  $V$  and  $T$  are unit vectors,  $1 \leq \|V\|_2, \|T\|_2 \leq \sqrt{n}$ .
- Since  $V$  diagonalizes  $\tilde{B}^{-1}\tilde{A}$  and therefore also  $n^{-\alpha}\tilde{B}^{-1}\tilde{A}$  and  $\kappa_V(n^{-\alpha}\tilde{B}^{-1}\tilde{A}) \leq \frac{n^{\alpha+2}}{\gamma}$ , [Remark 3.10](#) allows us to assume

$$\|V\|_2 \|V^{-1}\|_2 \leq \frac{n^{\alpha+2}}{\gamma} \quad (5.1.6)$$

without changing probabilities. Combined with the previous point, this implies  $\|V^{-1}\|_2 \leq \frac{n^{\alpha+2}}{\gamma}$ .

- The columns of  $T$  and  $V$  satisfy  $\|t_i - v_i\|_2 \leq \beta$  so  $\|T - V\|_2 \leq \sqrt{n}\beta$

- By the stability of singular values,  $\|T - V\|_2 \leq \sqrt{n}\beta$  implies  $\sigma_n(T) \geq \sigma_n(V) - \sqrt{n}\beta$ . Combining this with our upper bound on  $\|V^{-1}\|_2$  yields

$$\|T^{-1}\|_2 \leq \frac{n^{\alpha+2}}{\gamma - n^{\frac{2\alpha+5}{2}}\beta}. \quad (5.1.7)$$

- Because each diagonal entry of  $\Lambda$  is at most  $\sqrt{2}n^\alpha\omega$  from the corresponding diagonal entry of  $D$ ,  $\|\Lambda - D\|_2 \leq \sqrt{2}n^\alpha\omega$ .
- Since both  $(\tilde{A}, n^\alpha\tilde{B})$  and  $(D_1, D_2)$  have eigenvalues in  $D(0, 3)$ ,  $\|\Lambda\|_2, \|D\|_2 \leq 3n^\alpha$ .
- Finally,  $\|V^{-1} - T^{-1}\|_2 = \|T^{-1}(T - V)V^{-1}\|_2 \leq \|T^{-1}\|_2\|T - V\|_2\|V^{-1}\|_2$ .

Together, these imply the following bounds:

$$\|(V - T)\Lambda V^{-1}\|_2 \leq \|V - T\|_2\|\Lambda\|_2\|V^{-1}\|_2 \leq \sqrt{n}\beta \cdot 3n^\alpha \cdot \frac{n^{\alpha+2}}{\gamma} = \frac{3\beta}{\gamma}n^{\frac{4\alpha+5}{2}} \quad (5.1.8a)$$

$$\|T(\Lambda - D)V^{-1}\|_2 \leq \|T\|_2\|\Lambda - D\|_2\|V^{-1}\|_2 \leq \sqrt{n} \cdot \sqrt{2}n^\alpha\omega \cdot \frac{n^{\alpha+2}}{\gamma} = \frac{\sqrt{2}\omega}{\gamma}n^{\frac{4\alpha+5}{2}} \quad (5.1.8b)$$

$$\|TD(V^{-1} - T^{-1})\|_2 \leq \sqrt{n} \cdot 3n^\alpha \cdot \frac{n^{\alpha+2}}{\gamma - n^{\frac{2\alpha+5}{2}}\beta} \cdot \sqrt{n}\beta \cdot \frac{n^{\alpha+2}}{\gamma} = \frac{3\beta n^{3\alpha+5}}{\gamma(\gamma - n^{\frac{2\alpha+5}{2}}\beta)}. \quad (5.1.8c)$$

Now the choice of  $\beta$  in line 4 ensures  $\beta \leq \frac{\varepsilon\gamma}{12(1+4\gamma)}n^{-\frac{4\alpha+5}{2}}$ , so (5.1.8a) simplifies to

$$\|(V - T)\Lambda V^{-1}\|_2 \leq 3 \cdot \frac{\varepsilon\gamma}{12(1+4\gamma)n^{\frac{4\alpha+5}{2}}} \cdot \frac{n^{\frac{4\alpha+5}{2}}}{\gamma} = \frac{\varepsilon}{4(1+4\gamma)}. \quad (5.1.9)$$

Similarly, using this time the fact that  $\beta < \frac{\gamma}{2}n^{-\frac{2\alpha+5}{2}}$  and therefore  $\gamma - n^{\frac{2\alpha+5}{2}}\beta > \frac{\gamma}{2}$ , (5.1.8c) becomes

$$\|TD(V^{-1} - T^{-1})\|_2 \leq \frac{6}{\gamma^2}n^{3\alpha+5} \cdot \frac{\varepsilon\gamma^2}{24(1+4\gamma)}n^{-3\alpha-5} = \frac{\varepsilon}{4(1+4\gamma)}. \quad (5.1.10)$$

Finally,  $\omega = \frac{\gamma^4}{4}n^{-\frac{8\alpha+13}{3}}$  implies  $\omega \leq \frac{\varepsilon\gamma}{4\sqrt{2}(1+4\gamma)}n^{-\frac{4\alpha+5}{2}}$ , which allows us to upper bound (5.1.8b) as

$$\|T(\Lambda - D)V^{-1}\|_2 \leq \sqrt{2} \cdot \frac{\varepsilon\gamma}{4\sqrt{2}(1+4\gamma)n^{\frac{4\alpha+5}{2}}} \cdot \frac{n^{\frac{4\alpha+5}{2}}}{\gamma} = \frac{\varepsilon}{4(1+4\gamma)}. \quad (5.1.11)$$

Applying these to (5.1.5), we obtain

$$\|A - S D T^{-1}\|_2 \leq 4\gamma + (1+4\gamma) \left[ \frac{\varepsilon}{4(1+4\gamma)} + \frac{\varepsilon}{4(1+4\gamma)} + \frac{\varepsilon}{4(1+4\gamma)} \right] = 4\gamma + \frac{3}{4}\varepsilon. \quad (5.1.12)$$

Since  $\gamma = \frac{\varepsilon}{16}$  we conclude  $\|A - S D T^{-1}\|_2 \leq \varepsilon$ .  $\square$

## 5.2 Forward Error Guarantee and Computational Complexity

We might hope that Theorem 5.1 can provide a forward error guarantee in terms of the eigenvector condition number  $\kappa_V(A, B)$ . As we demonstrate below, this is possible when the input pencil is well-behaved (in particular regular with a full set of distinct and finite eigenvalues). The resulting Theorem 5.2 parallels a similar result of Banks et al. [9, Proposition 1.1].

**Theorem 5.2.** *Let  $A, B, \tilde{A}, \tilde{B} \in \mathbb{C}^{n \times n}$  with  $\|A\|_2 \leq 1$ . Assume that  $B$  is invertible and that the pencil  $(A, B)$  has a full set of distinct, finite eigenpairs  $\{(\lambda_i, v_i)\}_{i=1}^n$ . If  $\|A - \tilde{A}\|_2 \leq \varepsilon\sigma_n(B)\text{gap}(A, B)$  and  $\|B - \tilde{B}\|_2 \leq \varepsilon\sigma_n^2(B)\text{gap}(A, B)$  for*

$$\varepsilon \leq \frac{1}{32\kappa_V(A, B)}$$

then  $(\tilde{A}, \tilde{B})$  has no repeated eigenvalues and any set of corresponding eigenpairs  $\{(\tilde{\lambda}_i, \tilde{v}_i)\}_{i=1}^n$  satisfies

$$|\lambda_i - \tilde{\lambda}_i| \leq 4\text{gap}(A, B)\kappa_V(A, B)\varepsilon \quad \text{and} \quad \|v_i - \tilde{v}_i\|_2 \leq 24n\kappa_V(A, B)\varepsilon \quad \text{for all } i = 1, \dots, n$$

after multiplying the  $v_i$  by phases and reordering, if necessary.

*Proof.* We first note that  $\varepsilon < \frac{1}{32\kappa_V(A, B)}$  implies

$$\|B - \tilde{B}\|_2 \leq \frac{\sigma_n^2(B)\text{gap}(A, B)}{32\kappa_V(A, B)} \leq \frac{\sigma_n(B)}{16\kappa_V(A, B)} \leq \frac{\sigma_n(B)}{2}, \quad (5.2.1)$$

where the second inequality follows from  $\text{gap}(A, B) \leq 2\|B^{-1}A\|_2 \leq \frac{2}{\sigma_n(B)}$  (since  $\|A\|_2 \leq 1$ ). Thus, [Lemma 2.13](#) guarantees  $\sigma_n(\tilde{B}) \geq \sigma_n(B) - \|B - \tilde{B}\|_2 \geq \frac{\sigma_n(B)}{2}$ , so  $\tilde{B}$  is invertible. With this in mind, consider the matrices  $B^{-1}A$  and  $\tilde{B}^{-1}\tilde{A}$ , which are diagonalizable with the same eigenpairs as  $(A, B)$  and  $(\tilde{A}, \tilde{B})$  respectively. Using again the fact that  $\|A\|_2 \leq 1$ , we have

$$\begin{aligned} \|B^{-1}A - \tilde{B}^{-1}\tilde{A}\|_2 &= \|B^{-1}A - \tilde{B}^{-1}A + \tilde{B}^{-1}A - \tilde{B}^{-1}\tilde{A}\|_2 \\ &\leq \|B^{-1} - \tilde{B}^{-1}\|_2\|A\|_2 + \|\tilde{B}^{-1}\|_2\|A - \tilde{A}\|_2 \\ &\leq \|\tilde{B}^{-1}\|_2\|\tilde{B} - B\|_2\|B^{-1}\|_2 + \|\tilde{B}^{-1}\|_2\|A - \tilde{A}\|_2 \\ &\leq \frac{2}{\sigma_n(B)}\varepsilon\sigma_n^2(B)\text{gap}(A, B)\frac{1}{\sigma_n(B)} + \frac{2}{\sigma_n(B)}\varepsilon\sigma_n(B)\text{gap}(A, B) \\ &\leq 4\varepsilon\text{gap}(A, B). \end{aligned} \quad (5.2.2)$$

This implies that the eigenvalues of  $\tilde{B}^{-1}\tilde{A}$  belong to the  $4\varepsilon\text{gap}(A, B)$ -pseudospectrum of  $B^{-1}A$ , and moreover we can continuously deform the eigenvalues of  $B^{-1}A$  to those of  $\tilde{B}^{-1}\tilde{A}$  without leaving this pseudospectrum. Since  $\varepsilon < \frac{1}{4}$  and  $B^{-1}A$  is diagonalizable, single matrix Bauer-Fike ([Theorem 2.15](#)) therefore implies that  $\tilde{B}^{-1}\tilde{A}$ , and by extension  $(\tilde{A}, \tilde{B})$ , has a full set of distinct eigenvalues  $\lambda_1, \dots, \lambda_n$ . Bauer-Fike also guarantees that these eigenvalues can be ordered so that each  $\tilde{\lambda}_i$  satisfies

$$|\lambda_i - \tilde{\lambda}_i| \leq 4\text{gap}(A, B)\kappa_V(B^{-1}A)\varepsilon \quad (5.2.3)$$

for a corresponding eigenvalue  $\lambda_i$  of  $B^{-1}A$ . Recalling that  $\kappa_V(B^{-1}A) = \kappa_V(A, B)$ , we obtain the first guarantee.

The second guarantee follows from the proof of [\[9, Proposition 1.1\]](#) since the requirement  $\varepsilon < \frac{1}{32\kappa_V(A, B)}$  ensures by [\(5.2.2\)](#) that

$$\|B^{-1}A - \tilde{B}^{-1}\tilde{A}\|_2 \leq \frac{\text{gap}(B^{-1}A)}{8\kappa_V(B^{-1}A)}. \quad (5.2.4)$$

Note that while [\[9, Proposition 1.1\]](#) comes with norm assumptions on the matrices, these are not used in the proof of the eigenvector guarantee.  $\square$

Banks et al. state [\[9, Proposition 1.1\]](#) – the single matrix counterpart to [Theorem 5.2](#) – in terms of an eigenvalue problem condition number:

$$\kappa_{\text{eig}}(A) = \frac{\kappa_V(A)}{\text{gap}(A)}. \quad (5.2.5)$$

With this in mind, we could rewrite [Theorem 5.2](#) in terms of the similar quantity

$$\frac{\kappa_V(A, B)}{\sigma_n^3(B)\text{gap}(A, B)}. \quad (5.2.6)$$

While [\(5.2.6\)](#) does capture some of the challenges of the generalized eigenvalue problem (i.e., it is infinite if  $B$  is singular or  $(A, B)$  has a repeated eigenvalue) it is not invariant under scaling of  $A$  and  $B$  and is therefore not suitable as a condition number for the problem. For this reason, we choose instead to state the forward error guarantees in terms of  $\kappa_V(A, B)$ .

The proof of [9, Proposition 1.1] relies on some basic perturbation results for individual matrices summarized in [27]. Developing corresponding results for the generalized problem may allow for a similar forward error guarantee with looser requirements on  $\|A - \tilde{A}\|_2$  and  $\|B - \tilde{B}\|_2$ . In particular, we might hope to reduce or eliminate the factors of  $\sigma_n(B)$ . Absent these improvements, [Theorem 5.2](#) is fairly restrictive, requiring not only that  $(A, B)$  is regular and diagonalizable but that  $B$  is nonsingular. In part, this is a consequence of our version of Bauer-Fike, which makes many of the same assumptions and produces the same guarantees if used in the proof above. We consider a generalization to arbitrary regular pencils in [Appendix A](#). The singular pencil case is even more complex, requiring a different perturbation analysis altogether (see for example work of Lotz and Noferini [38]).

To wrap up this section, we compute the asymptotic complexity of **RPD** in terms of  $n$ , the size of the pencil  $(A, B)$ , and  $\varepsilon$ , the accuracy of the approximate diagonalization. Throughout, we assume that we have access to black-box algorithms for multiplying two  $n \times n$  matrices and computing the QR factorization of an  $n \times n$  matrix, which require  $T_{\text{MM}}(n)$  and  $T_{\text{QR}}(n)$  arithmetic operations respectively. For simplicity, we also assume access to QL/RQ algorithms (used in **GRURV**) that require  $T_{\text{QR}}(n)$  operations.

**Proposition 5.3.** *Exact arithmetic **RPD** requires at most*

$$O\left(\log(n) \log^2\left(\frac{n}{\varepsilon}\right) [T_{\text{QR}}(n) + T_{\text{MM}}(n)]\right)$$

*arithmetic operations.*

*Proof.* To compute complexity for **RPD** we track only matrix multiplication and QR, as all other building blocks have smaller complexity. We start by noting that line 2 of [Algorithm 6](#) implies  $\alpha = \mathcal{O}\left(\log_n\left(\frac{1}{\gamma}\right)\right)$ . Since  $\gamma = \Theta(\varepsilon)$ , we then have

$$n^\alpha = O\left(n^{\log_n(1/\gamma)}\right) = O\left(\frac{1}{\gamma}\right) = O\left(\frac{1}{\varepsilon}\right). \quad (5.2.7)$$

At the same time, we have in line 3

$$\epsilon > \frac{\gamma^5}{65n^{\frac{11\alpha+25}{3}}} = \Omega\left(\frac{\varepsilon^{26/3}}{n^{25/3}}\right). \quad (5.2.8)$$

Thus, line seven of **EIG** implies that the number of steps of repeated squaring required at any point in the recursion can be bounded asymptotically as

$$p = O\left(\log\left(\frac{n^\alpha}{\epsilon}\right)\right) = O\left(\log\left(\frac{n^{25/3}}{\varepsilon^{29/3}}\right)\right) = O\left(\log\left(\frac{n}{\varepsilon}\right)\right). \quad (5.2.9)$$

With this in mind, consider now working through one step of the divide-and-conquer process. Lines 8-15 of **EIG** make up the bulk of the work, executing a search over the grid lines for one that sufficiently splits the spectrum. For each line that is checked, we make one call to **IRS** and one call to **GRURV**. Now each step of repeated squaring consists of one  $2n \times 2n$  QR factorization and two  $n \times n$  matrix multiplications, therefore requiring  $T_{\text{QR}}(2n) + 2T_{\text{MM}}(n)$  operations. Meanwhile, applying **GRURV** to a product of two matrices requires  $3T_{\text{QR}}(n) + 2T_{\text{MM}}(n)$  operations. Combining this with (5.2.9), we conclude that each grid line checked results in

$$O\left(\log\left(\frac{n}{\varepsilon}\right) [T_{\text{QR}}(2n) + 2T_{\text{MM}}(n)] + 2T_{\text{QR}}(n) + 2T_{\text{MM}}(n)\right) = O\left(\log\left(\frac{n}{\varepsilon}\right) [T_{\text{QR}}(n) + T_{\text{MM}}(n)]\right) \quad (5.2.10)$$

operations. Since we check at most  $O\left(\log\left(\frac{1}{\omega}\right)\right)$  grid lines each time and

$$\omega = \frac{\gamma^4}{4n^{\frac{8\alpha+13}{3}}} = \Omega\left(\frac{\varepsilon^{20/3}}{n^{13/3}}\right), \quad (5.2.11)$$

we conclude that the operations totaled in (5.2.10) need to be performed at most  $O\left(\log\left(\frac{n}{\varepsilon}\right)\right)$  times. Hence, lines 8-15 of **EIG** take at most

$$O\left(\log^2\left(\frac{n}{\varepsilon}\right) [T_{\text{QR}}(n) + T_{\text{MM}}(n)]\right) \quad (5.2.12)$$



operations. Noting that the remainder of one step of **EIG** – i.e., the subsequent calls to **DEFLATE** – has complexity equal to that of checking one grid line, we conclude that (5.2.12) is the asymptotic complexity of one step of divide-and-conquer. Recalling that by selecting a grid line that sufficiently splits the spectrum at each step we ensure that only  $O(\log(n))$  steps of divide-and-conquer are necessary, we conclude that **RPD** executes at most

$$O\left(\log(n) \log^2\left(\frac{n}{\varepsilon}\right) [T_{\text{QR}}(n) + T_{\text{MM}}(n)]\right) \quad (5.2.13)$$

arithmetic operations.  $\square$

Since Demmel, Dumitriu, and Holtz have shown that QR reduces stably to matrix multiplication [17, §4.1], we can assume  $T_{\text{QR}}(n) = O(T_{\text{MM}}(n))$ . Thus, Proposition 5.3 implies that **RPD** can be implemented in  $O(\log(n) \log^2(\frac{n}{\varepsilon}) T_{\text{MM}}(n))$  operations. Up to log factors, then, **RPD** has the same asymptotic complexity as matrix multiplication, meaning it runs in nearly matrix multiplication time in exact arithmetic.

## 6 Numerical Examples

In this section, we consider a number of examples to investigate how pseudospectral divide-and-conquer performs in practice. Our first task is to adjust the parameters of **RPD** and **EIG** to make them more amenable to implementation; the values listed in the pseudocode of Algorithms 5 and 6 are prohibitively restrictive, hedging against the worst case to guarantee good results regardless of the inputs. With this in mind, we make the following relaxations.

- Rather than choosing the scaling factor  $\alpha$  based on the desired backward error, we fix  $\alpha = 3/2$ .
- Extracting the main dependence on  $\gamma$  and  $n$ , we set  $\epsilon = \beta = \omega = \gamma/n$ .
- We similarly limit the number of steps of repeated squaring to  $p = \lceil \log_2(n/\epsilon) \rceil$ .
- Finally, we drop the factor of  $1/n^3$  from the criteria used to compute  $k$  in line 12 of **EIG**.

While the choices listed above simplify the algorithm, they also affect the failure probability of **RPD**, which may now be large for certain combinations of  $n$  and  $\varepsilon$ . Since failure includes the possibility that **EIG** cannot find a sufficient dividing line, our implementation includes a fail-safe, defaulting to QZ (done in Matlab by calling `eig(A,B)`) when this occurs. While only one of the 5000 tests presented below made a call to QZ (on a  $2 \times 2$  subproblem no less), this kind of failure is a reality of the method and may be more frequent for certain problems. Accordingly, we present the following experiments as simply a proof of concept, and we do not consider run times nor do we use an explicitly parallel implementation of the algorithm. Throughout, all results were obtained in Matlab version R2023a.

We start by applying **RPD** to the following three examples, each of which presents a generalized eigenvalue problem with different conditioning:

1. **Planted Spectrum** – First, we consider a  $50 \times 50$  pencil  $(A, B)$  with equally spaced, real eigenvalues in the interval  $[-2, 2]$ . To obtain  $(A, B)$ , we fill a diagonal matrix  $\Lambda$  as  $\Lambda(j, j) = -2 + \frac{4(j-1)}{49}$  and set  $A = X\Lambda Y^{-1}$  and  $B = XY^{-1}$  for  $X$  and  $Y$  two independent, complex Gaussian matrices. In accordance with **RPD**, we then normalize the pencil so that  $\|A\|_2, \|B\|_2 \leq 1$ . We can think of this example as the best-case scenario, where  $\text{gap}(A, B)$  is large and  $B$  is far from singular.
2. **Jordan Block** – Next, we consider a  $50 \times 50$  pencil  $(A, B)$  with  $B = I$  and  $A = J_{50}(0)$ , where  $J_{50}(0)$  is a  $50 \times 50$  Jordan block with eigenvalue zero. This example tests a generalized eigenvalue problem with  $\text{gap}(A, B) = 0$ .
3. **Increasingly Singular  $B$**  – Finally, to explore the challenges associated with infinite eigenvalues, we consider a  $50 \times 50$  pencil whose second matrix  $B$  is made progressively closer to singular. To do this, we first construct a random  $M_1 = U\Sigma V^H$  where  $U$  and  $V$  are independent Haar matrices and  $\Sigma$  is diagonal with equally spaced (ascending) diagonal entries in the interval  $[1, 2]$ . We then construct

$M_2 = U\Lambda V^H$  for  $\Lambda$  a matrix whose only nonzero entry is  $\Lambda(1, 1) = 1$ . With  $M_1$  and  $M_2$ , we obtain a series of pencils

$$(A, B_\tau) = (I, M_1 - \tau M_2) \quad \tau \in [0, 1], \quad (6.0.1)$$

where, by construction,  $\sigma_{50}(B_\tau) \rightarrow 0$  as  $\tau \rightarrow 1$ . As in the first example,  $A$  and  $B_\tau$  are appropriately normalized before applying **RPD**. Note that before normalization  $\|B_\tau\|_2 = 2$  for all values of  $\tau$ .

We are interested in tracking the performance of **RPD** on these examples via a number of metrics. First and foremost, we want to verify a finite arithmetic counterpart to [Theorem 5.1](#): does **RPD** reliably produce accurate diagonalizations of each pencil? To measure diagonalization error, we compute

$$\log_{10} \left( \max \left\{ \|A - SDT^{-1}\|_2, \|B - SIT^{-1}\|_2 \right\} \right), \quad (6.0.2)$$

for  $S, D$ , and  $T$  the outputs of **RPD**, and we consider a run to be successful if this error is, at most,  $\log_{10}(\varepsilon)$ .

Next, we would like to obtain some indication of how efficient the divide-and-conquer process is. One way to do this is to catalog the relative split size at each step (i.e.,  $k/m$  in **EIG**). While we know that **EIG** guarantees that the relative split is at least 0.2 and at most 0.8, divide-and-conquer is most efficient if relative splits are close to 0.5 at each step.

Of course, the split size tells only part of the story. In fact, recalling the proof of [Proposition 5.3](#), the bulk of the work lies in finding a splitting line, meaning that even if splits are reliably near 50/50 the algorithm may be slow if we have to check too many. Assuming access to  $O(n^3)$  algorithms for matrix multiplication and QR, one step of our implementation requires  $O(\log(\frac{n}{\varepsilon})m^3l)$  operations, where  $l$  is the number of grid lines checked and  $m$  is the size of the current subproblem. Ignoring the  $\log(\frac{n}{\varepsilon})$  factor, we can do a pseudo-flop count by summing  $m^3l$  over all steps with  $m > 1$ . Moreover, we can easily compute an optimal value for this flop count by requiring at each step that  $l = 1$  and that the split is as close to 50/50 as possible. Dividing the actual count by the optimal one produces what we call a relative efficiency factor for each run (which tells us roughly how many times more work **RPD** is doing than the best-case scenario).

Histograms of each of these measures of performance are presented for all three examples in [Figures 4 to 6](#). In each test, we run **RPD** 500 times and note if calls to QZ are made. For the first two examples, we present results for decreasing values of  $\varepsilon$ , while for the third we change the value of  $\tau$  and fix  $\varepsilon = 10^{-5}$ .

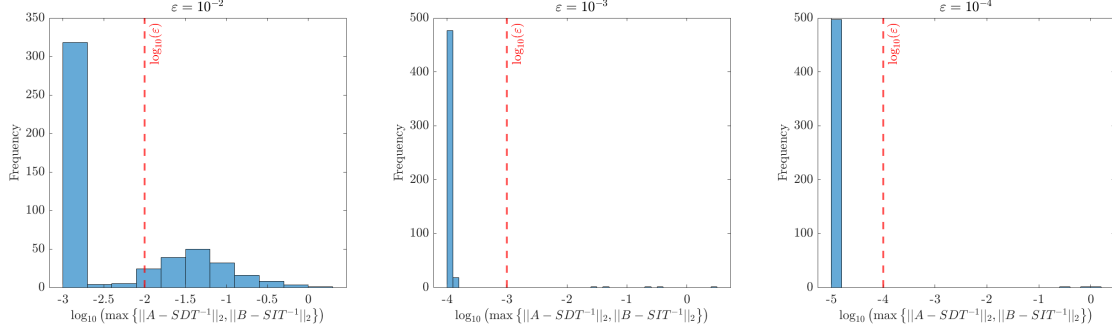
A few observations jump out immediately from these plots. As anticipated, **RPD** is capable of accurately diagonalizing all three of the example pencils, though the probability of failure appears fairly large when  $\varepsilon = 10^{-2}$  (especially for the Jordan block). It may seem counterintuitive that **RPD** is more likely to succeed when  $\varepsilon$  is small, but this is a consequence of our relaxed parameters, which become more restrictive (or equivalently more sensitive) as  $\varepsilon$  shrinks. In particular,  $\varepsilon = 10^{-5}$  was required for **RPD** to reliably diagonalize  $(A, B_\tau)$ ; when  $\varepsilon = 10^{-4}$ , **RPD** would frequently fail on this example, despite consistently diagonalizing the others, with seemingly no correlation to the value of  $\tau$ . With this in mind we caution again that this implementation can only be taken as a proof of concept and that a nuanced examination of the method's parameters would be required before applying it to larger or more complicated problems.

Interestingly, all three examples indicate that divide-and-conquer typically favors near-optimal eigenvalue splits. This carries through to the relative efficiency: our rough flop count shows that **RPD** is reliably doing only about three to four times the optimal amount of operations overall. Note that by ignoring the factor of  $\log(\frac{n}{\varepsilon})$  in this count we remove the primary dependence on  $\varepsilon$ , hence why the relative efficiencies don't change significantly as it decreases.

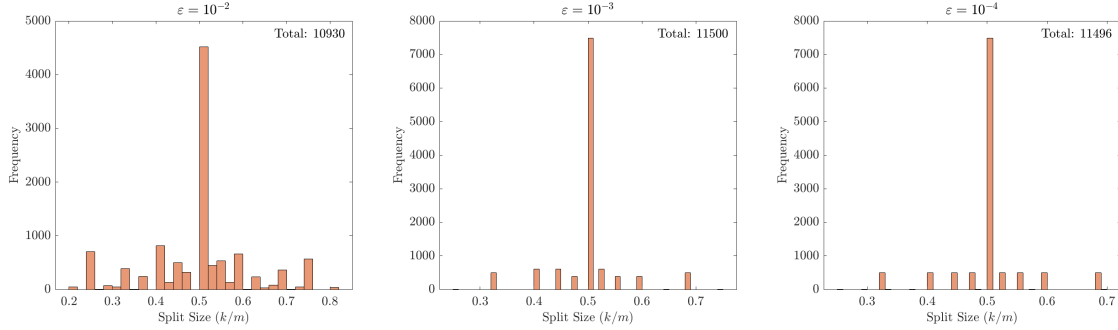
In all of the runs presented here only one defaulted to calling QZ. This occurred on a  $2 \times 2$  subproblem of the Jordan block example and indicates that shattering failed for that run. Though hopefully rare (as was the case here) this is to be expected on problems like the Jordan block, where repeated eigenvalues may not be sufficiently separated by the initial perturbation.

While these results are promising, we might be more interested in probing the boundaries of [Theorem 5.2](#). That is, when **RPD** succeeds on our examples, how accurate are the corresponding sets of approximate eigenvalues? With this in mind [Figure 7](#) provides eigenvalue approximation data for all three examples, where in each case we consider only approximations produced by successful runs.

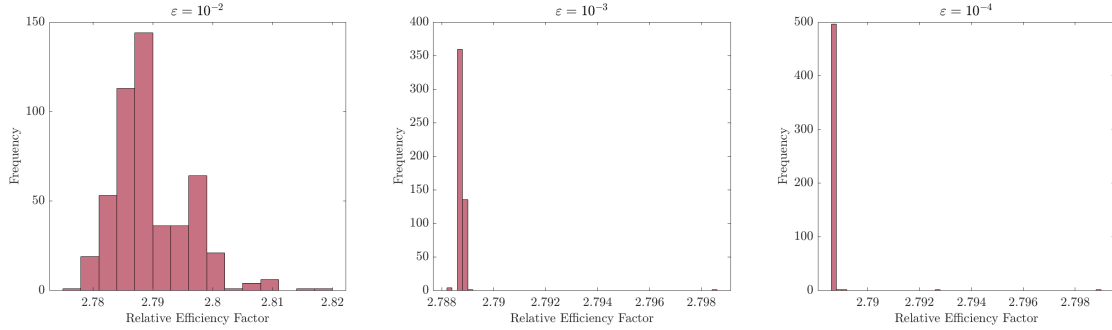
The results in these plots trace out nicely the relative challenge of extracting accurate eigenvalues from an accurate diagonalization. In the best case – the planted spectrum example – increasingly accurate diagonalizations provide correspondingly better eigenvalue approximations, as promised by [Theorem 5.2](#). The Jordan block example, on the other hand, demonstrates that when  $\text{gap}(A, B) = 0$  we cannot hope to



(a) Frequency of diagonalization error (6.0.2). We mark the  $\log_{10}(\epsilon)$  threshold for success in red. For this example  $\|A\|_2 = .967$  and  $\|B\|_2 = 1$ .

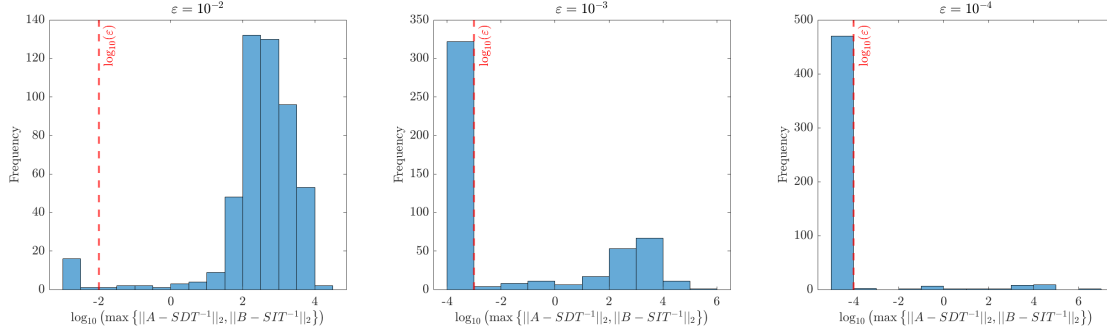


(b) Frequency of relative eigenvalue split sizes (i.e.,  $k/m$  in **EIG**). We record only successful splits here, which always satisfy  $0.2 \leq k/m \leq 0.8$ , and we do not include subproblems with  $m < 4$ , as these can only be split in one way. Since the total number of splits is variable (and dependent on the splits themselves) we record it at the top of each plot. This total is for all 500 tests; hence, dividing by 500 gives a rough average number of splits per run.

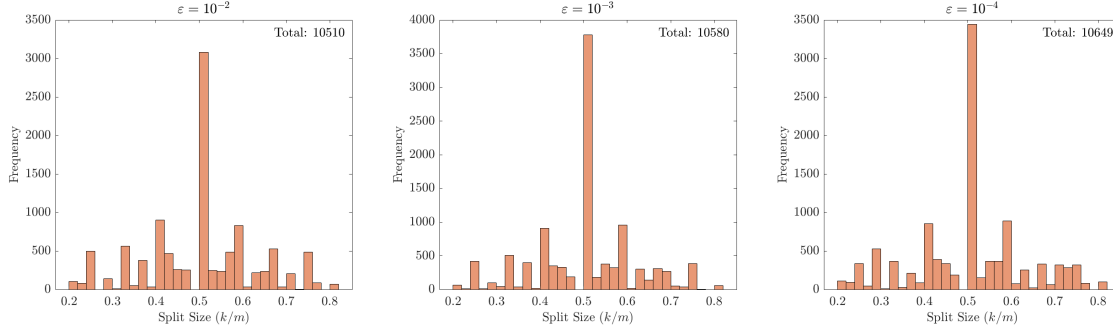


(c) Frequency of relative efficiency factor (i.e., the pseudo-flop count divided by its optimal value).

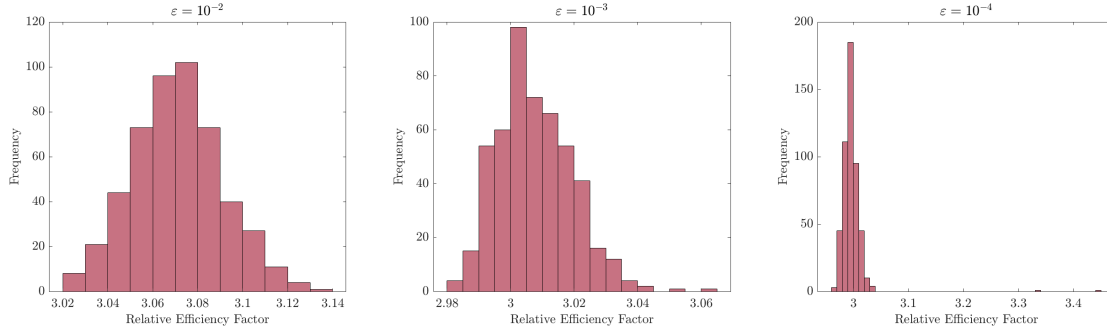
Figure 4: Performance data for **RPD** on the  $50 \times 50$  planted-spectrum example with decreasing values of  $\epsilon$ . Each plot corresponds to 500 runs of **RPD**. The divide-and-conquer process succeeded in all runs (i.e., no calls to **eig** were made).



(a) Same as (a) of Figure 4. For this example  $\|A\|_2 = \|B\|_2 = 1$ .

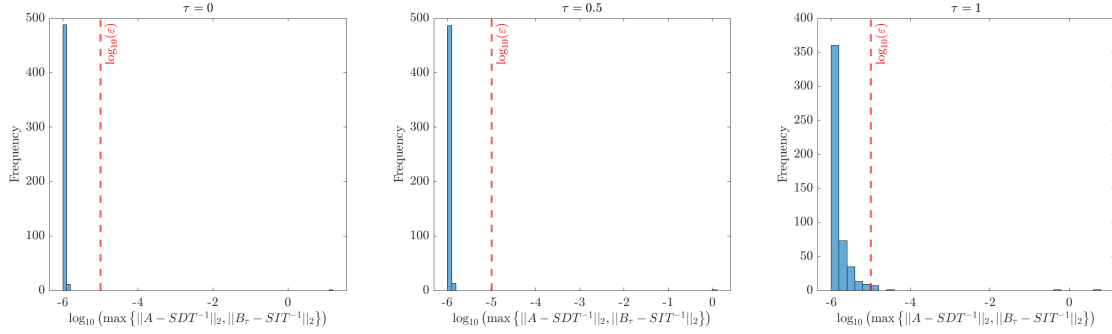


(b) Same as (b) of Figure 4.

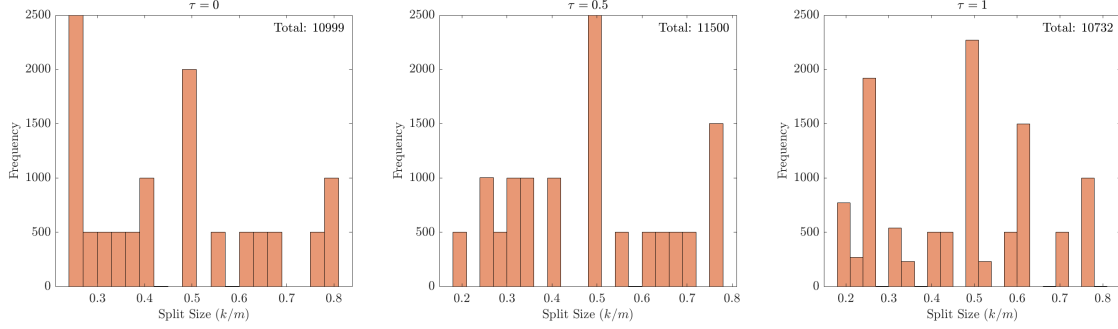


(c) Same as (c) of Figure 4

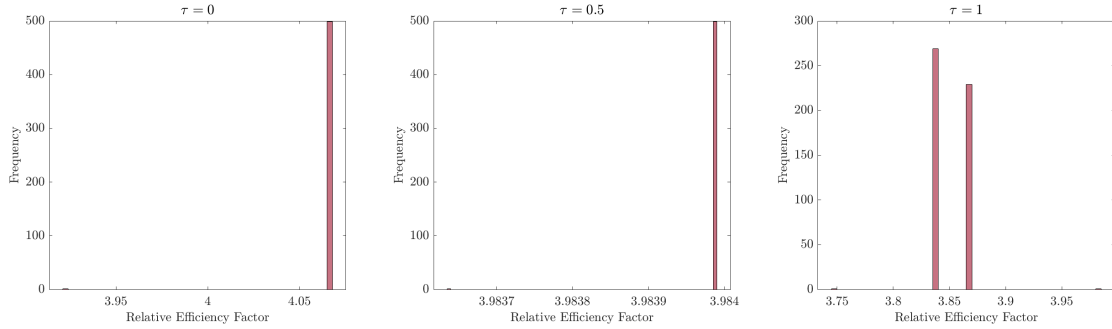
Figure 5: A repeat of Figure 4 for the  $50 \times 50$  Jordan block example. Once again, each plot corresponds to 500 applications of **RPD**. Of the cumulative 1500 runs used to produce these results, only one call to **eig** was made (on a subproblem of size  $2 \times 2$ ).



(a) Frequency of diagonalization error (6.0.2). For any value of  $\tau$  we have  $\|A\|_2 = 0.5$  and  $\|B_\tau\|_2 = 1$ .

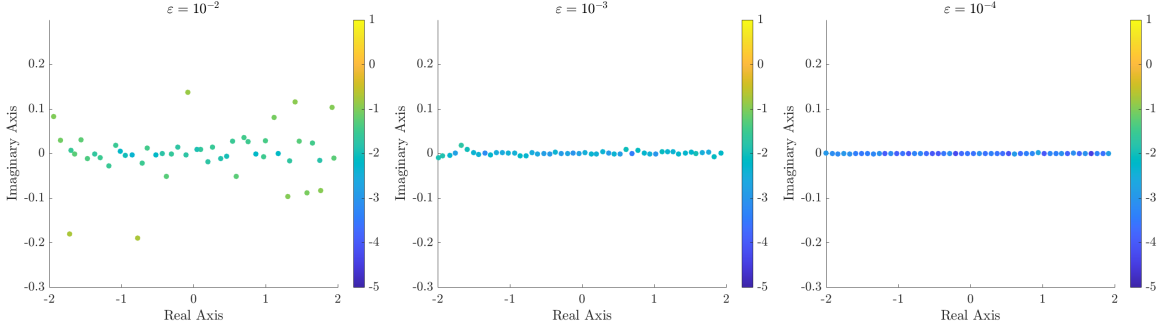


(b) Frequency of relative eigenvalue split sizes.

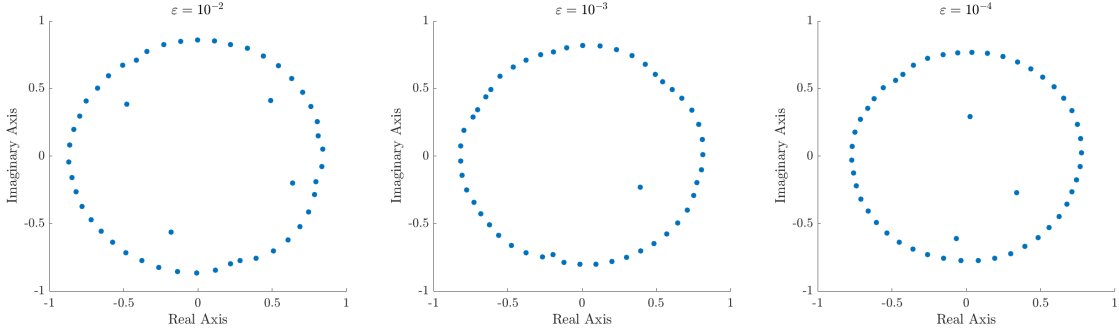


(c) Frequency of relative efficiency factor.

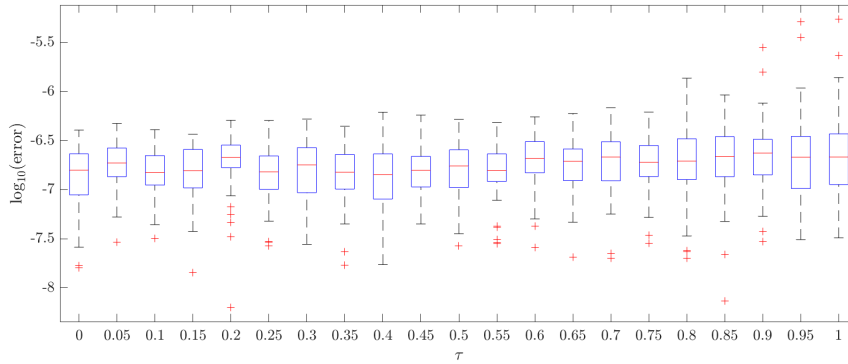
Figure 6: Performance data for **RPD** on the  $50 \times 50$  increasingly singular pencil  $(A, B_\tau)$ . Unlike the previous figures, these plots fix  $\epsilon = 10^{-5}$  and vary  $\tau$ , where  $B$  becomes closer to singular as  $\tau \rightarrow 1$ . The results presented for each value of  $\tau$  come from 500 runs of **RPD**, none of which defaulted to calling **eig**.



(a) Eigenvalue approximations for the planted spectrum example obtained from **RPD** with different values of  $\varepsilon$ . Each approximate eigenvalue is colored according to its accuracy, which is computed as  $\log_{10} |\tilde{\lambda}_i - \lambda_i|$  for  $\lambda_i$  and  $\tilde{\lambda}_i$  the true and approximate eigenvalues ordered by their real parts.



(b) Eigenvalue approximations for the Jordan block example obtained from **RPD** with different values of  $\varepsilon$ . The only true eigenvalue for this problem is zero.



(c) Boxplots of eigenvalue approximation errors for **RPD** applied to  $(A, B_\tau)$  with different values of  $\tau$ . Error is measured as  $\min_j |\lambda_i - D(j, j)|$ , where  $\lambda_i$  are the true eigenvalues of the pencil (computed via QZ) and  $D$  is the diagonal matrix produced by **RPD**. As in Figure 6, each run of **RPD** uses  $\varepsilon = 10^{-5}$ . For  $\tau = 1$ , the worst-case error (which is infinite) is omitted.

Figure 7: Eigenvalue approximation data for **RPD** applied to our three examples. We present here only results for successful runs – i.e., each set of approximate eigenvalues corresponds to a diagonalization with  $\|A - SDT^{-1}\|_2 \leq \varepsilon$  and  $\|B - SIT^{-1}\|_2 \leq \varepsilon$ .

Pseudospectral Divide-and-Conquer ( <a href="#">Algorithm 6</a> )			
QZ <a href="#">[41]</a>	Run 1	Run 2	Run 3
-2.089013	1.000013 + 0.000025i	1.000004 + 0.000006i	1.000002 + 0.000024i
1.000000	0.515949 - 0.520303i	1.884912 - 0.803207i	0.129337 - 0.121077i
0.445724	0.280363 - 0.067093i	0.358926 + 0.013113i	-0.368134 + 0.940716i
-0.014976	-1.701890 + 0.002810i	-1.518997 - 0.014526i	-4.469932 - 0.912286i

Table 2: Eigenvalues of the singular pencil (6.0.3) as computed by QZ and pseudospectral divide-and-conquer. We present three successful runs of **RPD**, each with  $\varepsilon = 10^{-6}$ .

recover repeated eigenvalues with any confidence, though this is also the case for classical backwards-stable algorithms like QZ. The final, infinite eigenvalue example is somewhere in between; while worst-case error balloons as  $B$  becomes more singular (to be expected as eigenvalues wander away to infinity), **RPD** still recovers the majority or even all of the finite eigenvalues. Note however that the measure of error used in this plot (i.e., the minimum distance from each true eigenvalue to an approximation) is somewhat weaker than we might hope. That is, a small worst-case error implies only that each true eigenvalue is close to an approximation, not that each true eigenvalue can be paired to a unique, nearby approximation.

To this point we have only applied pseudospectral divide-and-conquer to regular pencils. Recalling that singular pencils are a reality in many applications, we consider as a final test the following singular pencil taken from Lotz and Noferini [\[38\]](#):

$$A = \begin{pmatrix} 2 & -1 & -5 & -1 \\ 6 & -2 & -11 & -2 \\ 5 & 0 & -2 & 0 \\ 3 & 1 & 3 & 1 \end{pmatrix}, \quad B = \begin{pmatrix} 1 & -1 & -4 & -2 \\ 2 & -3 & -12 & -6 \\ -1 & -3 & -11 & -6 \\ -2 & -2 & -7 & -4 \end{pmatrix}. \quad (6.0.3)$$

The pencil  $(A, B)$  has only one eigenvalue at  $\lambda = 1$ . Practically speaking, recovering this eigenvalue via divide-and-conquer should be difficult due to the initial perturbation made by **RPD**. In fact, Lotz and Noferini show that an arbitrarily small (nonrandom) perturbation to  $(A, B)$  can send its eigenvalues to any four points in the complex plane. In spite of this, pseudospectral-divide-and-conquer finds the true eigenvalue to 5-6 digits of precision, as shown in [Table 2](#).

Of course, QZ also finds  $\lambda = 1$  to a remarkable 14 digits of precision. Motivated by this observation, Lotz and Noferini develop a theory of weak condition numbers to help explain the apparent stability of this eigenvalue. In some sense, the results in [Table 2](#) suggest an even more direct smoothed analysis explanation; though perturbations exist that produce arbitrary eigenvalues, the “average” or random case is likely to yield an eigenvalue near one. This echoes plot (c) of [Figure 7](#), demonstrating again that **RPD** is capable of producing accurate approximations for certain eigenvalues of pencils not covered by results like [Theorem 5.2](#).

Notice that the eigenvalues produced by QZ on this example are all real while those found by pseudospectral divide-and-conquer are complex. Since  $(A, B)$  is real, this is a consequence of the complex perturbation made by **RPD**. As we suggest in the next section, an open extension of this work could consider real or even structured random perturbations for certain problems. Finally, similar to the other examples, [Figure 8](#) provides a few empirical statistics for 500 runs of **RPD** on a normalized version of  $(A, B)$ .

## 7 Conclusion

In this paper, we have constructed an inverse-free routine for producing an approximate diagonalization of any matrix pencil  $(A, B)$ . The method, which rests on a divide-and-conquer eigensolver for the generalized eigenvalue problem, involves several threads of randomness. The most important of these is a random perturbation made to the input matrices, which regularizes the problem and allows the divide-and-conquer



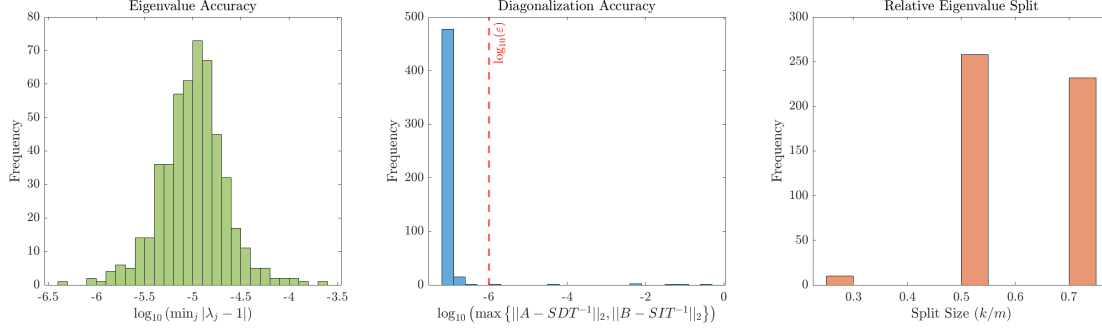


Figure 8: Statistics for 500 runs of **RPD** applied to a normalized version of the singular pencil (6.0.3) with  $\|A\|_2 = 0.694$ ,  $\|B\|_2 = 1$ , and  $\varepsilon = 10^{-6}$ . For the first plot,  $\{\lambda_i\}_{1 \leq i \leq 4}$  are the approximate eigenvalues obtained via divide-and-conquer. Once again, no runs defaulted to calling **eig**. As in the previous examples, we consider only splits on subproblems with  $m > 3$  for the third histogram; as a result, it records only the first split of each run, and the total number of splits is 500 (the number of runs).

process to succeed with high probability. Leveraging this result, our approach produces a provably accurate approximate diagonalization (in a backward error sense) for any input pencil in exact arithmetic, again with high probability. Moreover, the algorithm runs in nearly matrix multiplication time, establishing  $O(\log(n) \log^2(\frac{n}{\varepsilon}) T_{MM}(n))$  as an upper bound on the complexity of producing an exact arithmetic diagonalization of an  $n \times n$  pencil with backward error  $\varepsilon$ . Replacing  $B$  with the identity, this provides another nearly matrix multiplication time algorithm for diagonalizing a single matrix, representing an inverse-free counterpart to the algorithm of Banks et al. [9].

For interested readers, we note that there are a number of open problems and next steps related to this work, which we discuss briefly below.

- **Finite Arithmetic Analysis:** The most immediate open question concerns a finite arithmetic analysis of the algorithm. While we expect that the method will succeed with similar guarantees in finite arithmetic if stated properly, we have been unable to construct a proof. Appendix B explores some of the work done towards this end.
- **Hermitian/Deterministic Variants:** Throughout, we made no assumptions on the matrices of our pencil. Nevertheless, much attention has been paid to the Hermitian eigenvalue problem, where  $A$  is Hermitian and  $B$  Hermitian positive definite, meaning a version of this method adapted to that setting may be worth developing. The main difference here is the use of **DEFLATE**, as the left and right deflating subspaces of a Hermitian pencil are the same. More generally, we might hope to devise a deterministic way to produce the pseudospectral shattering result central to the method.
- **Perturbation Results for the Generalized Eigenvalue Problem:** In completing this work, we found that many of the useful perturbation results for the single matrix eigenvalue problem do not have counterparts for the generalized problem. In particular, there is a lack of results stated in ways that are useful for numerical purposes (i.e., using the Euclidean norm as opposed to a chordal metric). We hope that this work inspires more research in this direction, and we expect that developing better tools may improve the analysis presented here.

## 8 Acknowledgements

This work was supported by NSF grant DMS 2154099 and by Graduate Fellowships for STEM Diversity (GFSD). We thank Jess Banks, Jorge Garza-Vargas, and Nikhil Srivastava for their advice and feedback as well as Anne Greenbaum for helpful correspondence.

## A Alternative Versions of Bauer-Fike for Matrix Pencils

In this appendix, we discuss alternative formulations of [Theorem 2.20](#). As mentioned above, our version of Bauer-Fike is stated for easy use in the proof of [Theorem 3.11](#) and therefore appears somewhat unusual compared to existing perturbation results for the generalized eigenvalue problem. Nevertheless, it is essentially the same as standard bounds, as we demonstrate below. To do this, we introduce common notation from perturbation theory as presented in Stewart and Sun [\[51\]](#).

We begin by re-casting each eigenvalue  $\lambda$  as an ordered pair  $\langle \alpha, \beta \rangle$  such that  $\lambda = \frac{\alpha}{\beta}$ . In this notation, solutions to the generalized eigenvalue problem satisfy  $\beta Av = \alpha Bv$ . The main benefit of representing eigenvalues in this way is the natural inclusion of those at infinity, which now correspond to  $\beta = 0$ . Moreover, this definition links nicely with matrix pencil diagonalization; if  $(A, B) = (SD_1T^{-1}, SD_2T^{-1})$ , each diagonal entry of  $D_1$  and  $D_2$  contains a corresponding  $\alpha$  and  $\beta$ . Note that if  $(A, B)$  is regular, we can never have  $\alpha = \beta = 0$ .

Of course, there are infinitely many choices of  $\alpha$  and  $\beta$  that yield the same eigenvalue  $\lambda$ . For this reason, we can think of each eigenvalue  $\langle \alpha, \beta \rangle$  as a projective line – i.e., the subspace spanned by  $(\alpha \ \beta)^T$ . Accordingly, we measure distance between two eigenvalues  $\langle \alpha_1, \beta_1 \rangle$  and  $\langle \alpha_2, \beta_2 \rangle$  with the chordal metric:

$$\chi(\langle \alpha_1, \beta_1 \rangle, \langle \alpha_2, \beta_2 \rangle) = \frac{|\alpha_1\beta_2 - \beta_1\alpha_2|}{\sqrt{|\alpha_1|^2 + |\beta_1|^2}\sqrt{|\alpha_2|^2 + |\beta_2|^2}}. \quad (\text{A.0.1})$$

Dividing both the numerator and denominator of [\(A.0.1\)](#) by  $|\beta_1\beta_2|$ , we observe that if  $\lambda_1 = \frac{\alpha_1}{\beta_1}$  and  $\lambda_2 = \frac{\alpha_2}{\beta_2}$  then

$$\chi(\langle \alpha_1, \beta_1 \rangle, \langle \alpha_2, \beta_2 \rangle) = \frac{|\lambda_1 - \lambda_2|}{\sqrt{|\lambda_1|^2 + 1}\sqrt{|\lambda_2|^2 + 1}}. \quad (\text{A.0.2})$$

In other words, the chordal distance between  $\langle \alpha_1, \beta_1 \rangle$  and  $\langle \alpha_2, \beta_2 \rangle$  is half the Euclidean distance between the images of  $\lambda_1$  and  $\lambda_2$  under the stereographic projection. This ensures that the distance between any two eigenvalues is at most one, including eigenvalues at infinity.

Though perturbation results in terms of  $\chi$  originate with Stewart [\[49\]](#), the first version of Bauer-Fike stated in terms of the chordal distance for general matrices is due to Elsner and Sun [\[21\]](#), which we summarize below.

**Theorem A.1** (Elsner and Sun 1982). *Let  $(A, B)$  be a diagonalizable pencil with eigenvalues  $\langle \alpha_i, \beta_i \rangle$ . If  $T$  is any matrix of right eigenvectors of  $(A, B)$  and  $\langle \tilde{\alpha}_i, \tilde{\beta}_i \rangle$  are the eigenvalues of the regular pencil  $(\tilde{A}, \tilde{B})$ , then*

$$\max_i \min_j \chi(\langle \alpha_i, \beta_i \rangle, \langle \tilde{\alpha}_j, \tilde{\beta}_j \rangle) \leq \kappa(T) \|(AA^H + BB^H)^{-1/2}\|_2 \|(A - \tilde{A}, B - \tilde{B})\|_2$$

While [Theorem A.1](#) is more general than [Theorem 2.20](#), the two results are essentially the same under the assumptions made in [Section 2.2](#). To demonstrate this, suppose that  $(A, B)$  is diagonalizable and that  $B$  is nonsingular with  $\epsilon < \sigma_n(B)$ . If  $z \in \Lambda_\epsilon(A, B)$  then  $z$  is an eigenvalue of a pencil  $(\tilde{A}, \tilde{B})$  with  $\|A - \tilde{A}\|_2, \|B - \tilde{B}\|_2 \leq \epsilon$ . Thus, if  $\lambda$  is the eigenvalue of  $(A, B)$  closest to  $z$ , [Theorem A.1](#) and [\(A.0.2\)](#) imply

$$\frac{|z - \lambda|}{\sqrt{|z|^2 + 1}\sqrt{|\lambda|^2 + 1}} \leq \sqrt{2}\epsilon\kappa(T) \|(AA^H + BB^H)^{-1/2}\|_2 \quad (\text{A.0.3})$$

or, equivalently,

$$|z - \lambda| \leq \sqrt{2}\epsilon\kappa(T) \|(AA^H + BB^H)^{-1/2}\|_2 \sqrt{|z|^2 + 1}\sqrt{|\lambda|^2 + 1}. \quad (\text{A.0.4})$$

Applying [Lemma 2.19](#) to bound  $|z|$  and  $|\lambda|$  and noting  $\|(AA^H + BB^H)^{-1/2}\|_2 = \frac{1}{\sigma_n(A, B)}$ , we conclude that  $\Lambda_\epsilon(A, B)$  is contained in balls around the eigenvalues of  $(A, B)$  of radius

$$\sqrt{2}\epsilon \frac{\kappa(T)}{\sigma_n(A, B)} \left[ 1 + \left( \frac{\epsilon \|B^{-1}\|_2 + \|B^{-1}A\|_2}{1 - \epsilon \|B^{-1}\|_2} \right)^2 \right]. \quad (\text{A.0.5})$$

On one hand, the  $\sigma_n(A, B)$  in [\(A.0.5\)](#) is an improvement over the factor of  $\|B^{-1}\|_2$  in [Theorem 2.20](#), as  $\sigma_n(A, B) \geq \sigma_n(B)$ . At the same time, we pay the price in an additional factor of  $\sqrt{2}$  and the square on the

piece coming from [Lemma 2.19](#). Since  $\sigma_n(A, B) \geq \sigma_n(A)$ , [\(A.0.5\)](#) is likely a better bound if we know that  $A$  is far from singular, though in the proof of [Theorem 3.11](#) the only bounds on  $\sigma_n(A)$  available are the same as those for  $\sigma_n(B)$ . This means that, up to constants, a proof of shattering using [Theorem A.1](#) is the same as the one given above. In particular, Elsner and Sun’s result cannot be used to improve the dependence of  $\epsilon$  on  $n$ . Similarly, it would not change [Theorem 5.2](#).

Nevertheless, there is an important benefit of the generality of [Theorem A.1](#): the ability to control changes in the finite eigenvalues of a pencil with some at infinity. Up to this point, we have pursued a standard Bauer-Fike result that bounds  $\Lambda_\epsilon(A, B)$  by a union of balls around the eigenvalues of  $(A, B)$ . Because we know  $\Lambda_\epsilon(A, B)$  is unbounded if  $B$  is singular or  $\epsilon > \sigma_n(B)$ , [Theorem 2.20](#) and the alternate version [\(A.0.5\)](#) do not consider the case where  $B$  is singular. This ultimately carries through to our forward error bound [Theorem 5.2](#), which similarly requires that  $B$  is invertible. While we know that we can’t obtain any kind of forward error guarantees for the infinite eigenvalues of  $(A, B)$  with singular  $B$ , we would like to extend [Theorem 5.2](#) to the finite eigenvalues if possible. [Theorem A.1](#) offers one way to do this, producing the following proposition.

**Proposition A.2.** *Let  $(A, B)$  be a regular, diagonalizable pencil and let  $(\tilde{A}, \tilde{B})$  be a nearby pencil with  $\|A - \tilde{A}\|_2, \|B - \tilde{B}\|_2 \leq \epsilon$ . Suppose that  $\langle \alpha, \beta \rangle$  and  $\langle \tilde{\alpha}, \tilde{\beta} \rangle$  are eigenvalues of  $(A, B)$  and  $(\tilde{A}, \tilde{B})$ , where  $\langle \alpha, \beta \rangle$  is the closest eigenvalue of  $(A, B)$  to  $\langle \tilde{\alpha}, \tilde{\beta} \rangle$  in the chordal metric  $\chi$ . If  $\lambda = \frac{\alpha}{\beta}$  and  $\tilde{\lambda} = \frac{\tilde{\alpha}}{\tilde{\beta}}$  are both finite, then*

$$|\lambda - \tilde{\lambda}| \leq \sqrt{2}\epsilon \frac{\kappa_V(A, B)}{\sigma_n(A, B)} \sqrt{|\lambda|^2 + 1} \sqrt{|\tilde{\lambda}|^2 + 1}.$$

*Proof.* This follows directly from [Theorem A.1](#), noting that we can replace  $\kappa(T)$  with  $\kappa_V(A, B)$  by taking an infimum.  $\square$

Of course, this result is only useful if we can bound  $|\lambda|$  and  $|\tilde{\lambda}|$ , which is not necessarily straightforward. We do note, however, that  $\sigma_n(A, B)$  is guaranteed to be nonzero since  $(A, B)$  is regular.

To finish this section, we summarize other known variants of Bauer-Fike for the generalized eigenvalue problem (though this is by no means an exhaustive list). First, we note that [Theorem A.1](#) is the version stated by Stewart and Sun [[51](#), §VI Theorem 2.6] rewritten in terms of the canonical angle between the row spaces of  $(A, B)$  and  $(\tilde{A}, \tilde{B})$ . Stewart and Sun also include a version that swaps  $\kappa(T)$  for  $\|T\|_2 \|S^{-1}\|_2$ , where  $(S^{-1}AT, S^{-1}BT)$  is a diagonalization of  $(A, B)$  with the columns of  $S^{-1}$  and  $T$  normalized appropriately (see [[51](#), §VI Theorem 2.7]). This yields the simpler bound

$$\max_i \min_j \chi(\langle \alpha_i, \beta_i \rangle, \langle \tilde{\alpha}_j, \tilde{\beta}_j \rangle) \leq \|S^{-1}\|_2 \|T\|_2 \|(A - \tilde{A}, B - \tilde{B})\|_2. \quad (\text{A.0.6})$$

Note however that  $\|S^{-1}\|_2$  hides a dependence on the conditioning of  $A$  and  $B$  (recall for example that we construct our diagonalization above by taking  $S = BT$ ).

Minor improvements on [Theorem A.1](#) can be found in work of Elsner and Lancaster [[20](#)]. Meanwhile, Chu [[16](#)] stated their own version of Bauer-Fike consisting of four separate bounds, depending on whether the initial and perturbed eigenvalues are finite/infinite, which was subsequently generalized to matrix polynomials [[15](#)]. Finally, we note a recent sharp version of Shi and Wei [[48](#)] stated in terms of the sign-complex spectral radius.

## B Finite Arithmetic Analysis

In this appendix, we discuss the ongoing finite arithmetic analysis of **EIG** and **RPD**. We first outline our model of finite arithmetic computation and demonstrate some results for **GRURV** before exploring the challenges of analyzing **IRS** in this context.

### B.1 Black-Box Assumptions

Throughout, we assume a floating point arithmetic where

$$fl(x \circ y) = (x \circ y)(1 + \Delta), \quad |\Delta| \leq \mathbf{u} \quad (\text{B.1.1})$$

for basic operations  $\circ \in \{+, -, \times, \div\}$  and a machine precision  $\mathbf{u}(\varepsilon, n)$ , which is a function of the desired accuracy  $\varepsilon$  and the size of the problem  $n$ . We assume that  $\sqrt{x}$  can be evaluated in this way as well. (B.1.1) is a standard formulation for finite arithmetic computations (see for example [32]).

Throughout, we'll think of  $\mathbf{u}$  as inverse polynomial in  $n$ . In practice, we choose  $\mathbf{u}$  based on our error analysis to ensure either true backward stability or, if that's not possible, the slightly weaker logarithmic stability of Demmel, Dumitriu, and Holtz [17]. With this in mind, we further assume access to black-box algorithms for Gaussian sampling, matrix multiplication, and QR/QL, which we summarize below. These follow Banks et al. [9] to allow for easy connection with their finite arithmetic analysis.

**Assumption B.1** (Gaussian Sampling). There exists a  $c_N$ -stable Gaussian sampler  $N(\sigma)$  that takes  $\sigma \in \mathbb{R}_{\geq 0}$  and outputs  $\tilde{G} = N(\sigma)$  satisfying  $|\tilde{G} - G| \leq c_N \sigma \mathbf{u}$  for some  $G \sim \mathcal{N}_{\mathbb{C}}(0, \sigma^2)$ .

**Assumption B.2** (Matrix Multiplication). There exists a  $\mu_{\text{MM}}(n)$ -stable multiplication algorithm  $\mathbf{MM}(\cdot, \cdot)$  satisfying

$$\|\mathbf{MM}(A, B) - AB\|_2 \leq \mu_{\text{MM}}(n) \mathbf{u} \|A\|_2 \|B\|_2$$

in  $T_{\text{MM}}(n)$  arithmetic operations. Here, as in the rest of this appendix,  $AB$  represents the exact arithmetic product of  $A$  and  $B$ .

**Assumption B.3** (QR Factorization). There exists a  $\mu_{\text{QR}}(n)$ -stable QR algorithm  $\mathbf{QR}(\cdot)$  satisfying

1.  $[Q, R] = \mathbf{QR}(A)$ ,
2.  $R$  is exactly upper triangular/trapezoidal,
3. There exists  $A'$  and unitary  $Q'$  such that  $A' = Q'R$  with

$$\|Q' - Q\|_2 \leq \mu_{\text{QR}}(n) \mathbf{u}, \quad \|A' - A\|_2 \leq \mu_{\text{QR}}(n) \mathbf{u} \|A\|_2,$$

in  $T_{\text{QR}}(n)$  arithmetic operations.

For simplicity, we further assume access to a QL algorithm  $\mathbf{QL}(\cdot)$  that satisfies similar guarantees as in Assumption B.3 with the same parameter  $\mu_{\text{QR}}(n)$ . Note that for these routines we can always guarantee a truly triangular result in finite arithmetic by forcing entries above/below the diagonal to be zero.

## B.2 Two Matrix GRURV

In our algorithm, **EIG** only ever applies **GRURV** to a pair of matrices in one of the following ways: **GRURV**(2,  $A_1, A_2, -1, 1$ ) or **GRURV**(2,  $A_1, A_2, 1, -1$ ). Under the finite arithmetic setting established above, the first of these proceeds as follows.

**GRURV**(2,  $A_1, A_2, -1, 1$ ):

1.  $[U_2, R_2, V] = \mathbf{RURV}(A_2)$
2.  $X = \mathbf{MM}(A_1^H, U_2)$
3.  $[U, R_1^H] = \mathbf{QL}(X)$

There are three sources of error here: **RURV** in step one, matrix multiplication in step two, and QL in step three. The latter two are controlled by Assumption B.2 and Assumption B.3 respectively. To control error in finite arithmetic **RURV**, we use work of Banks et al. [9, Lemma C.17] (which is itself built on Assumption B.1). Under the additional assumptions

$$4\|A_2\|_2 \max\{c_N \mu_{\text{MM}}(n) \mathbf{u}, c_N \mu_{\text{QR}}(n) \mathbf{u}\} \leq \frac{1}{4} \leq \|A_2\|_2 \quad \text{and} \quad 1 \leq \min\{\mu_{\text{MM}}(n), \mu_{\text{QR}}(n), c_N\} \quad (\text{B.2.1})$$

this yields the following.

**Theorem B.4.** *Let  $[U, R_1, R_2, V] = \mathbf{GRURV}(2, A_1, A_2, -1, 1)$  in finite arithmetic for two matrices  $A_1$  and  $A_2$ . Assuming (B.2.1), there exist matrices  $\tilde{A}_1, \tilde{A}_2$  and unitary  $\tilde{U}, \tilde{V}$ , such that  $\tilde{A}_1^{-1} \tilde{A}_2 = \tilde{U} R_1^{-1} R_2 \tilde{V}$  and*

1.  $\tilde{V}$  is Haar distributed.
2.  $\|U - \tilde{U}\|_2 \leq \mu_{QR}(n)\mathbf{u}$ .
3.  $\|A_1 - \tilde{A}_1\|_2 \leq [\mu_{QR}(n)\mathbf{u} + \mu_{MM}(n)\mathbf{u}(1 + \mu_{QR}(n)\mathbf{u}) + \mu_{QR}(n)\mathbf{u}(1 + \mu_{MM}(n)\mathbf{u})(1 + \mu_{QR}(n)\mathbf{u})] \|A_1\|_2$ .
4. For every  $1 > \alpha > 0$  and  $t > 2\sqrt{2} + 1$ , the event that both
  - $\|V - \tilde{V}\|_2 \leq \frac{8tn^{3/2}}{\alpha} c_N \mu_{QR}(n)\mathbf{u} + \frac{10n^2}{\alpha} \mathbf{u}$
  - $\|A_2 - \tilde{A}_2\|_2 \leq \left( \frac{9tn^{3/2}}{\alpha} c_N \mu_{QR}(n)\mathbf{u} + 2\mu_{MM}(n)\mathbf{u} + \frac{10n^2}{\alpha} c_N \mathbf{u} \right) \|A_2\|_2$
 occurs with probability at least  $1 - 2e\alpha^2 - 2e^{-t^2n}$ .

*Proof.* Beginning with finite arithmetic guarantees for **RURV**, [9, Lemma C.17] implies that there exists unitary matrices  $\tilde{U}_2$  and  $\tilde{V}$  and a matrix  $\tilde{A}_2$  such that  $\tilde{A}_2 = \tilde{U}_2 R_2 \tilde{V}$ , where  $\tilde{V}$  is Haar distributed and  $\|U_2 - \tilde{U}_2\|_2$ ,  $\|V - \tilde{V}\|_2$ , and  $\|A_2 - \tilde{A}_2\|_2$  can all be controlled. In particular,

$$\|U_2 - \tilde{U}_2\|_2 \leq \mu_{QR}(n)\mathbf{u}. \quad (\text{B.2.2})$$

Consequently, [Assumption B.2](#) guarantees that in step two above

$$\|X - A_1^H U_2\|_2 \leq \mu_{MM}(n)\mathbf{u} \|U_2\|_2 \|A_1\|_2 \leq \mu_{MM}(n)\mathbf{u}(1 + \mu_{QR}(n)\mathbf{u}) \|A_1\|_2. \quad (\text{B.2.3})$$

Lastly, [Assumption B.3](#) implies that there exists a unitary matrix  $\tilde{U}$  and a matrix  $\tilde{X}$  such that  $\tilde{X} = \tilde{U} R_1^H$  with

$$\|X - \tilde{X}\|_2 \leq \mu_{QR}(n)\mathbf{u} \|X\|_2. \quad (\text{B.2.4})$$

With this in mind, let  $\tilde{A}_1 = \tilde{U}_2 \tilde{X}^H$ . By construction, we have

$$\tilde{A}_1^{-1} \tilde{A}_2 = (\tilde{U}_2 \tilde{X}^H)^{-1} \tilde{U}_2 R_2 \tilde{V} = (R_1 \tilde{U}^H)^{-1} R_2 \tilde{V} = \tilde{U} R_1^{-1} R_2 \tilde{V}, \quad (\text{B.2.5})$$

which means  $\tilde{U} R_1^{-1} R_2 \tilde{V}$  is a generalized rank-revealing factorization of  $\tilde{A}_1^{-1} \tilde{A}_2$ . Now the distance between  $A_2$  and  $\tilde{A}_2$  follows directly from [9, Lemma C.17], as does the analogous result for  $\tilde{V}$ . Additionally, we observe

$$\begin{aligned} \|A_1 - \tilde{A}_1\|_2 &= \|A_1 - \tilde{U}_2 \tilde{X}^H\|_2 \\ &\leq \|A_1^H \tilde{U}_2 - \tilde{X}\|_2 \\ &= \|A_1^H \tilde{U}_2 - A_1^H U_2 + A_1^H U_2 - X + X - \tilde{X}\|_2 \\ &\leq \|A_1^H (\tilde{U}_2 - U_2)\|_2 + \|A_1^H U_2 - X\|_2 + \|X - \tilde{X}\|_2 \\ &\leq \|A_1\|_2 \mu_{QR}(n)\mathbf{u} + \mu_{MM}(n)\mathbf{u}(1 + \mu_{QR}(n)\mathbf{u}) \|A_1\|_2 + \mu_{QR}(n)\mathbf{u} \|X\|_2. \end{aligned} \quad (\text{B.2.6})$$

Since (B.2.3) implies

$$\begin{aligned} \|X\|_2 &\leq \mu_{MM}(n)\mathbf{u}(1 + \mu_{QR}(n)\mathbf{u}) \|A_1\|_2 + \|A_1^H U_2\|_2 \\ &\leq \mu_{MM}(n)\mathbf{u}(1 + \mu_{QR}(n)\mathbf{u}) \|A_1\|_2 + \|A_1\|_2 (1 + \mu_{QR}(n)\mathbf{u}) \\ &= (1 + \mu_{MM}(n)\mathbf{u})(1 + \mu_{QR}(n)\mathbf{u}) \|A_1\|_2, \end{aligned} \quad (\text{B.2.7})$$

this becomes

$$\|A_1 - \tilde{A}_1\|_2 \leq [\mu_{QR}(n)\mathbf{u} + \mu_{MM}(n)\mathbf{u}(1 + \mu_{QR}(n)\mathbf{u}) + \mu_{QR}(n)\mathbf{u}(1 + \mu_{MM}(n)\mathbf{u})(1 + \mu_{QR}(n)\mathbf{u})] \|A_1\|_2. \quad (\text{B.2.8})$$

Finally recalling (B.2.2), we have all of the listed bounds.  $\square$

While [Theorem B.4](#) applies explicitly to **GRURV**(2,  $A_1, A_2, -1, 1$ ) it also covers **GRURV**(2,  $A_1, A_2, 1, -1$ ); the latter only swaps **RURV** and **QL** for **RULV** and **QR**, thereby providing the same guarantees since **QR** and **QL** satisfy essentially the same assumptions.

### B.3 Finite Arithmetic IRS

We turn now to **IRS**. Consider computing  $[A_p, B_p] = \mathbf{IRS}(A, B, p)$  in finite arithmetic. To simplify the analysis, we'll assume  $\mu_{\text{MM}}(n)\mathbf{u}, \mu_{\text{QR}}(2n)\mathbf{u} \leq \tau \in (0, 1)$  for some small  $\tau$  (again inverse polynomial in  $n$ ), and we'll let  $A_0 = A$  and  $B_0 = B$  be the  $n \times n$  input matrices.

The very first step of repeated squaring computes a QR factorization  $[Q, R] = \mathbf{QR} \begin{pmatrix} B_0 \\ -A_0 \end{pmatrix}$ , where by

[Assumption B.3](#) there exist nearby matrices  $\tilde{A}_0, \tilde{B}_0$  and unitary  $\tilde{Q}$  such that

$$\begin{pmatrix} \tilde{B}_0 \\ -\tilde{A}_0 \end{pmatrix} = \tilde{Q}R \quad (\text{B.3.1})$$

with

$$\|A_0 - \tilde{A}_0\|_2, \|B_0 - \tilde{B}_0\|_2 \leq \left\| \begin{pmatrix} B_0 \\ -A_0 \end{pmatrix} - \begin{pmatrix} \tilde{B}_0 \\ -\tilde{A}_0 \end{pmatrix} \right\|_2 \leq \tau \sqrt{\|A_0\|_2^2 + \|B_0\|_2^2}. \quad (\text{B.3.2})$$

Combining (B.3.2) with [Assumption B.2](#), it's not hard to show that  $A_1$  and  $B_1$  – our finite arithmetic outputs after one step – are “close” to  $\tilde{Q}_{12}^H \tilde{A}_0$  and  $\tilde{Q}_{22}^H \tilde{B}_0$ , the exact arithmetic result of one step of **IRS** applied to  $\tilde{A}_0$  and  $\tilde{B}_0$ . Here, “close” means

$$\|A_1 - \tilde{Q}_{12}^H \tilde{A}_0\|_2 \leq O(\tau)\|A_0\|_2 \quad \text{and} \quad \|B_1 - \tilde{Q}_{22}^H \tilde{B}_0\|_2 \leq O(\tau)\|B_0\|_2, \quad (\text{B.3.3})$$

assuming  $\|A_0\|_2$  and  $\|B_0\|_2$  are of the same order (as is the case for the matrices **IRS** is applied to in **EIG**).

To generalize (B.3.3) to the  $(p+1)^{\text{st}}$  step of repeated squaring, suppose that  $A_p$  and  $B_p$  are the result of  $p$  finite arithmetic steps of **IRS** applied to  $A_0$  and  $B_0$  while  $\tilde{A}_p$  and  $\tilde{B}_p$  are the outputs of  $p$  exact arithmetic steps applied to  $\tilde{A}_0$  and  $\tilde{B}_0$ . The  $(p+1)^{\text{st}}$  step of finite arithmetic **IRS** then proceeds as follows:

1.  $[Q, R] = \mathbf{QR} \begin{pmatrix} B_p \\ -A_p \end{pmatrix}$
2.  $A_{p+1} = \mathbf{MM}(Q_{12}^H, A_p)$
3.  $B_{p+1} = \mathbf{MM}(Q_{22}^H, B_p)$ .

Note that we recycle the notation  $Q$  and  $R$  in item 1 for simplicity; in practice these are of course different for each value of  $p$ . We now make the following observations:

- As in the first step above, [Assumption B.3](#) implies the existence of matrices  $\tilde{A}_p$  and  $\tilde{B}_p$  such that

$$\begin{pmatrix} \tilde{B}_p \\ -\tilde{A}_p \end{pmatrix} = \tilde{Q}R \quad (\text{B.3.4})$$

where  $\tilde{Q}$  is truly unitary,  $\|Q - \tilde{Q}\|_2 \leq \tau$ , and  $\|A_p - \tilde{A}_p\|_2, \|B_p - \tilde{B}_p\|_2 \leq \tau \sqrt{\|A_p\|_2^2 + \|B_p\|_2^2}$ .

- Using  $\|Q_{12}\|_2, \|Q_{22}\|_2 \leq \|Q\|_2 \leq 1 + \tau$ , [Assumption B.2](#) implies

$$\|A_{p+1} - Q_{12}^H A_p\|_2 \leq \tau(1 + \tau)\|A_p\|_2 \quad \text{and} \quad \|B_{p+1} - Q_{22}^H B_p\|_2 \leq \tau(1 + \tau)\|B_p\|_2. \quad (\text{B.3.5})$$

- Again thinking of  $\tilde{Q}_{12}^H \tilde{A}_p$  and  $\tilde{Q}_{22}^H \tilde{B}_p$  as the exact arithmetic outputs of one step of **IRS** applied to  $\tilde{A}_p$  and  $\tilde{B}_p$ , we note

$$\begin{aligned} \|A_{p+1} - \tilde{Q}_{12}^H \tilde{A}_p\|_2 &= \|A_{p+1} - Q_{12}^H A_p + Q_{12}^H A_p - \tilde{Q}_{12}^H A_p + \tilde{Q}_{12}^H A_p - \tilde{Q}_{12}^H \tilde{A}_p\|_2 \\ &\leq \|A_{p+1} - Q_{12}^H A_p\|_2 + \|Q_{12} - \tilde{Q}_{12}\|_2 \|A_p\|_2 + \|\tilde{Q}_{12}\|_2 \|A_p - \tilde{A}_p\|_2 \\ &\leq (2\tau + \tau^2)\|A_p\|_2 + \tau \sqrt{\|A_p\|_2^2 + \|B_p\|_2^2}. \end{aligned} \quad (\text{B.3.6})$$

Making the same argument for  $B_{p+1}$  and  $\tilde{Q}_{22}^H \tilde{B}_p$  we conclude

$$\|A_{p+1} - \tilde{Q}_{12}^H \tilde{A}_p\|_2 \leq O(\tau)\|A_p\|_2 \quad \text{and} \quad \|B_{p+1} - \tilde{Q}_{22}^H \tilde{B}_p\|_2 \leq O(\tau)\|B_p\|_2, \quad (\text{B.3.7})$$

again assuming that  $\|A_p\|_2$  and  $\|B_p\|_2$  are of the same order.

We would next like to argue that the exact QR factorization (B.3.4) is close to an exact QR factorization of  $\begin{pmatrix} \bar{B}_p \\ -\bar{A}_p \end{pmatrix}$ . To do this, assume we have access to  $\|A_p - \bar{A}_p\|_2$  and  $\|B_p - \bar{B}_p\|_2$ . In the argument to come, we bound error inductively, where (B.3.3) is the base case (corresponding to  $p = 1$ ). With this in mind, we have

$$\|\tilde{A}_p - \bar{A}_p\|_2 \leq \|\tilde{A}_p - A_p\|_2 + \|A_p - \bar{A}_p\|_2 \leq \tau \sqrt{\|A_p\|_2^2 + \|B_p\|_2^2} + \|A_p - \bar{A}_p\|_2 \quad (\text{B.3.8})$$

and therefore, since the same bound holds for  $\|\tilde{B}_p - \bar{B}_p\|_2$ ,

$$\begin{aligned} \left\| \begin{pmatrix} \tilde{B}_p \\ -\tilde{A}_p \end{pmatrix} - \begin{pmatrix} \bar{B}_p \\ -\bar{A}_p \end{pmatrix} \right\|_2 &\leq \left( \|\tilde{A}_p - \bar{A}_p\|_2^2 + \|\tilde{B}_p - \bar{B}_p\|_2^2 \right)^{1/2} \\ &\leq \left[ 2\theta_p \tau^2 + 2\sqrt{\theta_p} \tau (\|A_p - \bar{A}_p\|_2 + \|B_p - \bar{B}_p\|_2) + \|A_p - \bar{A}_p\|_2^2 + \|B_p - \bar{B}_p\|_2^2 \right]^{1/2}, \end{aligned} \quad (\text{B.3.9})$$

where  $\theta_p = \|A_p\|_2^2 + \|B_p\|_2^2$ . Moreover,

$$\sigma_n \begin{pmatrix} \tilde{B}_p \\ -\tilde{A}_p \end{pmatrix} \geq \sigma_n \begin{pmatrix} B_p \\ -A_p \end{pmatrix} - \left\| \begin{pmatrix} \tilde{B}_p \\ -\tilde{A}_p \end{pmatrix} - \begin{pmatrix} B_p \\ -A_p \end{pmatrix} \right\|_2 \geq \sigma_n \begin{pmatrix} B_p \\ -A_p \end{pmatrix} - \sqrt{2\theta_p} \tau. \quad (\text{B.3.10})$$

Thus, a standard perturbation result of Sun [52, Theorem 1.6] states that as long as

$$\beta_p = \frac{[2\theta_p \tau^2 + 2\sqrt{\theta_p} \tau (\|A_p - \bar{A}_p\|_2 + \|B_p - \bar{B}_p\|_2) + \|A_p - \bar{A}_p\|_2^2 + \|B_p - \bar{B}_p\|_2^2]^{1/2}}{\sigma_n \begin{pmatrix} B_p \\ -A_p \end{pmatrix} - \sqrt{2\theta_p} \tau} < 1, \quad (\text{B.3.11})$$

there exists an exact QR factorization

$$\begin{pmatrix} \bar{B}_p \\ -\bar{A}_p \end{pmatrix} = UR' \quad (\text{B.3.12})$$

with

$$\|\tilde{Q} - U\|_2 \leq \sqrt{n}(1 + \sqrt{2}) \frac{\beta_p}{1 - \beta_p}. \quad (\text{B.3.13})$$

Setting  $\bar{A}_{p+1} = U_{12}^H \bar{A}_p$  and  $\bar{B}_{p+1} = U_{22}^H \bar{B}_p$ , we can now bound the error  $\|A_{p+1} - \bar{A}_{p+1}\|_2$  as follows:

$$\begin{aligned} \|A_{p+1} - \bar{A}_{p+1}\|_2 &= \|A_{p+1} - \tilde{Q}_{12}^H \tilde{A}_p + \tilde{Q}_{12}^H \tilde{A}_p - \tilde{Q}_{12}^H \bar{A}_p + \tilde{Q}_{12}^H \bar{A}_p - \bar{A}_{p+1}\|_2 \\ &\leq \|A_{p+1} - \tilde{Q}_{12}^H \tilde{A}_p\|_2 + \|\tilde{A}_p - \bar{A}_p\|_2 + \|\tilde{Q}_{12} - U_{12}\|_2 \|\bar{A}_p\|_2 \\ &\leq (2\tau + \tau^2) \|A_p\|_2 + 2\sqrt{\theta_p} \tau + \|A_p - \bar{A}_p\|_2 + \sqrt{n}(1 + \sqrt{2}) \frac{\beta_p}{1 - \beta_p} \|\tilde{A}_0\|_2. \end{aligned} \quad (\text{B.3.14})$$

For the last inequality, we use the fact that  $\|\bar{A}_p\|_2 \leq \|\tilde{A}_0\|_2$  since  $\bar{A}_p$  is obtained from  $\tilde{A}_0$  via exact arithmetic **IRS**. Making the parallel argument for  $B_{p+1}$ , we then have a final set of bounds

$$\begin{aligned} \|A_{p+1} - \bar{A}_{p+1}\|_2 &\leq O(\tau) \|A_p\|_2 + \|A_p - \bar{A}_p\|_2 + \sqrt{n}(1 + \sqrt{2}) \frac{\beta_p}{1 - \beta_p} \|\tilde{A}_0\|_2 \\ \|B_{p+1} - \bar{B}_{p+1}\|_2 &\leq O(\tau) \|B_p\|_2 + \|B_p - \bar{B}_p\|_2 + \sqrt{n}(1 + \sqrt{2}) \frac{\beta_p}{1 - \beta_p} \|\tilde{B}_0\|_2. \end{aligned} \quad (\text{B.3.15})$$

The dependence on  $\|A_p\|_2$  and  $\|B_p\|_2$  in (B.3.15) is not an issue; in fact,  $\|A_{p+1}\|_2 \leq (1 + \tau)^2 \|A_p\|_2$  and  $\|B_{p+1}\|_2 \leq (1 + \tau)^2 \|B_p\|_2$ , meaning norms grow by, at most, tiny constants. The factor of  $\sqrt{n}$ , on the other hand, is a problem. Recalling that we take logarithmically many steps of repeated squaring in **EIF**, multiplying by a factor of  $\sqrt{n}$  each time will cause error to grow at a rate faster than can be controlled if  $\mathbf{u}$  is inverse polynomial in  $n$ . This is ultimately a consequence of Sun's perturbation bound, which is stated



in terms of the Frobenius norm  $\|\cdot\|_F$ . While useful from a perturbation theory perspective, the Frobenius norm is problematic numerically, requiring a conversion to the two norm that incurs a  $\sqrt{n}$ .

This begs the question, can we obtain a better perturbation bound? Ostensibly, Sun’s result is stated in terms of the Frobenius norm because it rests on the following inequality: given  $L \in \mathbb{C}^{n \times n}$  a lower triangular matrix with real diagonal entries,

$$\|L\|_F \leq \frac{1}{\sqrt{2}} \|L + L^H\|_F. \quad (\text{B.3.16})$$

Unfortunately, no inequality of the form  $\|L\|_2 \leq C \|L + L^H\|_2$  for a positive constant  $C$  can exist (multiply the matrix in [13, Example 3.3] by  $i$  for a counterexample). Nevertheless, work of Bhatia [13] implies

$$\|L\|_2 \leq O(\log(n)) \|L + L^H\|_2, \quad (\text{B.3.17})$$

meaning Sun’s proof can be adapted to replace the  $\sqrt{n}$  factor with  $\log(n)$ .

This provides an improvement over (B.3.15), but it still isn’t good enough to control overall error. That is, taking  $O(\log(n))$  steps would cause error to grow like  $O(\log(n)^{\log(n)}) = O(n^{\log(\log(n))})$ , which is more than polynomial. Without access to better QR perturbation bounds, our only hope is to argue that at each step

$$\beta_p = O\left(\frac{1}{\log(n)}\right), \quad (\text{B.3.18})$$

therefore canceling the  $\log(n)$  factor. Practically speaking, this boils down to showing

$$\sigma_n \begin{pmatrix} B_p \\ -A_p \end{pmatrix} = \Omega(\log(n)). \quad (\text{B.3.19})$$

Now in **FIG**, the inputs of **IRS** are linear combinations of the perturbed and scaled matrices  $\tilde{A}$  and  $n^\alpha \tilde{B}$ , meaning with high probability (B.3.19) holds for  $p = 0$ . Nevertheless, it is still an open question whether or not this is preserved as repeated squaring proceeds.

In our experiments,  $\sigma_n \begin{pmatrix} B_p \\ -A_p \end{pmatrix}$  decreases as **IRS** runs, though not by much, lending support to the idea that (B.3.19) should hold for all  $p$  as long as the corresponding value at  $p = 0$  is sufficiently large. The challenge to proving this in general stems from the fact that  $A_p$  and  $B_p$  are obtained from  $A_{p-1}$  and  $B_{p-1}$  by multiplying by  $n \times n$  pieces of a nearly unitary  $2n \times 2n$  matrix  $Q$ . In particular, no non-trivial lower bound can exist for the smallest singular value of the  $n \times n$  pieces of  $Q$  used. In some sense, this reflects the fact that our black-box assumptions for QR are insufficient to analyze **IRS**; the portion of Assumption B.3 relevant to  $Q$  isn’t strong enough while the guarantees for  $R$  are not needed.

## References

- [1] Björn Adlerborn, Bo Kågström, and Daniel Kressner. A parallel QZ algorithm for distributed memory HPC systems. *SIAM Journal on Scientific Computing*, 36(5):C480–C503, 2014.
- [2] Michael Aizenman, Ron Peled, Jeffrey Schenker, Mira Shamir, and Sasha Sodin. Matrix regularizing effects of Gaussian perturbations. *Communications in Contemporary Mathematics*, 19(03):1750028, 2017.
- [3] Luis Miguel Anguas, María Isabel Bueno, and Froilán M. Dopico. A comparison of eigenvalue condition numbers for matrix polynomials. *Linear Algebra and its Applications*, 564:170–200, 2019.
- [4] Z. D. Bai. Circular law. *The Annals of Probability*, 25(1):494–529, 1997.
- [5] Zhaojun Bai, James Demmel, and Ming Gu. An inverse free parallel spectral divide and conquer algorithm for nonsymmetric eigenproblems. *Numerische Mathematik*, 76:279–308, 1997.
- [6] Grey Ballard, James Demmel, and Ioana Dumitriu. Minimizing communication for eigenproblems and the singular value decomposition. *ArXiv*, abs/1011.3077, 2010.

- [7] Grey Ballard, James Demmel, Ioana Dumitriu, and Alexander Rusciano. A generalized randomized rank-revealing factorization. *ArXiv*, abs/1909.06524, 2019.
- [8] Grey Ballard, James Demmel, Olga Holtz, and Oded Schwartz. Minimizing communication in numerical linear algebra. *SIAM Journal on Matrix Analysis and Applications*, 32:866–901, 09 2011.
- [9] Jess Banks, Jorge Garza-Vargas, Archit Kulkarni, and Nikhil Srivastava. Pseudospectral shattering, the sign function, and diagonalization in nearly matrix multiplication time. *Foundations of Computational Mathematics*, pages 1–89, 2022.
- [10] Jess Banks, Archit Kulkarni, Satyaki Mukherjee, and Nikhil Srivastava. Gaussian regularization of the pseudospectrum and davis’ conjecture. *Communications on Pure and Applied Mathematics*, 74:2114–2131, 10 2021.
- [11] F. L. Bauer and C. T. Fike. Norms and exclusion theorems. *Numerische Mathematik*, 2(1):137–141, Dec 1960.
- [12] A.N. Beavers and E.D. Denman. A new similarity transformation method for eigenvalues and eigenvectors. *Mathematical Biosciences*, 21(1):143–169, 1974.
- [13] Rajendra Bhatia. Pinching, trimming, truncating, and averaging of matrices. *The American Mathematical Monthly*, 107(7):602–608, 2000.
- [14] Tony F. Chan. Rank revealing QR factorizations. *Linear Algebra and its Applications*, 88-89:67–82, 1987.
- [15] Eric King-wah Chu. Perturbation of eigenvalues for matrix polynomials via the Bauer-Fike theorems. *SIAM Journal on Matrix Analysis and Applications*, 25(2):551–573, 2003.
- [16] King-Wah Eric Chu. Exclusion theorems and the perturbation analysis of the generalized eigenvalue problem. *SIAM Journal on Numerical Analysis*, 24(5):1114–1125, 1987.
- [17] James Demmel, Ioana Dumitriu, and Olga Holtz. Fast linear algebra is stable. *Numerische Mathematik*, 108:59–91, Oct 2007.
- [18] Alan Edelman. Eigenvalues and condition numbers of random matrices. *SIAM Journal on Matrix Analysis and Applications*, 9(4):543–560, 1988.
- [19] Alan Edelman and N. Raj Rao. Random matrix theory. *Acta Numerica*, 14:233–297, 2005.
- [20] L. Elsner and P. Lancaster. The spectral variation of pencils of matrices. *Journal of Computational Mathematics*, 3(3):262–274, 1985.
- [21] Ludwig Elsner and Ji guang Sun. Perturbation theorems for the generalized eigenvalue problem. *Linear Algebra and its Applications*, 48:341–357, 1982.
- [22] Thomas Ericsson and Axel Ruhe. The spectral transformation Lánczos method for the numerical solution of large sparse generalized symmetric eigenvalue problems. *Mathematics of Computation*, 35:1251–1268, 1980.
- [23] Brendan Farrell and Roman Vershynin. Smoothed analysis of symmetric random matrices with continuous distributions. *Proceedings of the American Mathematical Society*, 144, 12 2012.
- [24] Ricardo D. Fierro, Per Christian Hansen, and Peter Søren Kirk Hansen. UTV tools: Matlab templates for rank-revealing UTV decompositions. *Numerical Algorithms*, 20:165–194, 1999.
- [25] Valérie Fraysse, Michel Gueury, Frank Nicoud, and Vincent Toumazou. Spectral portraits for matrix pencils. 1996.
- [26] Judith D. Garduber and Alan J. Laub. A generalization of the matrix-sign-function solution for algebraic Riccati equations. *International Journal of Control*, 44(3):823–832, 1986.

- [27] Anne Greenbaum, Ren-Cang Li, and Michael L. Overton. First-order perturbation theory for eigenvalues and eigenvectors. *SIAM Review*, 62(2):463–482, 2020.
- [28] Ming Gu and Stanley C. Eisenstat. Efficient algorithms for computing a strong rank-revealing QR factorization. *SIAM Journal on Scientific Computing*, 17(4):848–869, 1996.
- [29] M. R. Guarracino, C. Cifarelli, O. Seref, and P. M. Pardalos. A classification method based on generalized eigenvalue problems. *Optimization Methods and Software*, 22(1):73–81, 2007.
- [30] Ernst Hairer and Gerhard Wanner. *Solving Ordinary Differential Equations II. Stiff and Differential-Algebraic Problems*, volume 14. 01 1996.
- [31] Desmond J. Higham and Nicholas J. Higham. Structured backward error and condition of generalized eigenvalue problems. *SIAM Journal on Matrix Analysis and Applications*, 20(2):493–512, 1998.
- [32] Nicholas J. Higham. *Accuracy and Stability of Numerical Algorithms*. Society for Industrial and Applied Mathematics, Second edition, 2002.
- [33] Michiel E. Hochstenbach, Christian Mehl, and Bor Plestenjak. Solving singular generalized eigenvalue problems by a rank-completing perturbation. *SIAM Journal on Matrix Analysis and Applications*, 40(3):1022–1046, 2019.
- [34] Roger A. Horn and Charles R. Johnson. *Matrix Analysis*. Cambridge University Press, 2 edition, 2012.
- [35] Y. Hua and T.K. Sarkar. Matrix pencil method for estimating parameters of exponentially damped/undamped sinusoids in noise. *IEEE Transactions on Acoustics, Speech, and Signal Processing*, 38(5):814–824, 1990.
- [36] Bo Kågström and Daniel Kressner. Multishift variants of the QZ algorithm with aggressive early deflation. *SIAM Journal on Matrix Analysis and Applications*, 29(1):199–227, 2007.
- [37] L. Kronecker. *Algebraische Reduction der Schaaren bilinearer Formen*. Sitzungsberichte der Preussischen Akademie der Wissenschaften. 1890.
- [38] Martin Lotz and Vanni Noferini. Wilkinson’s bus: Weak condition numbers, with an application to singular polynomial eigenproblems. *Foundations of Computational Mathematics*, 20, 03 2020.
- [39] Alexander N. Malyshev. Parallel algorithm for solving some spectral problems of linear algebra. *Linear Algebra and its Applications*, 188-189:489–520, 1993.
- [40] O.L. Mangasarian and E.W. Wild. Multisurface proximal support vector machine classification via generalized eigenvalues. *IEEE Transactions on Pattern Analysis and Machine Intelligence*, 28(1):69–74, 2006.
- [41] C. B. Moler and G. W. Stewart. An algorithm for generalized matrix eigenvalue problems. *SIAM Journal on Numerical Analysis*, 10(2):241–256, 1973.
- [42] J. D. Roberts. Linear model reduction and solution of the algebraic Riccati equation by use of the sign function†. *International Journal of Control*, 32(4):677–687, 1980.
- [43] R. Roy and T. Kailath. ESPRIT-estimation of signal parameters via rotational invariance techniques. *IEEE Transactions on Acoustics, Speech, and Signal Processing*, 37(7):984–995, 1989.
- [44] Mark Rudelson and Roman Vershynin. The Littlewood–Offord problem and invertibility of random matrices. *Advances in Mathematics*, 218(2):600–633, 2008.
- [45] Tetsuya Sakurai and Hiroshi Sugiura. A projection method for generalized eigenvalue problems using numerical integration. *Journal of Computational and Applied Mathematics*, 159(1):119–128, 2003.
- [46] Ahmed H. Sameh and John A. Wisniewski. A trace minimization algorithm for the generalized eigenvalue problem. *SIAM Journal on Numerical Analysis*, 19(6):1243–1259, 1982.

- [47] Arvind Sankar, Daniel A. Spielman, and Shang-Hua Teng. Smoothed analysis of the condition numbers and growth factors of matrices. *SIAM Journal on Matrix Analysis and Applications*, 28(2):446–476, 2006.
- [48] Xinghua Shi and Yimin Wei. A sharp version of Bauer–Fike’s theorem. *Journal of Computational and Applied Mathematics*, 236(13):3218–3227, 2012.
- [49] G. W. Stewart. Gershgorin theory for the generalized eigenvalue problem  $Ax = \lambda Bx$ . *Mathematics of Computation*, 29(130):600–606, 1975.
- [50] G. W. Stewart. Updating a rank-revealing ULV decomposition. *SIAM Journal on Matrix Analysis and Applications*, 14(2):494–499, 1993.
- [51] G.W. Stewart and J. Sun. *Matrix Perturbation Theory*. Computer Science and Scientific Computing. Elsevier Science, 1990.
- [52] Ji-Guang Sun. Perturbation bounds for the Cholesky and QR factorizations. *BIT Numerical Mathematics*, 31(2):341–352, jun 1991.
- [53] Terence Tao and Van Vu. Random matrices: the distribution of the smallest singular values. *Geometric and Functional Analysis*, 20, 04 2009.
- [54] Lloyd N. Trefethen and Mark Embree. *Spectra and Pseudospectra: The Behavior of Nonnormal Matrices and Operators*. Princeton University Press, 2020.
- [55] Roman Vershynin. *High-Dimensional Probability: An Introduction with Applications in Data Science*. Cambridge Series in Statistical and Probabilistic Mathematics. Cambridge University Press, 2018.
- [56] Robert C. Ward. The combination shift QZ algorithm. *SIAM Journal on Numerical Analysis*, 12(6):835–853, 1975.
- [57] David S. Watkins. Performance of the QZ algorithm in the presence of infinite eigenvalues. *SIAM Journal on Matrix Analysis and Applications*, 22(2):364–375, 2000.